NASA TECHNICAL NOTE

NASA TN D-6292

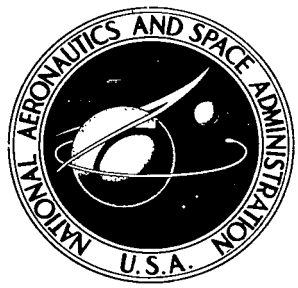

EXPERIMENTAL INVESTIGATION OF THE USE OF SLOTTED TEST-SECTION WALLS TO REDUCE WALL INTERFERENCE FOR HIGH-LIFT-MODEL TESTING

by Kalman J. Grunwald

Langley Research Center
Hampton, Va. 23365

NATIONAL AERONAUTICS AND SPACE ADMINISTRATION • WASHINGTON, D. C. • JUNE 1971

1. Report No.	2. Government Accession No.	3. Recipient's Catalog No.
NASA TN D-6292		

4. Title and Subtitle	5. Report Date
EXPERIMENTAL INVESTIGATION OF THE USE OF SLOTTED TEST-SECTION WALLS TO REDUCE WALL INTERFERENCE FOR HIGH-LIFT-MODEL TESTING	June 1971
	6. Performing Organization Code
7. Author(s)	8. Performing Organization Report No.
Kalman J. Grunwald	L-6884
	10. Work Unit No.
9. Performing Organization Name and Address	721-01-10-06
NASA Langley Research Center Hampton, Va. 23365	11. Contract or Grant No.
	13. Type of Report and Period Covered
12. Sponsoring Agency Name and Address	Technical Note
National Aeronautics and Space Administration Washington, D.C. 20546	14. Sponsoring Agency Code

15. Supplementary Notes

16. Abstract

An investigation of various test-section configurations with slotted sidewalls, both slotted and open lower boundaries, and slotted and closed upper boundaries was carried out in a small wind tunnel. Additional variables investigated include slot width and slot length. A full-span, jet-flap model with an aspect ratio of 4.0 was tested in a large test section to obtain essentially free-air conditions and in a small test section with closed walls as well as slotted walls to obtain a measure of the effectiveness of the slotted-wall configurations in reducing the wall effects. The model was also fitted with a horizontal tail to obtain a measure of the wall effects and the effectiveness of the slotted walls in reducing these wall effects at the tail.

The results of the investigation indicated that the use of test-section configurations with three and four slotted walls resulted in large reductions in the wall-interference effects.

17. Key Words (Suggested by Author(s))	18. Distribution Statement
Slotted tunnel walls Wall interference Wind-tunnel corrections V/STOL	Unclassified – Unlimited

19. Security Classif. (of this report)	20. Security Classif. (of this page)	21. No. of Pages	22. Price*
Unclassified	Unclassified	72	$3.00

*For sale by the National Technical Information Service, Springfield, Virginia 22151

EXPERIMENTAL INVESTIGATION OF THE USE OF SLOTTED TEST-SECTION WALLS TO REDUCE WALL INTERFERENCE FOR HIGH-LIFT-MODEL TESTING

By Kalman J. Grunwald
Langley Research Center

SUMMARY

An investigation of various test-section configurations with slotted sidewalls, both slotted and open lower boundaries, and slotted and closed upper boundaries was carried out in a small wind tunnel. Additional variables investigated include slot width and slot length. A full-span, jet-flap model with an aspect ratio of 4.0 was tested in a large test section to obtain essentially free-air conditions and in a small test section with closed walls as well as slotted walls to obtain a measure of the effectiveness of the slotted-wall configurations in reducing the wall effects. The model was also fitted with a horizontal tail to obtain a measure of the wall effects, and the effectiveness of the slotted walls in reducing these wall effects at the tail.

The results of the investigation indicated that the use of test-section configurations with three and four slotted walls resulted in large reductions in the wall-interference effects.

INTRODUCTION

The wind-tunnel testing of V/STOL and STOL models accentuates the wall-induced interference problems common to all wind-tunnel tests of aircraft models. Increases in the magnitude of the wall effects arise from the large wake-deflection angles and associated high-lift coefficients encountered in V/STOL and STOL model tests.

Three approaches can be taken to obtain free-air data from wind-tunnel tests. The wall effects can be minimized by (1) using a sufficiently small ratio of model to tunnel size, (2) using special test-section configurations, or (3) correcting the wind-tunnel data for the effects of the test-section walls (refs. 1 to 8). Using small models is undesirable because of the low Reynolds number and impractical because of the difficulty of providing the model power. Using very large tunnels presents another alternative; however, such facilities are few and of limited availability.

An approach to the second alternative, the development of special test-section configurations to minimize wall effects, was proposed in reference 9 in which the use of slotted sidewalls and an open lower boundary in a deep narrow tunnel was suggested for this purpose. Reference 9 explored this possibility theoretically but pointed out that certain practical problems, such as viscous effects of flow through the slots, made experimental development of such a test section necessary.

The third alternative, the use of wall corrections, is the only practical approach presently available. The classical theory (for example, ref. 1) for unpowered models has been extended to V/STOL models in references 2 and 3, which take into account the deflection of the wake trailing from the model. Several investigations (refs. 3 to 6) have shown that this theory can adequately correct the test data from a fairly wide variety of models for reasonable ratios of model size to tunnel size.

The present test was undertaken to investigate wall-interference effects when test-section configurations with slotted and open walls were used. A full-span, jet-flap model was used to represent the class of V/STOL models which distribute their lift over the span. This model was tested in a large test section to obtain near-free-air data and in the research test section with closed walls as well as various configurations of slotted walls to obtain a measure of the effectiveness of the slotted-wall configurations in reducing wall effects. The test-section variables included slot width and length, slots in two, three, and four walls, as well as an open floor as proposed in reference 9.

SYMBOLS

A schematic presentation of the positive sense of forces, moments, and angles with respect to the model is presented in figure 1. Values are given in both SI and U.S. Customary Units. The measurements and calculations were made in U.S. Customary Units.

A_m model momentum area, $\frac{\pi b^2}{4}$, m^2 (ft^2)

A_T tunnel cross-sectional area, m^2 (ft^2)

b model wing span, meters (feet)

B tunnel width, meters (feet)

C_D drag coefficient, $\frac{D}{qS}$

C_L	lift coefficient, $\frac{L}{qS}$
$C_{N,T}$	tail-normal-force coefficient, $\frac{N_{tail}}{qS}$
C_μ	jet-momentum coefficient, $\frac{T_{static}}{qS}$
D	drag, newtons (pounds)
H	tunnel height, meters (feet)
i_t	tail incidence, degrees
L	lift, newtons (pounds)
l_c	ceiling-slot length, meters (feet)
l_d	tunnel test-section length, meters (feet)
l_f	floor-slot length, meters (feet)
l_R	distance from the entrance of the test section to the rear of reentry lip, meters (feet)
l_s	sidewall-slot length, meters (feet)
N_{tail}	tail normal force, newtons (pounds)
q	dynamic pressure, $\frac{1}{2}\rho V_\infty^2$, N/m^2 (lb/ft^2)
S	wing area, 232.3 cm^2 (36 in^2)
w_c	ceiling-slot (width) opening, cm (inches)
w_f	floor-slot opening, cm (inches)
w_s	sidewall-slot opening, cm (inches)
T_{static}	static thrust, newtons (pounds)

V_∞ free-stream velocity, m/sec (ft/sec)

α angle of attack, degrees

α_T tail angle of attack, degrees

ρ density, kg/m^3 (slugs/ft^3)

JET-FLAP MODEL

The jet-flap model (figs. 2, 3, and 4) was of relatively simple design and consisted of a wing, fuselage, and horizontal tail. The wing had an aspect ratio of 4 (figs. 3 and 4), employed a modified NACA 4415 airfoil section, and was 30.5 cm (12 inches) in span. High-pressure air was piped through the fuselage to the wing center section (fig. 3), then distributed across the span, and ejected from rectangularly shaped nozzles at 90° to the chord plane at the trailing edge. Measurements along the jet span indicated a uniform distribution with no noticeable drop off of airflow as the wing tips or center were approached. The wing was supported independently of the fuselage by a three-component internal strain-gage balance. A 0.32-cm (0.12-inch) transition strip of No. 60 carborundum grains (0.032-cm (0.012-inch) mean-grain diameter) was installed on the wing and tail beginning at the 8-percent chord.

The horizontal tail had an aspect ratio of 4, employed a NACA 0012 airfoil section, and had a span of 17.3 cm (6.8 inches). It was mounted on a two-component internal strain-gage balance and had the capability of being varied in tail incidence from a nominal setting of -10° to +40° in 5° increments. The entire model could be varied in angle of attack from -20° to +20°.

The model fuselage was an extension of the sting support through which the high-pressure air lines and the strain-gage leads were passed. The wing and tail were mounted separately from the fuselage; and therefore, the wing and tail forces and moments were measured in the presence of the fuselage but no fuselage force measurements were obtained. The fuselage also had a 0.32-cm (0.12-inch) transition strip of No. 60 carborundum grains approximately 2.54 cm (1 inch) behind the nose.

TEST PROCEDURE AND ACCURACY

The tests were run through a range of C_μ values to cover conditions from near-hovering to conventional flight. The C_μ value is an indication of the speed range. At low values, the flight is more nearly conventional; as C_μ is increased, powered lift becomes predominant and hovering flight is approached. The thrusts used to determine

the appropriate values of C_μ were based on a static calibration. A typical run in the tunnel consisted of varying model angle of attack through a range of -15^o to $+20^o$ in 1^o increments. For each of these runs, the value of C_μ was fixed. The tail-incidence i_t settings were selected so that at each C_μ a zero value of tail-normal-force coefficient $C_{N,T}$ could be achieved.

In an effort to obtain consistency, support equipment, sting, air line, and fairing were kept identical when the model was moved from one tunnel to another. However, no matter how much effort was put into maintaining consistency, anomalous discrepancies in the data did occur.

One of these discrepancies occurred when data from the closed model tunnel were compared with data from the Langley 300-MPH 7- by 10-foot tunnel (near-free-air condition). Initially, it was anticipated that the power-off data (near zero angle of attack, zero wing lift, and zero tail normal force) for the model in the closed model tunnel could be shifted to fall directly in line with the data from the 7- by 10-foot tunnel. By this method, a constant angle correction could be applied to the remainder of the closed-model-tunnel data. This technique would eliminate the necessity for running flow-angularity tests in each facility. However, when this technique was applied and the wing lifts were set the same, the tail normal force did not correspond (approximately a 1^o offset). A compromise adjustment was made to all the model tunnel data of $1/2^o$ in order to bring the zero C_μ data more closely in line with the near-free-air data from the 7- by 10-foot tunnel.

In wind-tunnel tests of this type, it is difficult to quote accuracy limits because the electrical measuring and recording equipment are at least an order of magnitude more accurate than the actual scatter in the data. The difficulty in holding test conditions precisely and nonmeasurable fluctuations (from the average values) in tunnel dynamic pressures introduce errors. In order to reduce the magnitude of the fluctuations in the data, each α point presented in the text is the average of 10 measured values over a 10-second time interval. The best measure of data accuracy, therefore, comes from data repeatability and data scatter. Repeat runs, which are shown only for near-free-air data from the 7- by 10-foot tunnel, of almost all the data tested within this paper were made. The tests in the 7- by 10-foot tunnel were run on three separate occasions; all the test data are presented and the data scatter is indicated. From the results of these tests and the scatter observed in any one curve, the measure of accuracy can be determined. For data where repeat runs are not presented, the accuracy level is the same order as those runs where it is presented.

MODEL TUNNEL

An open-circuit model tunnel was constructed and installed in a large room for the present investigation. A three-view drawing of the tunnel is presented in figure 5.

In an effort to provide good-quality flow, both a honeycomb and a screen were placed in the tunnel entrance. The honeycomb was 20.3 cm (8 inches) deep and consisted of 1.9-cm (3/4-inch) hexagonal elements with 0.008-cm (0.003-inch) wall thickness. The screen was ordinary 5.5- by 7-per-cm (14- by 18-per-inch) mesh window screen. A 6-to-1 contraction ratio was provided from the tunnel entrance to the test section. The effective length and wall configuration of the test section could be varied. The fixed-pitch drive fan was driven by an electric motor through a variable-frequency model-motor power supply.

A remote-control angle-of-attack system was provided. For all the tests, the model was mounted in the inverted position to simplify model and test-section-configuration changes.

TEST SECTIONS

The rectangular 3.05-meter-long (10-foot) test section of the model tunnel was 57.1 cm (22.5 inches) wide by 82.0 cm (32.25 inches) high. (See fig. 6.) Divergence of 2.54 cm per 3.05 m (1 inch per 10 feet), which was approximately $1/2^{\circ}$, was built into the floor and ceiling of the test section to compensate for boundary-layer growth.

The test section was designed to allow for sidewall slotting and for ceiling and floor replacement. (See figs. 7 and 8.) The sidewalls were built with four slots having beveled edges. (See fig. 7.) These slots could be closed or opened to any position up to 2.5 percent of the sidewall height per slot or a maximum of 10-percent opening per wall. Simple wood fillers were used to achieve any desired slot lengths. The tunnel floor and ceiling, whose orientation is taken with respect to the model, could be removed or replaced with slotted walls containing six 1.3-cm-wide (0.5-inch) unbeveled slots. These walls would have approximately 13 percent opening per wall.

The tunnel-test-section configurations in which the jet-flap model was tested have been separated into four general categories for convenience of discussion. A tabular listing of these tunnel configurations and relative dimensions are presented in table I.

The first test section employed was the Langley 300-MPH 7- by 10-foot tunnel, which was used to provide the near-free-air data as a basis of comparison $\left(\text{where } A_m/A_T = 0.01\right)$. Although not completely correction free, the 7- by 10-foot tunnel does closely represent the free-air condition. A sketch of the model wing indicating its

TABLE I.- DETAILED DESCRIPTION OF TUNNEL CONFIGURATIONS

Description of tunnel	A_M/A_T	l_d/H	l_R/H	l_s/H	l_f/H	l_c/H	w_s/H (four slots)	w_f/B (six slots)	w_c/B (six slots)
7' × 10' tunnel (near free air)	0.01	1.50	------	-------	-------	-------	-------	--------	-------
Model tunnel:									
Closed-wall test section	0.15	3.72	------	-------	-------	-------	-------	--------	-------
Slotted-wall test section:									
Floor slotted only	0.15	3.72		No slots	1.48	No slots	No slots	0.13	No slots
Sidewalls slotted only	0.15	3.72	No	1.86	No slots	No slots	0.10	No slots	No slots
Sidewalls, floor slotted	0.15	3.72	reentry	1.86	1.48	No slots	0.10	0.13	No slots
Sidewalls, floor, ceiling slotted	0.15	3.72	lip	1.86	1.48	1.48	0.10	0.13	0.13
Sidewalls, ceiling slotted	0.15	3.72		1.86	No slots	1.48	0.10	No slots	0.13
Sidewalls, floor, ceiling slotted	0.15	3.72		0.93	1.48	1.48	0.10	0.13	0.13
Screened-floor, slotted sidewall test section:									
Screened floor, sidewalls slotted	0.15	3.72	1.86	1.86	1.08		0.10		
Screened floor, sidewalls slotted	0.15	3.72	2.80	1.86	2.01	Ceiling	0.10	Floor	Ceiling
Screened floor, sidewalls slotted	0.15	3.72	3.25	1.86	2.48	closed	0.10	screened	closed
Screened floor, sidewalls slotted	0.15	3.72	3.72	3.72	2.95		0.10		
Screened floor, sidewalls slotted	0.15	3.72	2.80	1.86	2.02		0.05		

orientation in the tunnel and also its relative size to the 7- by 10-foot tunnel can be seen in figure 6. A photograph of the model in the 7- by 10-foot tunnel can be seen in figure 4.

The second test section used was the 57.2- by 81.9-cm (22.50- by 32.25-inch) model tunnel employing the closed-wall configuration. A sketch of the test-section cross section showing model orientation and relative model size to tunnel size is also shown in figure 6 $\left(\text{where } A_m/A_T = 0.15\right)$.

The third test section (see fig. 7) includes the configurations in which the walls were slotted or a combination of slotted and closed. The slotted-wall configurations include (1) floor slotted, (2) sidewalls slotted, (3) floor and sidewalls slotted, (4) all four walls slotted, (5) ceiling and sidewalls slotted, (6) all four walls slotted, however, shorter length sidewall slots than in the other configuration with four walls slotted. A more detailed description of each of the tunnel-wall configurations is presented in table I.

The fourth test section (see fig. 8) includes configurations having a screened floor, which was intended to represent an open boundary, four equally wide slots in each sidewall totaling 10 percent of each sidewall area, and a closed ceiling. All tests in this test section required a relatively large three-sided reentry lip at the rear of the open floor (fig. 9) and a 5.5- by 7-per-cm (14- by 18-per-inch) mesh screen over the open floor (fig. 10), the primary purpose of which was to eliminate excessive tunnel pulsations. Different test-section lengths were used during the tests and are as follows: 89 cm

(35 inches), 165 cm (65 inches), 203 cm (80 inches), and 241 cm (95 inches). One series of tests was also run with 5-percent opening in each sidewall for the 165-cm-long (65-inch) test section.

PRESENTATION OF RESULTS

Three separate series of tests of the model in the 7- by 10-foot tunnel were made and corrected for wall interference using the interference factors of references 7 and 8 and effective skew angle as determined in reference 3. These corrected data are presented in figure 11 and also on all other data figures 12 to 18 as a base point for comparison with other tunnel configurations. A listing of the data figures is included below:

Tunnel configuration	A_m/A_T	Figure
7- by 10-foot	0.01	11
Model tunnel:		
Closed	0.15	12
Open floor, slotted sidewalls	0.15	13 to 15
Slotted walls	0.15	16 to 18

DISCUSSION

Closed Test Section

Wall interference on lift and drag.- In order to evaluate the effect of wall slotting, it was first necessary to establish two basic conditions. The first, the free-air condition, which represents the goal that wall slotting and wall corrections attempt to achieve, was determined from tests of the jet-flap model in the 7- by 10-foot tunnel. (See figs. 11 to 18.) The second, the closed-wall condition, which represents the condition of maximum constraint, was determined from tests in the closed model tunnel. The aforementioned conditions would not be complete without applying wall corrections to the closed-tunnel data. (Wall-interference corrections for the 7- by 10-foot tunnel amounted to approximately $1/2^{\circ}$ at the highest C_μ values.) These corrections were applied by use of the general techniques presented in references 7 and 8 with effective skew angle computed as in reference 3. The small differences in C_μ resulting from the horizontal interference velocities have been removed from the lift data by finding dC_L/dC_μ from closely spaced test runs in the 7- by 10-foot tunnel and then subtracting an amount equal to $\left(dC_L/dC_\mu\right)\Delta C_\mu$ from the lift coefficient. For tail normal force, the behavior of $dC_{N,T}/dC_\mu$ was very erratic with respect to both C_μ and α; consequently, no similar correction has been applied to the tail-normal-force data. The actual changes

in C_μ as a result of the horizontal interference were small for this model. The basic data and these data corrected for wall interference for the closed model tunnel are presented in figure 12.

An example of the effectiveness of the closed-tunnel correction can be seen in figure 12(c) at $C_\mu = 1.5$. For this condition with corrections applied to the closed-model-tunnel data and compared with the near-free-air data, the stall angle is matched.

The test data (lift, drag, and tail-normal-force coefficients) are presented as a function of α or α_T in figure 12 for a momentum-coefficient range from $C_\mu = 0$ (no blowing) to $C_\mu = 10.0$ (high blowing). The expected wall-induced upwash, which increases the angle of attack at the model, is apparent in the data for the closed model tunnel. Wall recirculation effects limited the range of data to which usable corrections could be applied. Recirculation of the flow leaving the powered model caused flow breakdown in the tunnel. This flow impinged on the floor, spread, flowed up the sidewalls, and met at the ceiling, where it separated. This phenomenon is discussed in detail in references 10, 11, 12, and 13. The wake-deflection angle (based on momentum considerations) beyond which flow disturbances can occur is computed to be 43°. (See ref. 11.) This angle is obtained at $\alpha \approx 5^\circ$ for $C_\mu = 5.0$. (See fig. 12(e).) At this angle of attack and above, the wing and resulting data are affected by recirculation.

Wall interference on tail normal force.- In order to isolate the wall interference at the tail region, a separate strain-gage balance was used to support the tail and thereby measure tail normal force. The test conditions under which the tail-normal-force data were measured correspond to those for the wing forces. In figure 12, data from the 7- by 10-foot tunnel are compared with data from the closed model tunnel at various tail-incidence angles. Wall corrections have also been applied to the tail-normal-force data from the closed model tunnel and are presented in figure 12.

Because of the low normal-force coefficient at which the tail is operating and its small size with respect to the test section, the wall effects due to the tail itself at both wing and tail locations can be assumed to be small when compared with the wall effects due to the wing. Therefore, any tail-normal-force differences between the data obtained in the small tunnel and the near-free-air data obtained in the 7- by 10-foot tunnel may be attributed to wall effects arising from the wing. A longitudinal wall-interference gradient in the tunnel may also contribute to these differences.

The uncorrected closed-tunnel tail data of figure 12 show large displacements and slope changes of a type similar to that experienced at the wing. These effects are obviously induced by wall interference, and application of wall corrections does reduce this interference effect at the lower C_μ values (C_μ from 0 to 3.0). However, the corrected data, at the higher C_μ's of 5 and 10, do not result in good correlation with

free-air data as would be expected, since the flow throughout the test section was affected by recirculation.

Rather large unexpected displacements with near-zero wing lift and near-zero tail normal force at small negative angles of attack occurred in the tail-normal-force data at $C_\mu = 0$. (See fig. 12(a).) Tests were repeated for these conditions in both the near-free-air and the closed-model-tunnel conditions with the same results as the data presented. A satisfactory explanation of this result is not available; however, this discrepancy cannot be caused by wall interference because of the low lifts involved.

Open-Floor (Screened) and Slotted-Sidewall Test Section

One of the tunnel configurations employed during the tests had an open floor and slotted sidewalls. This configuration was conceived by the author of reference 9. The screened-floor boundary which was used for the "open floor" tests was found to be necessary to eliminate undesirable tunnel airflow pulsations and was not believed to violate the assumption of the open floor. The uncorrected lift, drag, and tail-normal-force coefficients of the jet-flap model for various configurations of the open-floor test sections are presented in figures 13 and 14. Figure 13 shows the effect of test-section length with 10-percent slotted sidewalls, and figure 14 compares the data for 5-percent and 10-percent slotted sidewalls. Wall corrections based on reference 9 were applied to the data for the 5-percent slotted-sidewall configuration of figure 14, and the results are presented in figure 15. A complete description of each of the wall configurations is presented in table I.

Wall interference on lift, drag, and tail-normal-force coefficients.- As can be seen from the data presented in figure 13, the configuration with open floor and slotted sidewalls of 10-percent slot opening appears to give force-data results independent of tunnel slot length or open-floor length. Of even greater significance is the good correlation of the wing-lift data using these test-section configurations with the free-air data and the fair correlation of the tail data. The model drag-coefficient data of figure 13 also show only negligible effects of tunnel-wall constraint.

Effect of sidewall-slot percent opening.- Tests were also conducted to determine the effect of percent sidewall-slot opening with the open-floor configuration. The lift, drag, and tail-normal-force coefficients for 5- and 10-percent slot openings are compared in figure 14. The data for 5-percent slot opening are more nearly correction free throughout the range tested. This trend is particularly evident at the tail region. The drag-coefficient data of figure 14 again indicate only negligible wall-interference effects.

Correction of data for the open-floor (screened) and slotted-sidewalls test section.- A major limitation for the use of slotted and open-boundary wind-tunnel test sections is the lack of an adequate wall-interference theory to correct model data taken with these

wall configurations. An analytic approach to establishing a zero tunnel-boundary lift interference on a small powered lift model was undertaken in reference 9. In this reference, zero interference on such a model is determined by using a tunnel with a closed upper wall, screened floor, and slotted sidewalls; however, the theory is regarded as unreliable for predicting the sidewall-slot widths required because of the boundary-layer effects on slots of such small size. Correction factors for a helicopter-type lifting element for the aforementioned configuration test section have been developed within the text of reference 9. The theoretical tunnel conditions analyzed in reference 9 are somewhat different than those tested. Because of an error, as discussed in reference 9, in the initial estimation of the slot opening, a wall slotting as small as that recommended was not tested. However, reference 9 does give numerical results for a tunnel with a sidewall slotting of 4.55 percent per wall and a width-to-height ratio of 1.5. These corrections were applied to the wing and tail data although the tunnel used during the investigation had a slot opening of 5 percent per wall and 1.43 width-to-height ratio.

The screened floor used during the tests caused the powered wake vortex to dissipate. Since the theory assumes the wake terminates at the floor, the screen installation is highly desirable in that it causes the test conditions to approximate more nearly the mathematical model assumed in the analysis.

The interference factors applied to the data were taken from figure 6 of reference 9. The streamwise interference factor $\delta_{R,x}$ and the upwash interference factor $\delta_{R,z}$ have been used for $\alpha = 0^{o}$ and applied to the lift and drag of the wing. The interference factor applied to the tail normal force was determined from an interpolation and an extrapolation of the upwash interference factor $\delta_{R,z}$ at the nondimensionalized station at which interference is computed with respect to the lifting element $\frac{x}{h} = 0.3$ and 0.5. The tail quarter-chord is located at position $\frac{x}{h} = 0.327$ with respect to the wing quarter-chord.

When these corrections are applied to the data of figure 15, a maximum of -2^{o} change in angle of attack and a 2-percent increase in free-stream dynamic pressure are computed.

As can be seen in figure 15, corrections do not significantly alter the comparison of the uncorrected data with the free-air data. Further expansion of the theory to include finite span, tail position, and other factors would be desirable. These results, therefore, point to the need for continued analytic and experimental work of this nature in order to develop wall-correction theory on slotted tunnels at high-lift conditions.

Slotted Test Section

In an attempt to reduce lift-induced wall interference, a number of other slotted test-section configurations were investigated. The slotted-wall configurations include:

(1) floor slotted, (2) sidewalls slotted, (3) floor and sidewalls slotted, (4) all four walls slotted, (5) ceiling and sidewalls slotted, (6) all four walls slotted, however, shorter length sidewall slots than in the other four-wall-slotted configuration. A more detailed description of each of the tunnel-wall configurations is presented in table I.

Wall interference on lift and drag coefficients.- The effect of wall slotting on wing-lift coefficient is evident in figure 16(c) ($C_\mu = 1.5$). By referring to figure 12(c), it can be seen that the data for the floor slotted only corresponds very closely to the uncorrected data for the fully closed model tunnel. As more walls are slotted, the effects of wall constraint are reduced, and in the four-wall-slotted configuration, an overcorrecting tendency can be noted. This general trend is in evidence throughout all the data of figure 16; however, at the higher C_μ's of 5 and 10, the difference between the three-wall-slotted (floor and sidewalls) and the four-wall-slotted condition appears to be negligible. This result may indicate a reduction in sensitivity of the slotted ceiling at the higher lifts. Other factors such as ceiling separation or flow recirculation may be the cause. Further indication that the slotted ceiling is ineffective in reducing wall interference at the high-lift conditions can be found in the data of figure 17. This comparison shows the configuration with the ceiling and sidewall slotted to be less effective in reducing wall interference than those with the floor and sidewall slotted at all powered-lift conditions tested (C_μ = 0.5 to 10.0).

The most notable result of wall slotting is the agreement that has been obtained with free-air data by using either the three- or four-wall-slotted configurations of figure 16. At the wing, the data from these wall configurations correspond closely with the free-air data throughout most of the α range.

By examining figure 12(c) and figure 16(c), which are representative of the data, it can be seen that the lift coefficients for the three- and four-wall-slotted configurations are of the same order of agreement with free-air data as are the data for the closed tunnel corrected for wall interference. It, therefore, follows that this tunnel-slotting technique might be employed with reasonably good results.

The effects of sidewall-slot length are shown in figure 18. The four-wall slotted condition was tested at ratios of slot length to tunnel height of 1.86 and 0.93. The data indicate no effect of changes in length.

The drag-coefficient data for all the slotted-tunnel configurations are presented in figures 16, 17, and 18. As can be seen from the data, wall interference on drag in these slotted tunnels is negligible.

Wall interference on tail normal force.- From the tail-normal-force data of figures 16 and 17, it appears that the three- and four-wall-slotted configurations are also the most desirable in reducing wall interference at the tail region.

Although these configurations are the most desirable and certainly give better results than the closed-tunnel configuration, they do not completely correct the data to the free-air condition.

In conclusion, it may be stated that wall interference at the tail region may be significantly reduced by the use of slotted-wall configurations, but that the complete elimination of these effects was not accomplished with any of the tested configurations. It should be emphasized that the reductions in wall interference indicated in these tests apply to the jet-flap model tested herein in a tunnel of similar length-to-width ratio. A different type of high-lift configuration may show quite different results. For example, models having longer longitudinal extent, such as the tandem rotor or tandem-ducted configurations, could show appreciably larger wall interference on the overall configuration than has been evident in the present investigation. Furthermore the ratio of tunnel height to width is a significant parameter. For deep narrow tunnels of the type tested herein, slotting the sidewalls is highly effective in changing wall interference. On the other hand, in a shallow wide tunnel slotting the floor and ceiling would be more significant.

CONCLUDING REMARKS

The results of the investigation indicate that the wall interference at the wing may be nearly eliminated for high-lift, jet-flap models by the use of a wind-tunnel configuration with three or four walls slotted. Under the same testing conditions, reductions in the wall interference at the tail of the model were also experienced.

A slotted-sidewall, open-floor, closed-ceiling test-section configuration was also employed during tests of the jet-flap model. This configuration also gave near-interference-free results for the wing. However, at the tail, wall effects were still in evidence. This configuration was less desirable overall in reducing the wall interference than were the three- and four-wall-slotted tunnels.

It should also be emphasized that the reductions in wall interference indicated in these tests apply to the jet-flap model tested herein in a tunnel of similar height-to-width ratio. A different type of high-lift configuration may show quite different results. For example, models having longer longitudinal extent, such as the tandem-rotor or tandem-ducted configurations, could show appreciably larger wall interference on the overall configuration than has been evident in the present investigation.

Langley Research Center,
National Aeronautics and Space Administration,
Hampton, Va., May 11, 1971.

REFERENCES

1. Glauert, H.: The Elements of Aerofoil and Airscrew Theory. Second ed., Cambridge Univ. Press, 1947. (Reprinted 1948.)

2. Heyson, Harry H.: Linearized Theory of Wind-Tunnel Jet-Boundary Corrections and Ground Effect for VTOL-STOL Aircraft. NASA TR R-124, 1962.

3. Heyson, Harry H.; and Grunwald, Kalman J.: Wind-Tunnel Boundary Interference for V/STOL Testing. Conference on V/STOL and STOL Aircraft, NASA SP-116, 1966, pp. 409-434.

4. Grunwald, Kalman J.: Experimental Study of Wind-Tunnel-Wall Effects and Wall Corrections for a General-Research V/STOL Tilt-Wing Model With Flap. NASA TN D-2887, 1965.

5. Davenport, Edwin E.; and Kuhn, Richard E.: Wind-Tunnel-Wall Effects and Scale Effects on a VTOL Configuration With a Fan Mounted in the Fuselage. NASA TN D-2560, 1965.

6. Staff of Powered-Lift Aerodynamics Section, NASA Langley Res. Center: Wall Effects and Scale Effects in V/STOL Model Testing. AIAA Aerodynamic Testing Conference, Mar. 1964, pp. 8-16.

7. Heyson, Harry H.: Use of Superposition in Digital Computers to Obtain Wind-Tunnel Interference Factors for Arbitrary Configurations, With Particular Reference to V/STOL Models. NASA TR R-302, 1969.

8. Heyson, Harry H.: Fortran Programs for Calculating Wind-Tunnel Boundary Interference. NASA TM X-1740, 1969.

9. Wright, Ray H.: Research on Design of Test Sections for Small Wind-Tunnel Boundary Interference V/STOL Model. NASA TR R-286, 1968.

10. Rae, William H., Jr.: Limits on Minimum-Speed V/STOL Wind-Tunnel Tests. J. Aircraft, vol. 4, no. 3, May-June 1967, pp. 249-254.

11. Heyson, Harry H.: Wind-Tunnel Wall Effects at Extreme Force Coefficients. Ann. N.Y. Acad. Sci., vol. 154, art. 2, Nov. 22, 1968, pp. 1074-1093.

12. Heyson, Harry H.: Theoretical Study of Conditions Limiting V/STOL Testing in Wind Tunnels With Solid Floor. NASA TN D-5819, 1970.

13. Rae, William H., Jr.; and Shindo, Shojiro: Comments on V/STOL Wind Tunnel Data at Low Forward Speeds. Vol. II of Aerodynamics of Rotary Wing and V/STOL Aircraft, Cornell Aeronaut. Lab., Inc., and U.S. Army Aviat. Mater. Lab., June 1969.

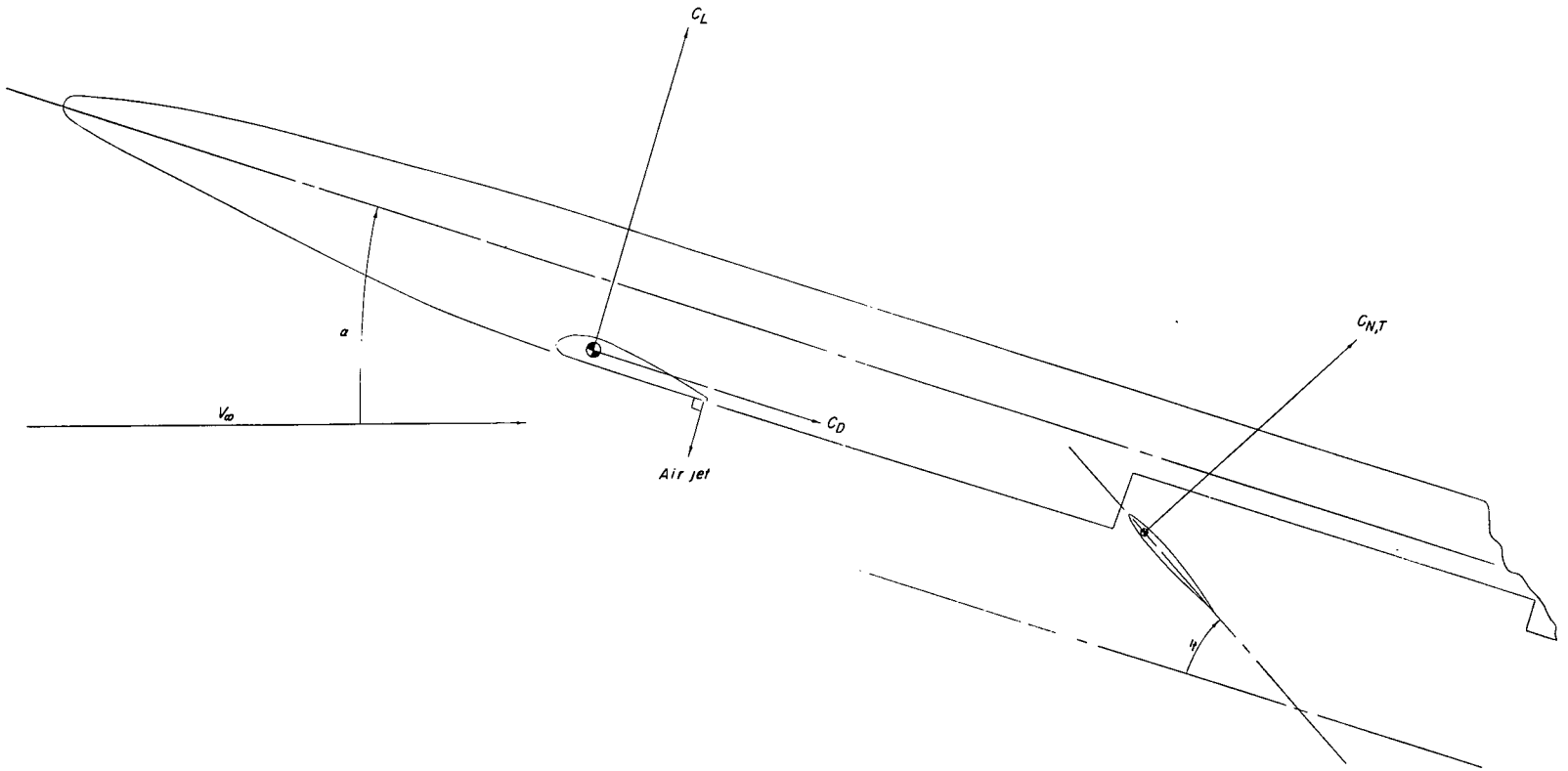

Figure 1.- Positive direction of forces, moments, and angles on model.

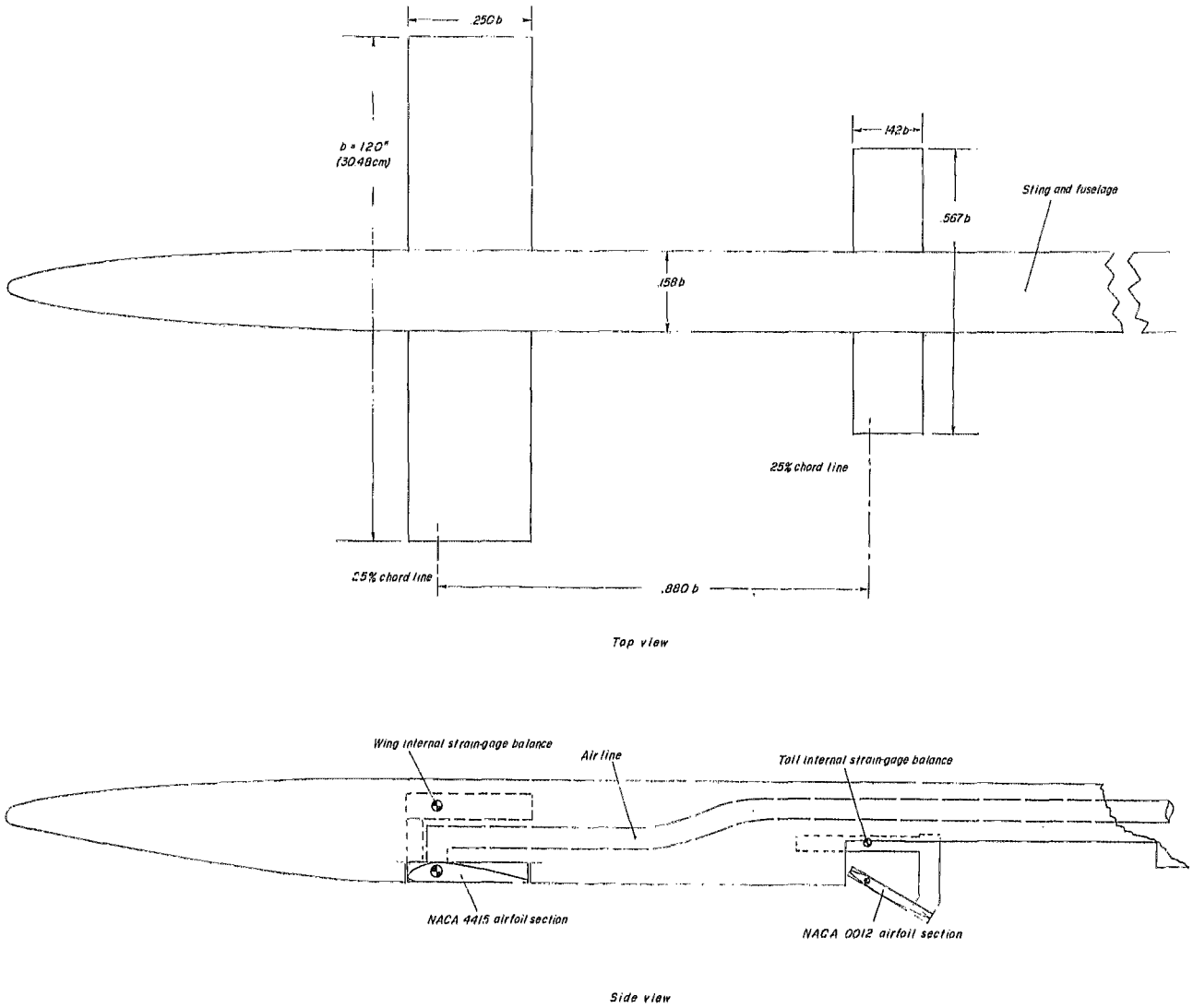

Figure 2.- Drawing of jet-flap model with pertinent dimensions given.

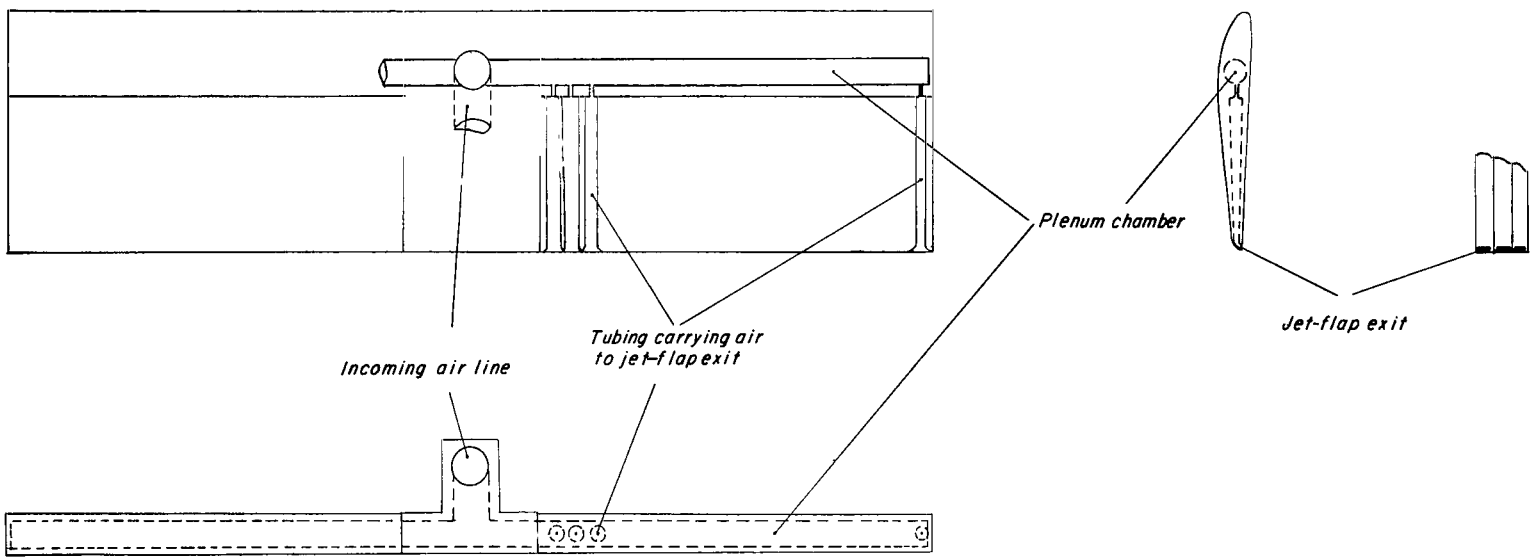

Figure 3.- Drawing of jet-flap wing, indicating the internal detail of air passage to jet-flap exit.

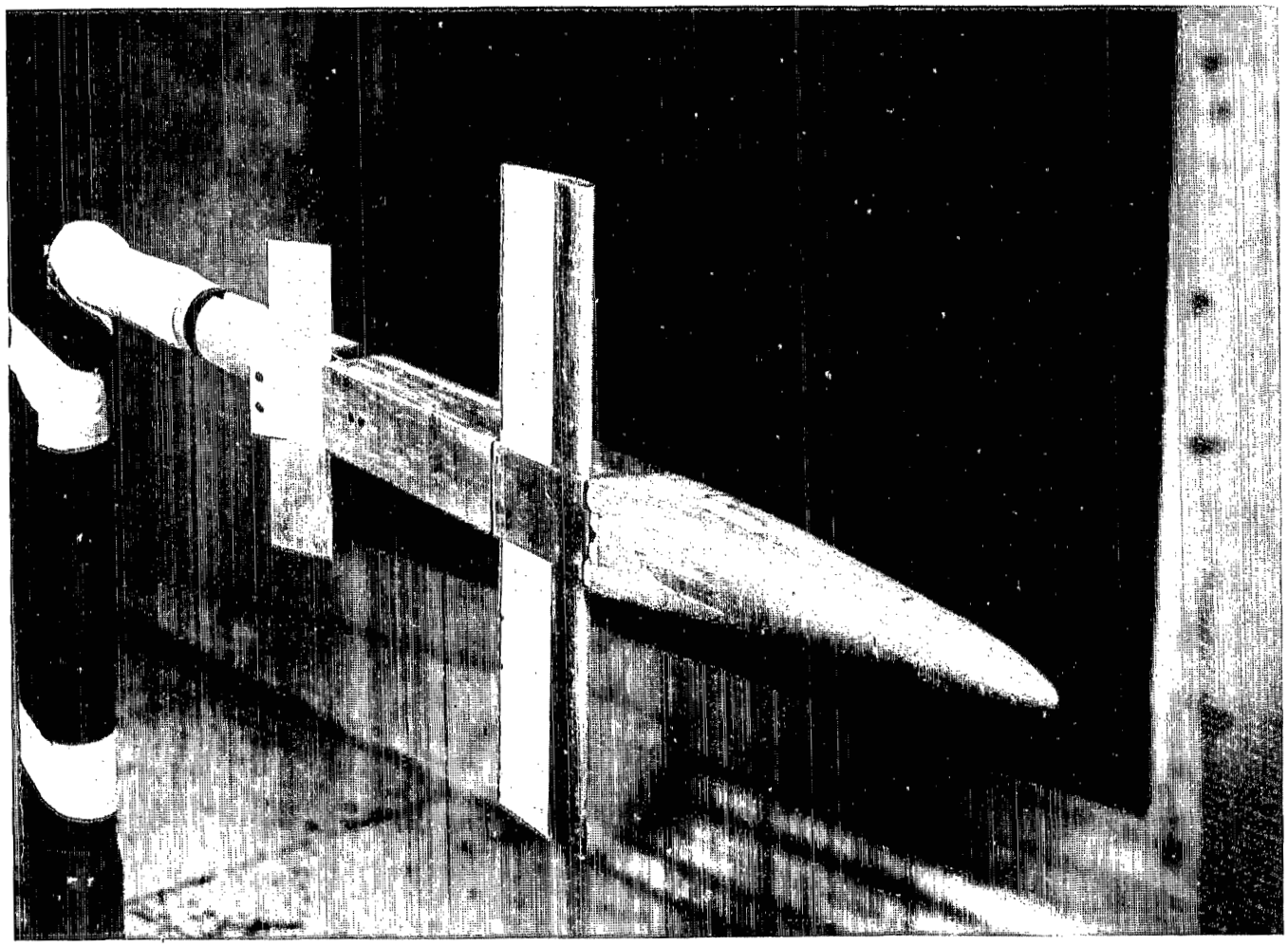

L-66-2977

Figure 4.- Jet-flap model in Langley high-speed 7- by 10-foot tunnel.

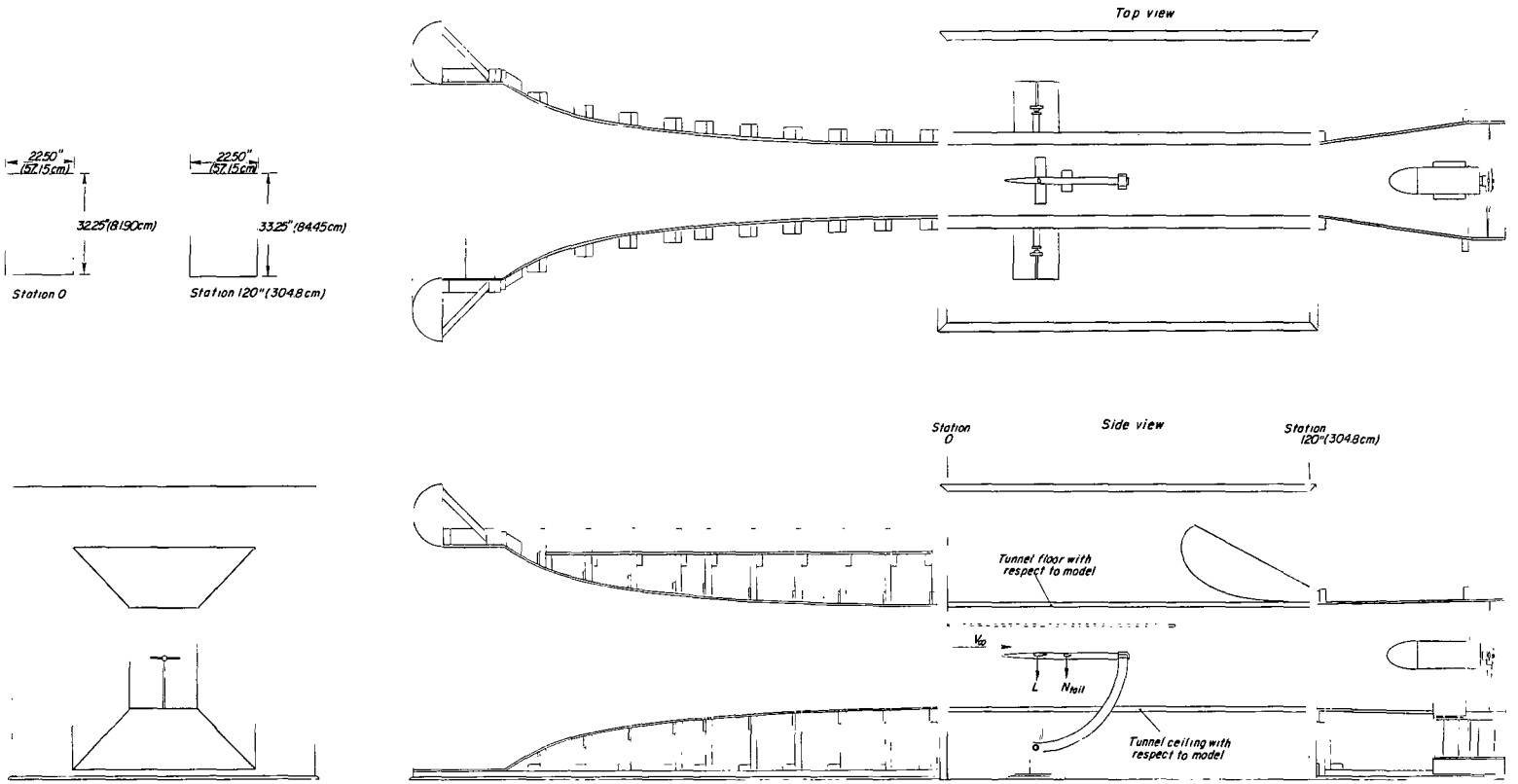

Figure 5.- Three-view drawing of model tunnel, showing tunnel and model orientation.

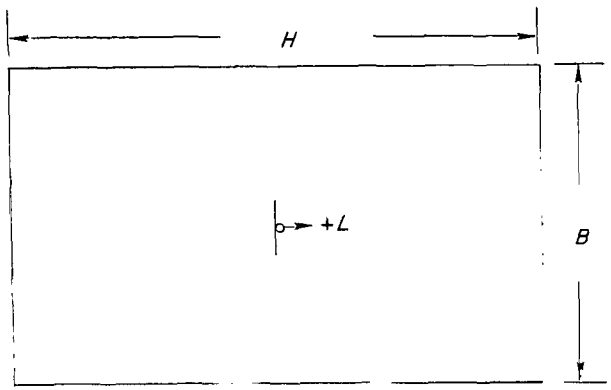

7'x10' closed tunnel
(2.124 m x 3.048m)

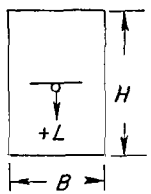

22.5"x 32.25" closed tunnel
(57.1 cm x 82.0cm)

Figure 6.- Relative size and orientation of model to tunnel.

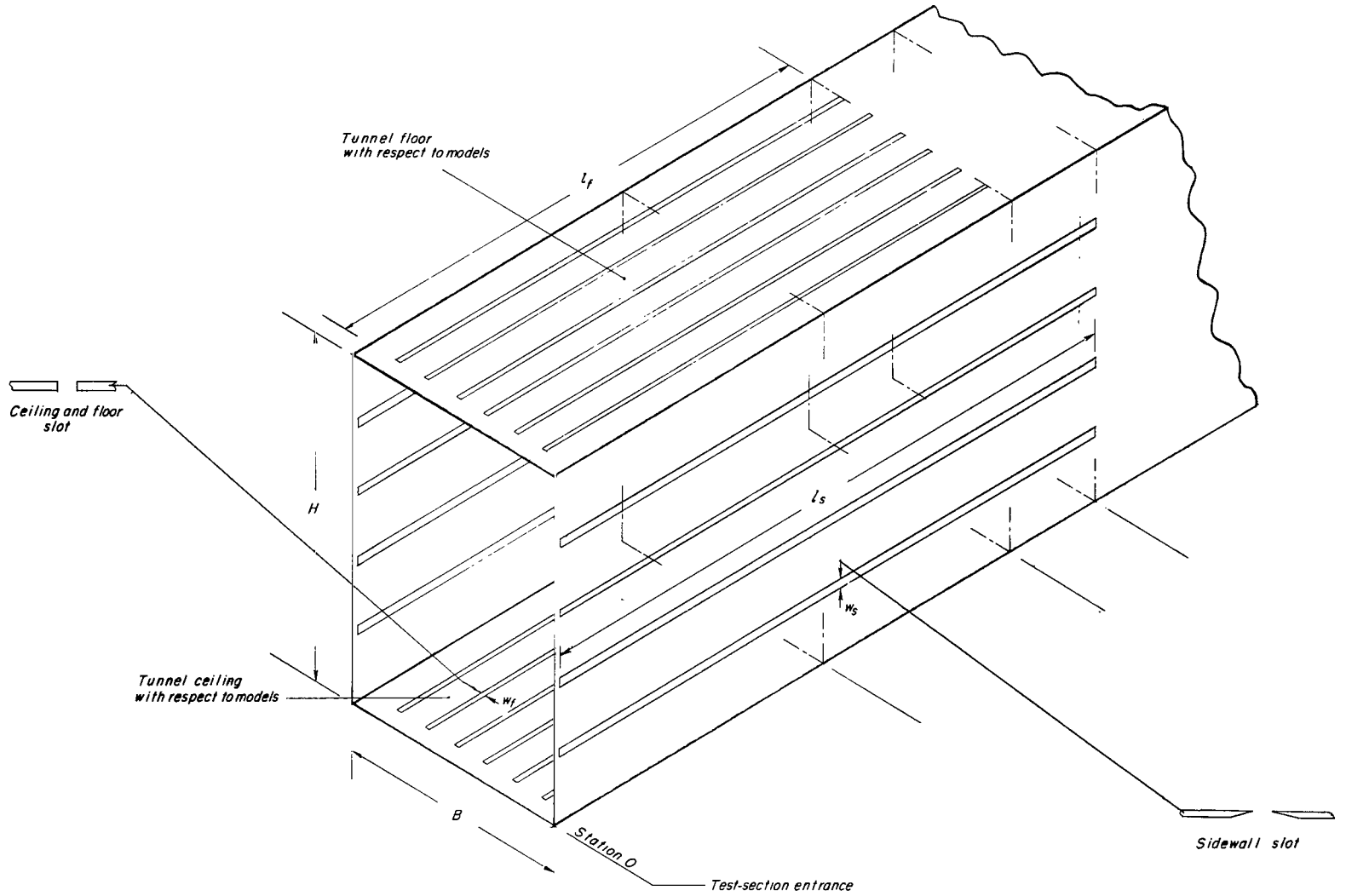

Figure 7.- Drawing of test section for slotted configuration with shape of slots indicated.

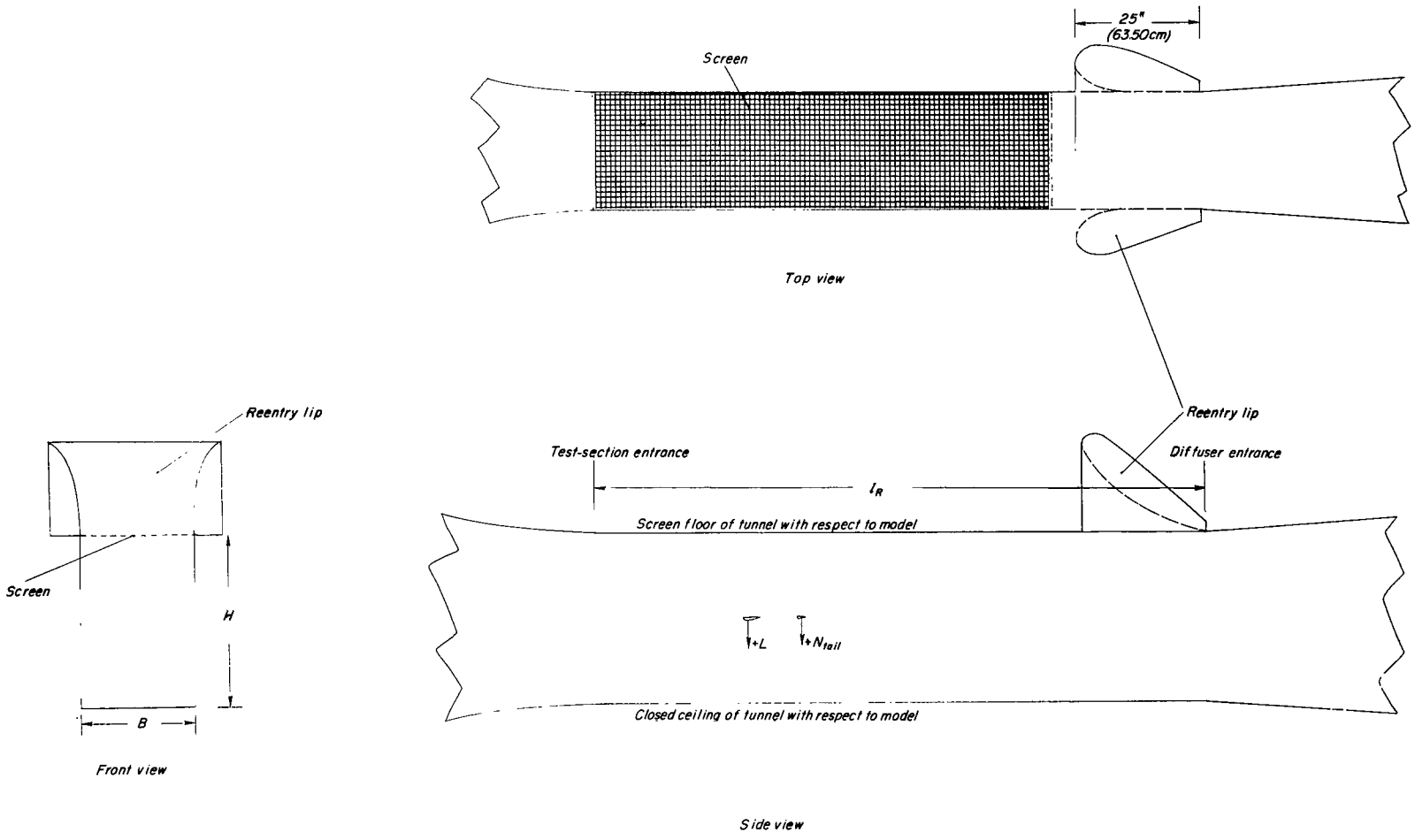

Figure 8.- Three-view drawing of screened-floor and slotted-sidewall configuration.

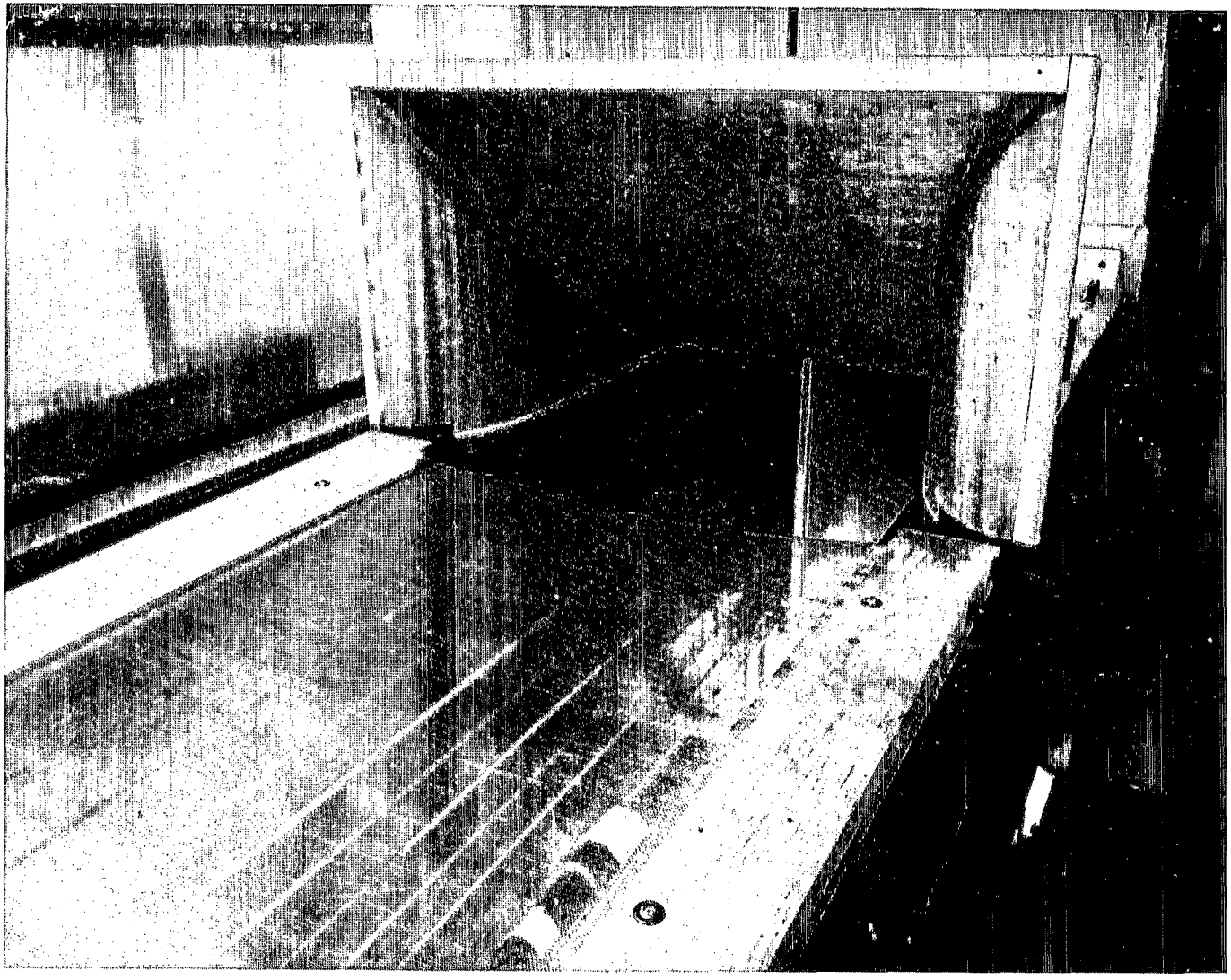

L-65-9398

Figure 9.- Reentry lip used on model tunnel.

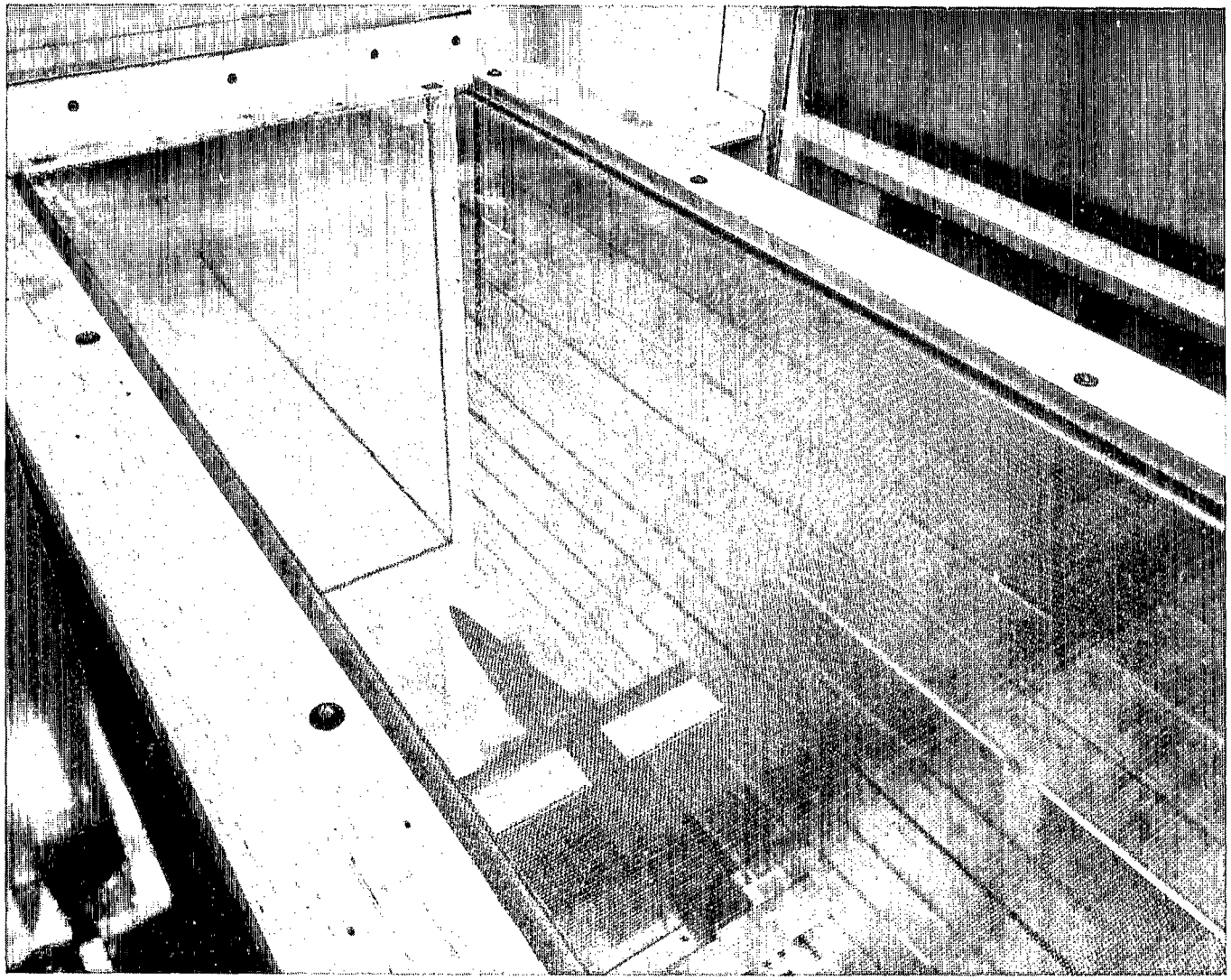

L-65-9401

Figure 10.- Model tunnel showing screen installation.

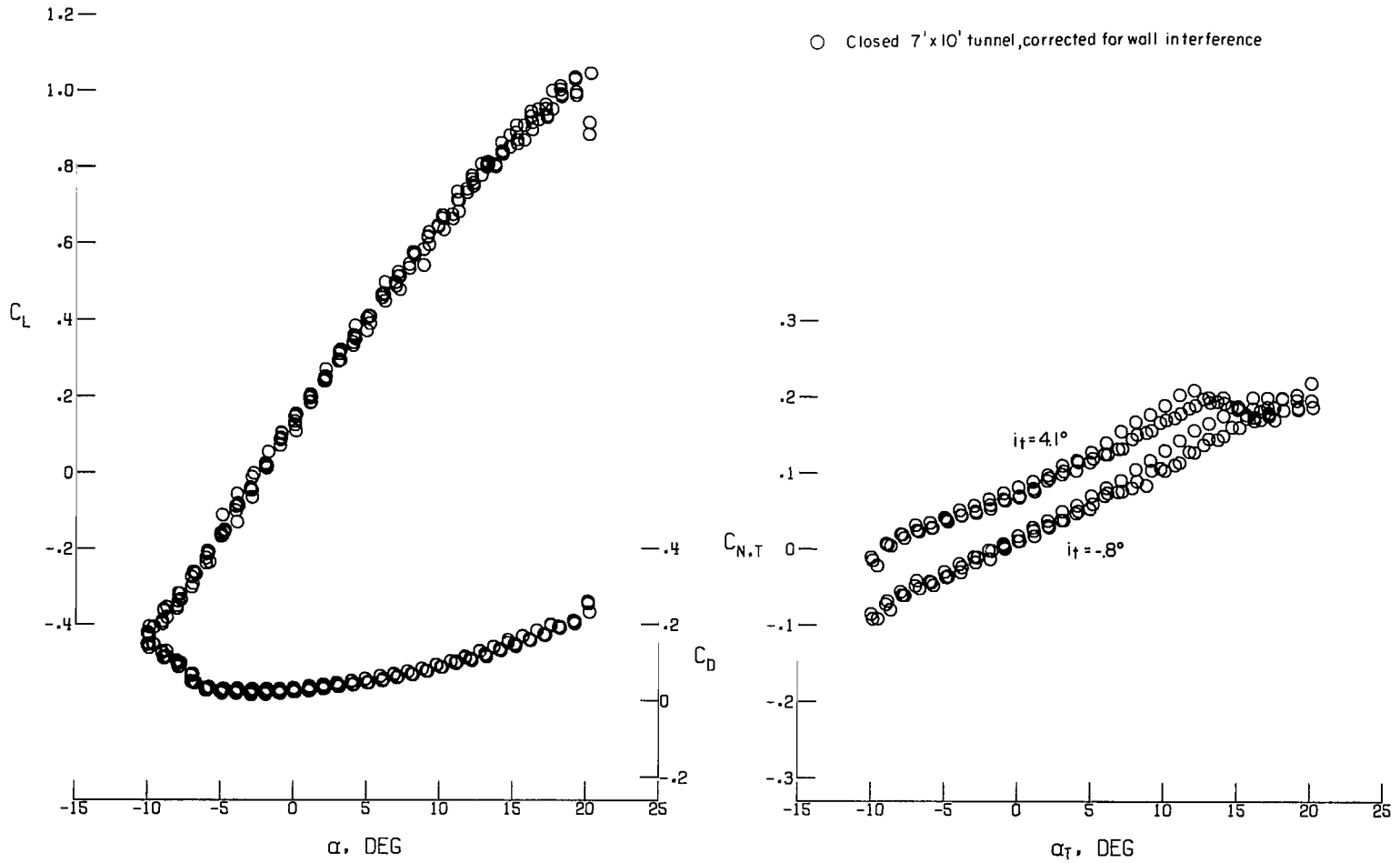

(a) $C_\mu = 0$.

Figure 11.- Lift, drag, and tail-normal-force coefficients on jet-flap model tested on three separate occasions in the 7- by 10-foot tunnel (wall corrections applied).

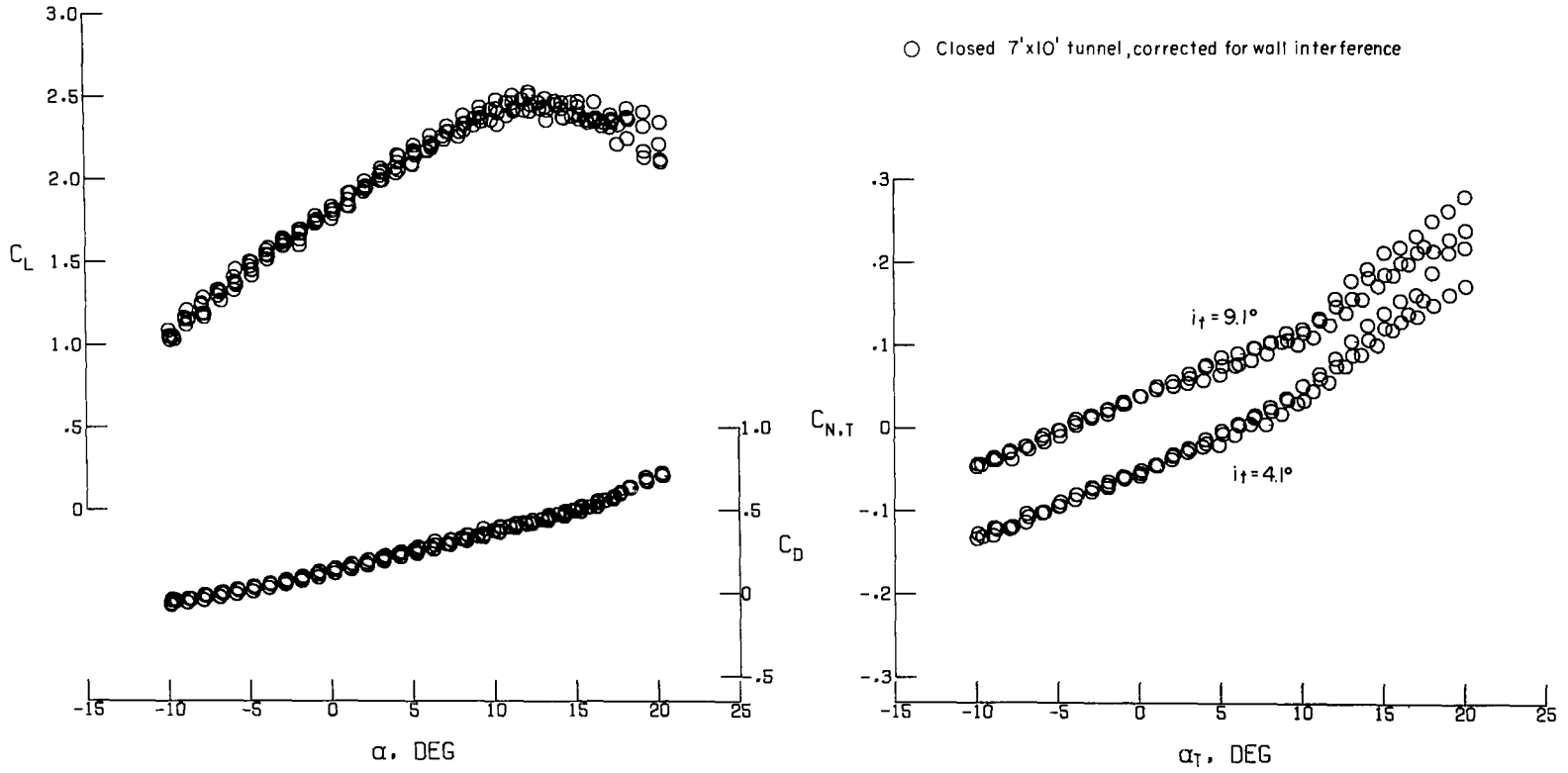

(b) $C_\mu = 0.5$.

Figure 11.- Continued.

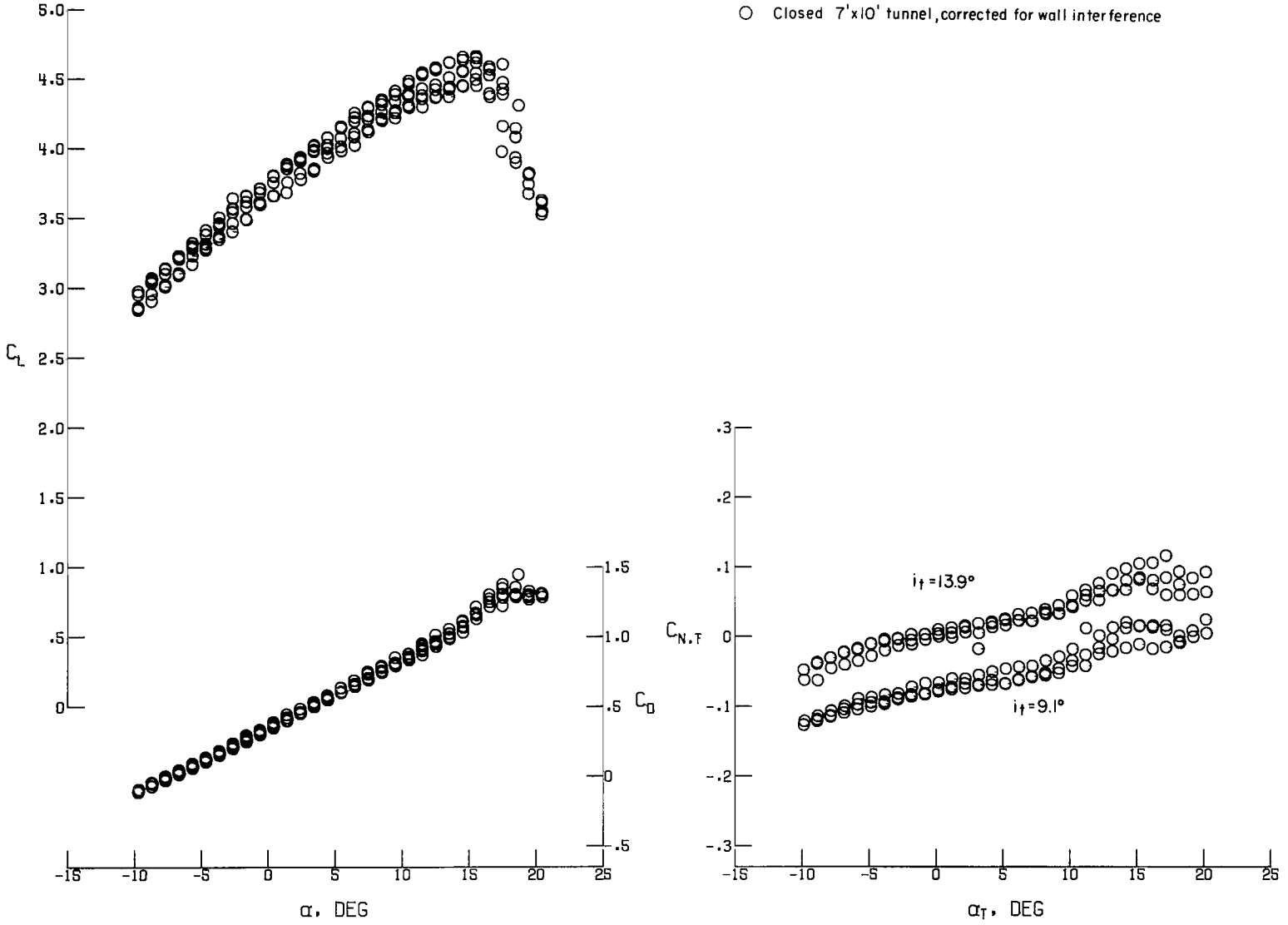

(c) $C_\mu = 1.5$.

Figure 11.- Continued.

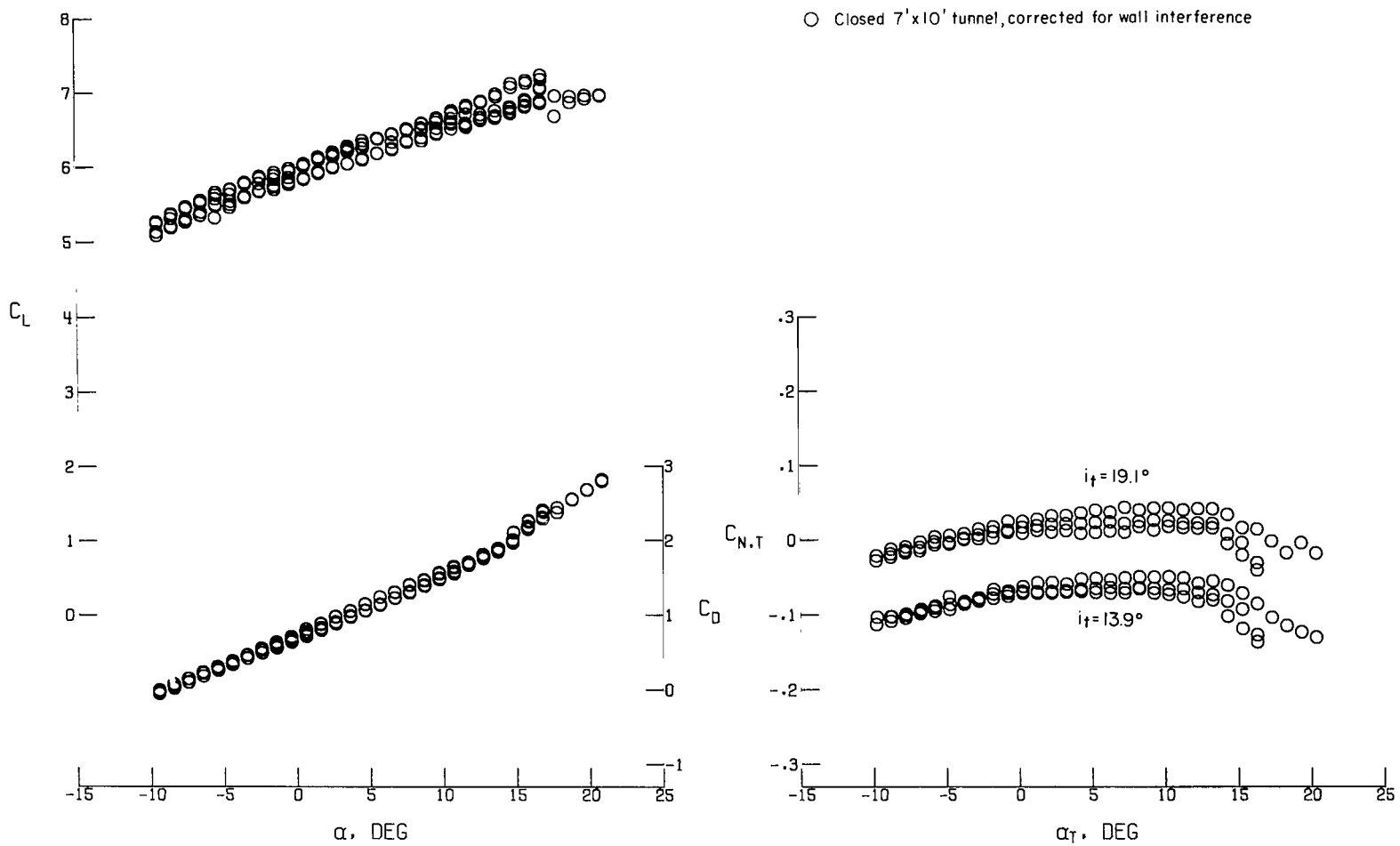

(d) C_μ = 3.0.

Figure 11.- Continued.

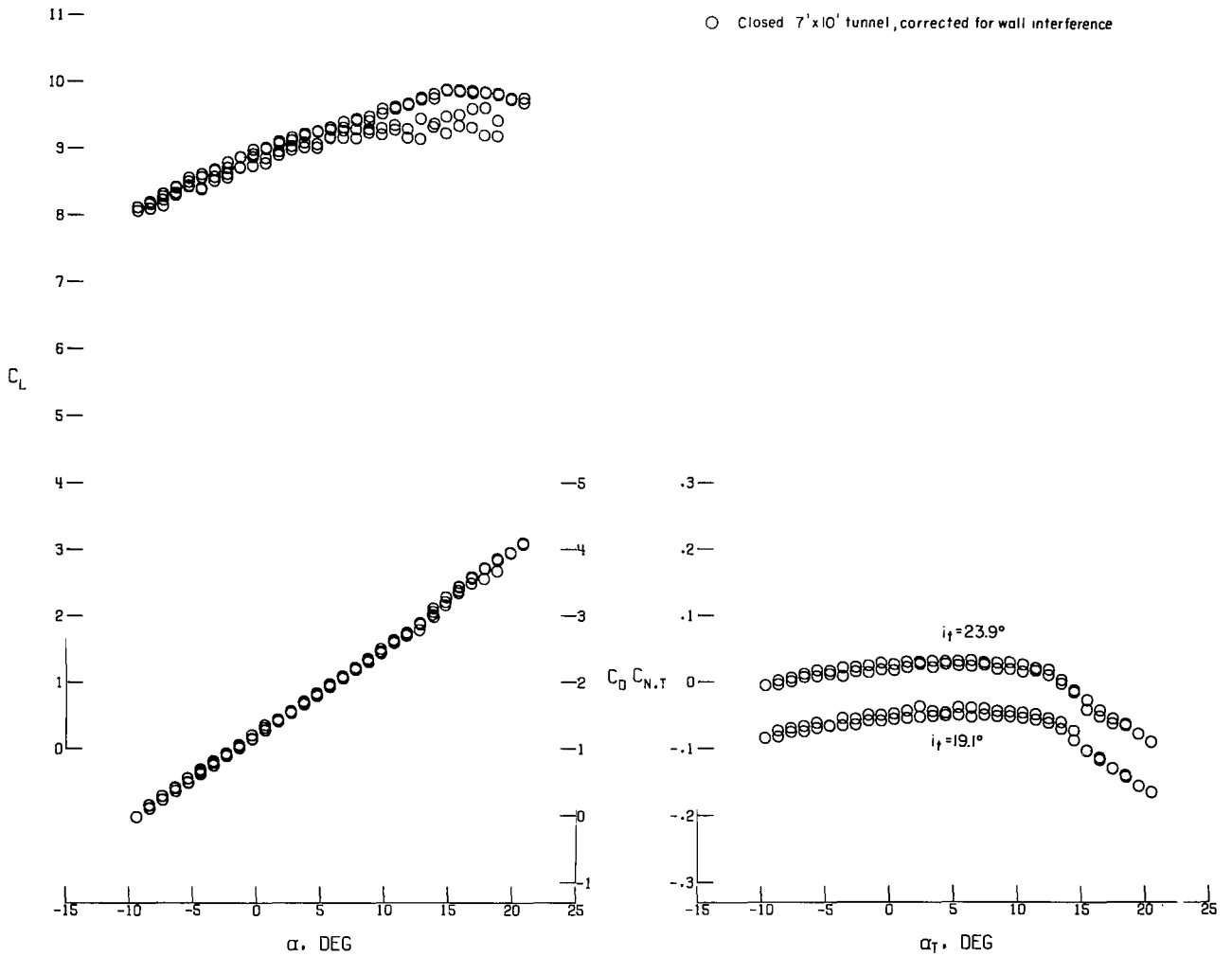

(e) C_μ = 5.0.

Figure 11.- Continued.

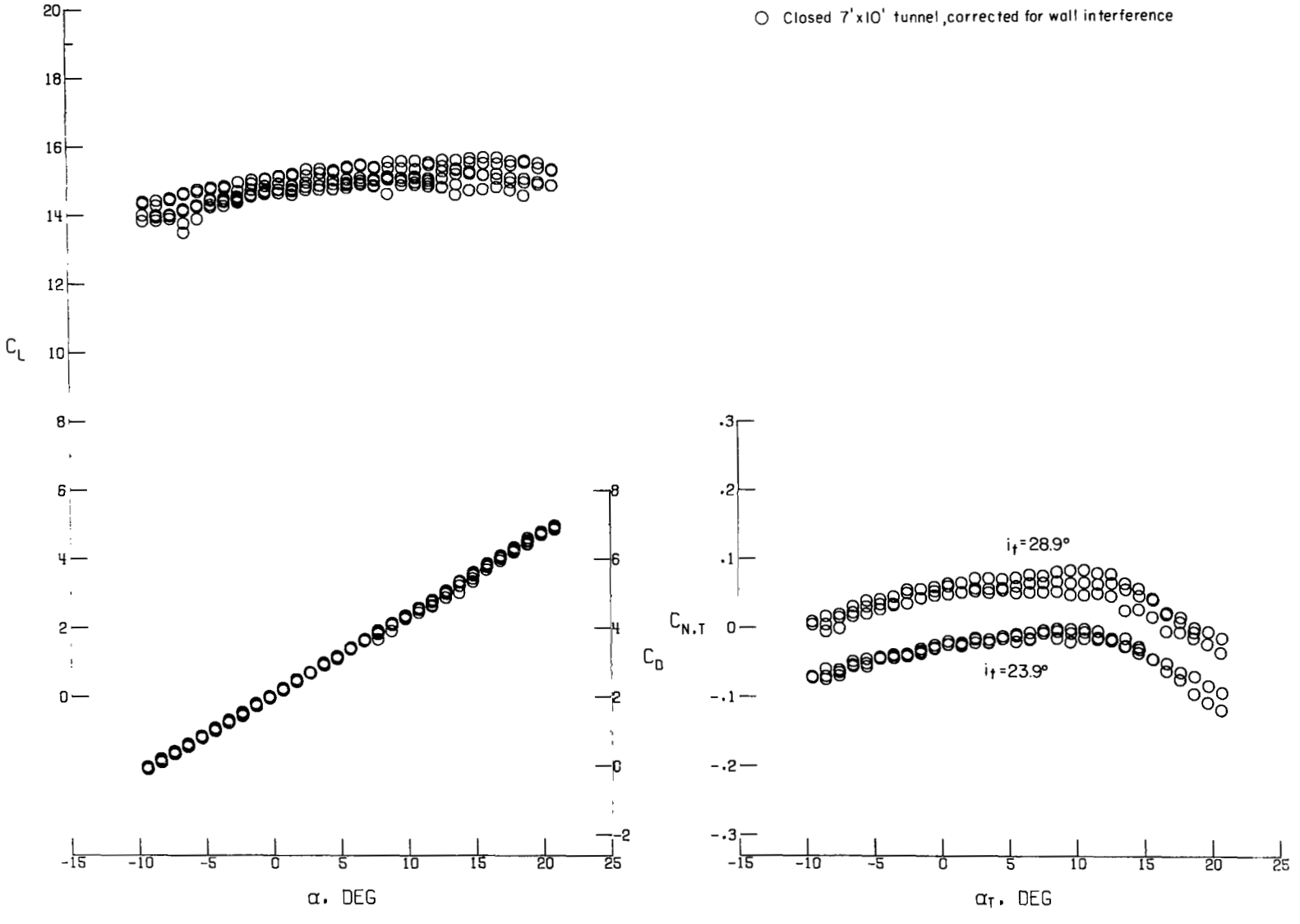

(f) C_μ = 10.0.

Figure 11.- Concluded.

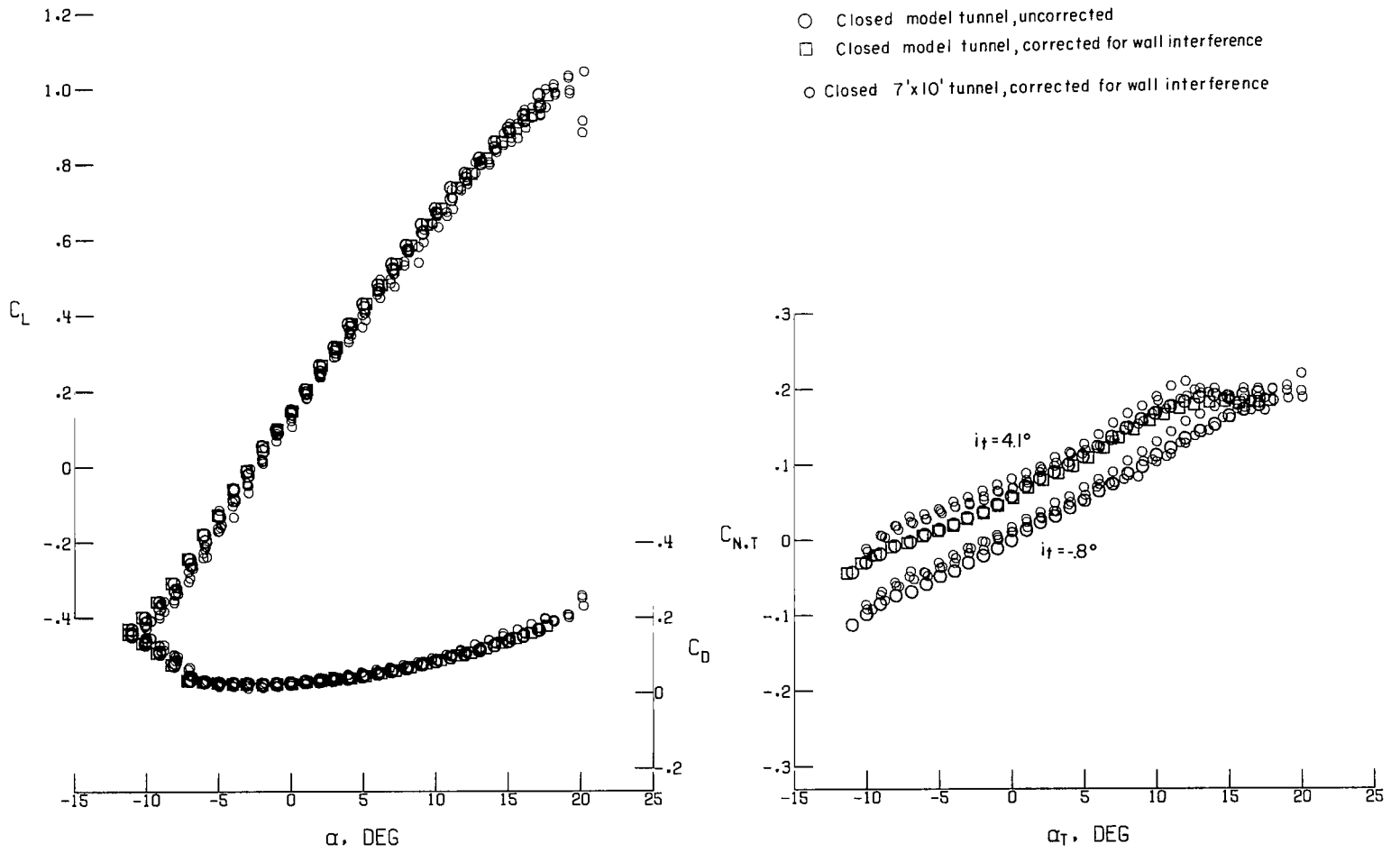

(a) $C_\mu = 0$.

Figure 12.- Effect of tunnel area on lift, drag, and tail-normal-force coefficients on jet-flap model (model-tunnel data presented as measured and also corrected for wall interference).

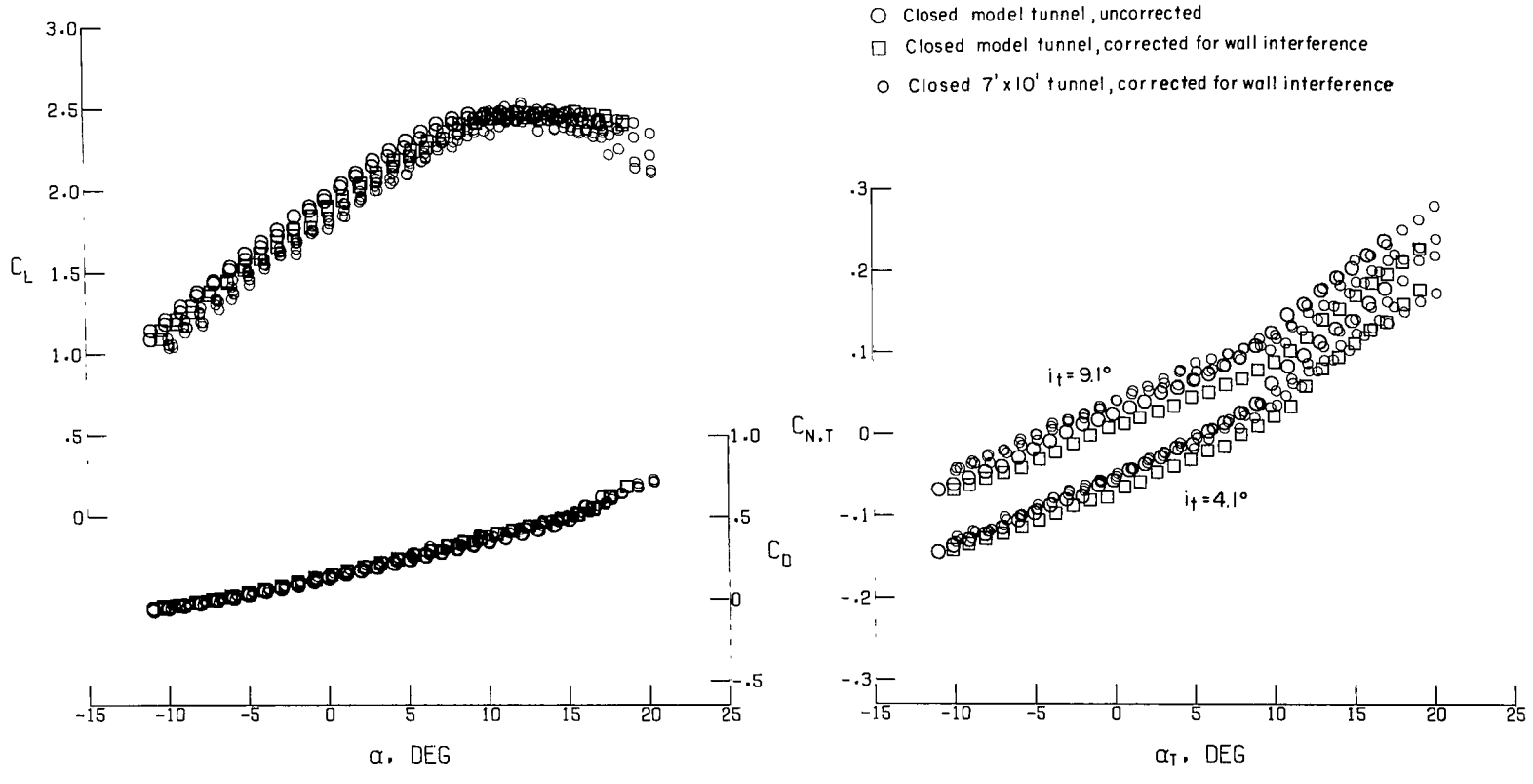

(b) $C_\mu = 0.5$.

Figure 12.- Continued.

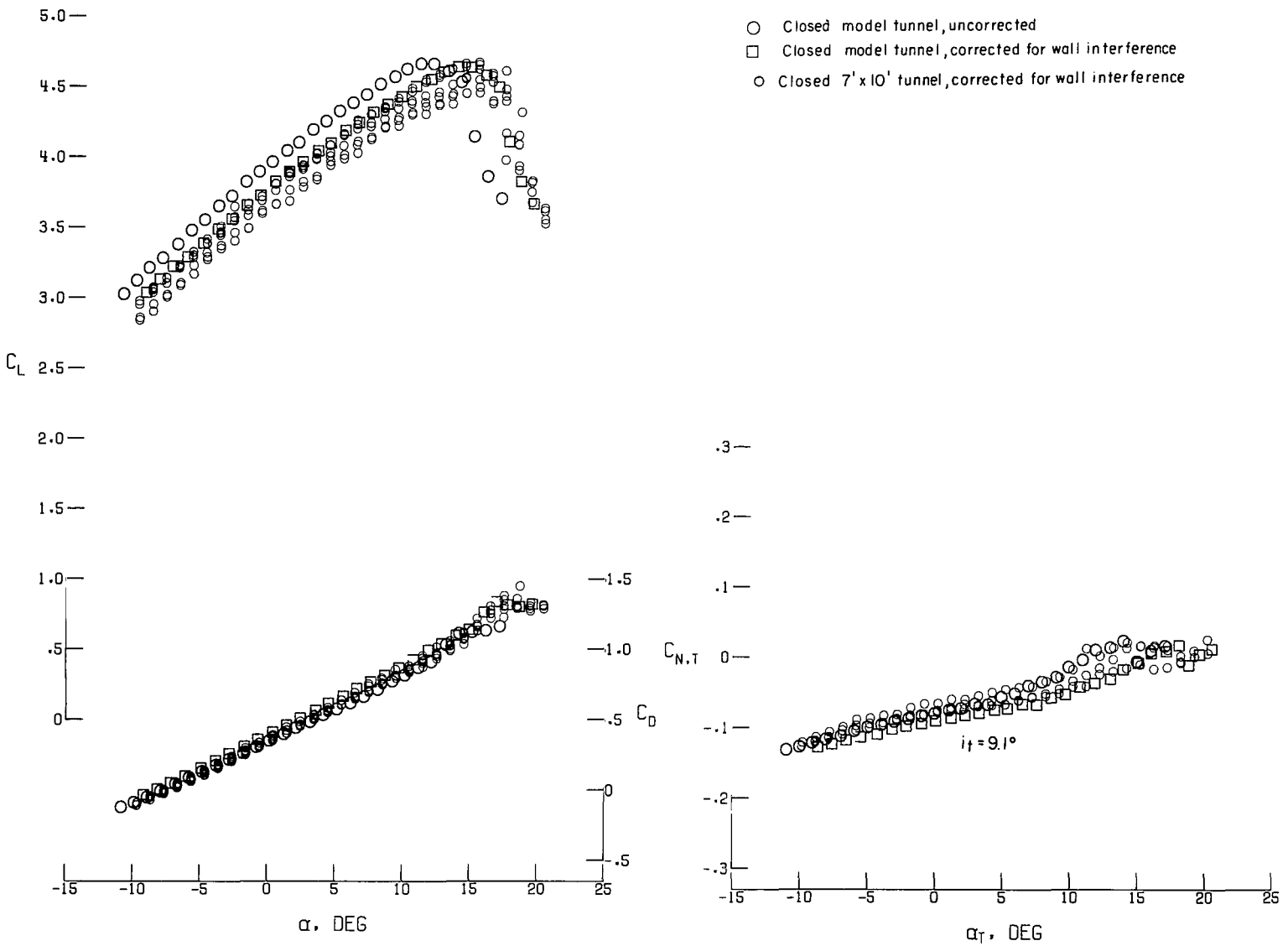

(c) C_μ = 1.5.

Figure 12.- Continued.

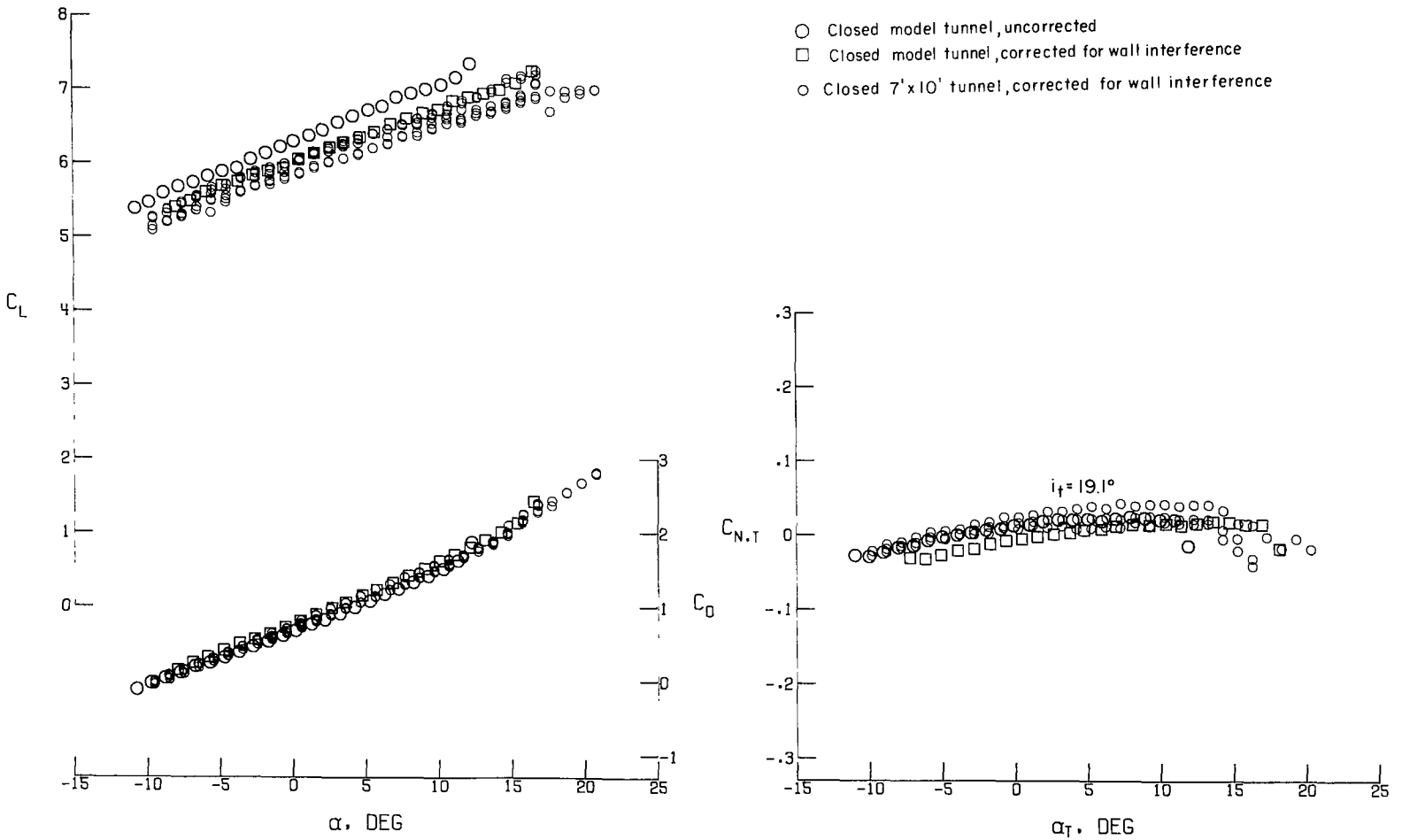

(d) C_μ = 3.0.

Figure 12.- Continued.

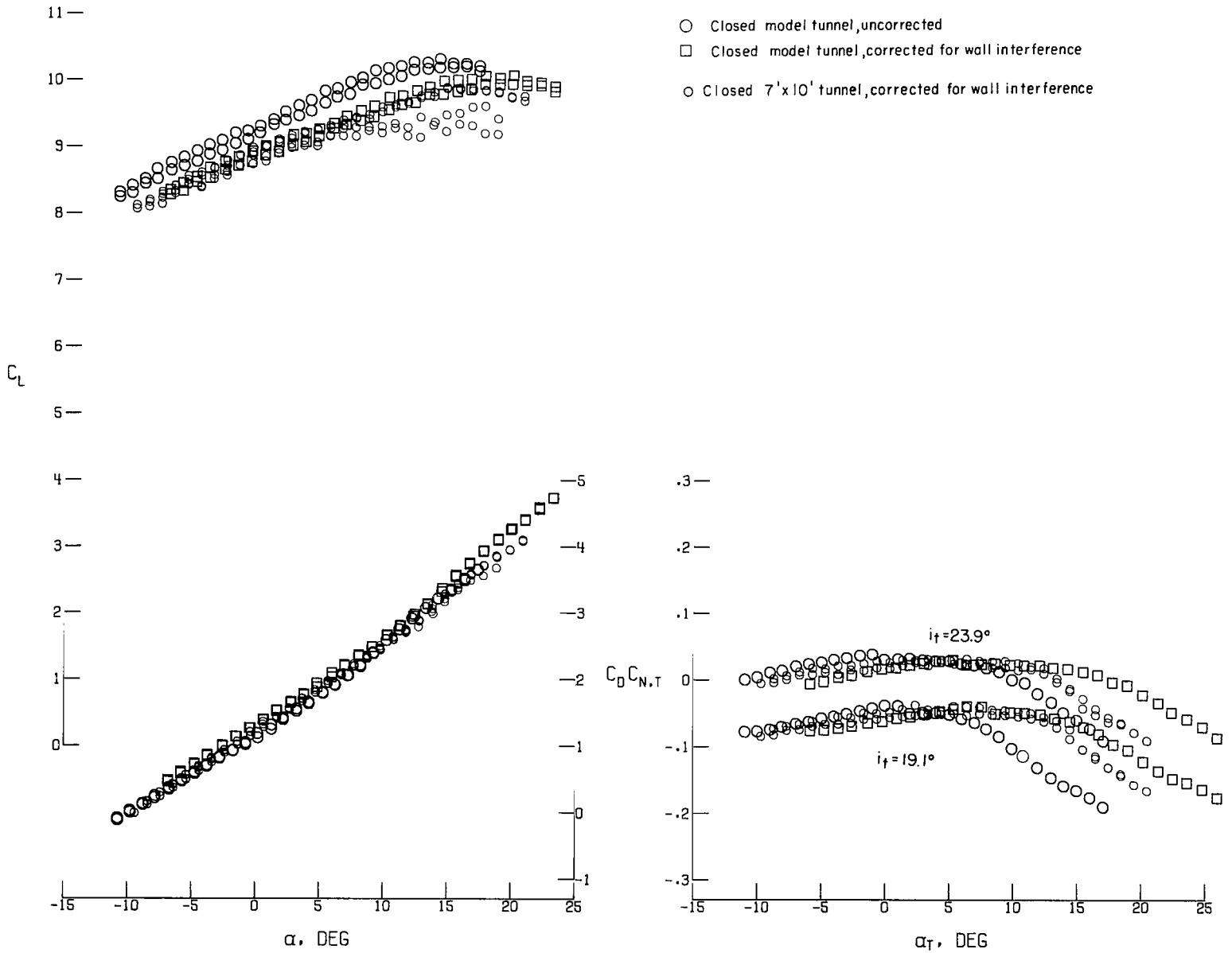

(e) C_μ = 5.0.

Figure 12.- Continued.

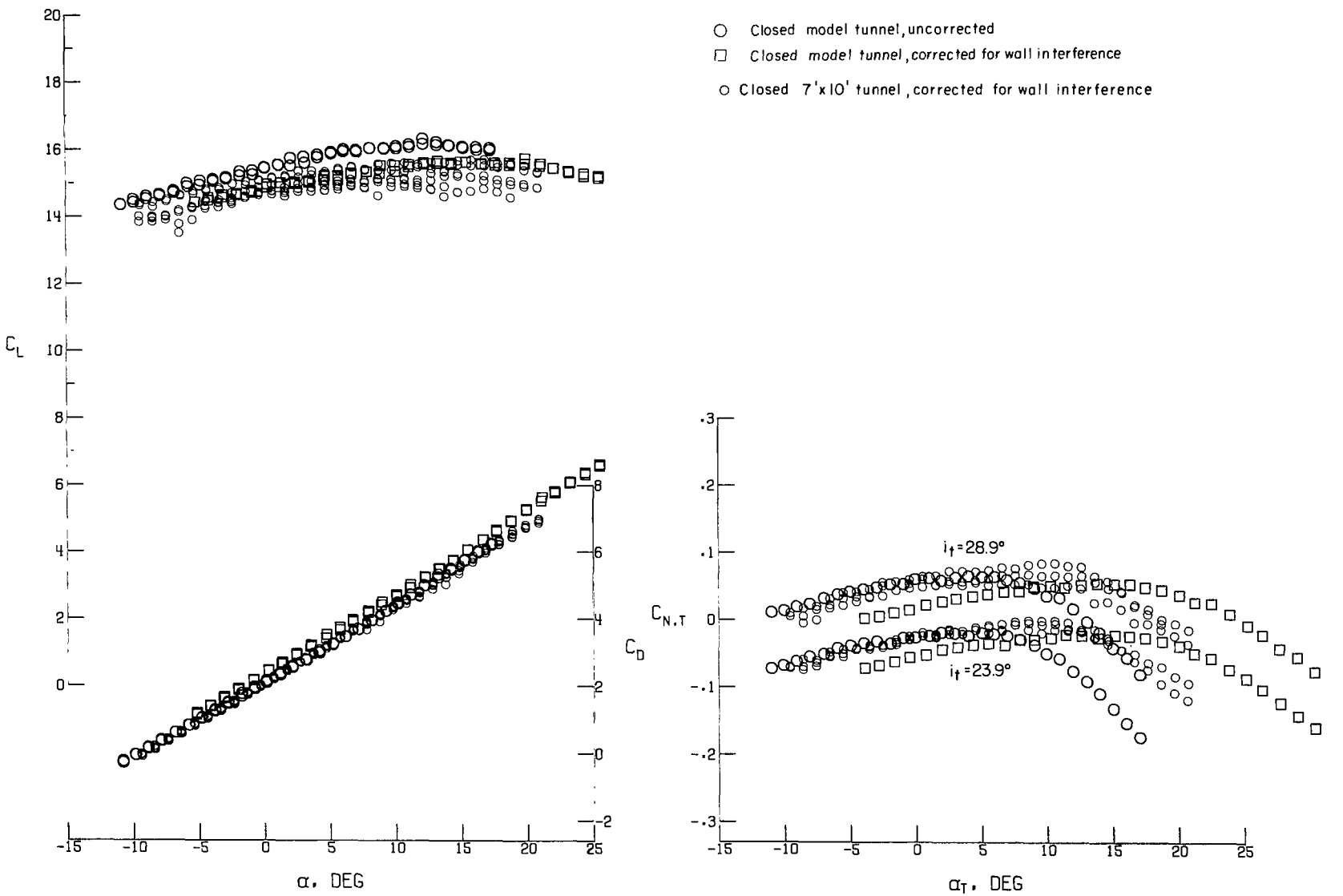

(f) C_μ = 10.0.

Figure 12.- Concluded.

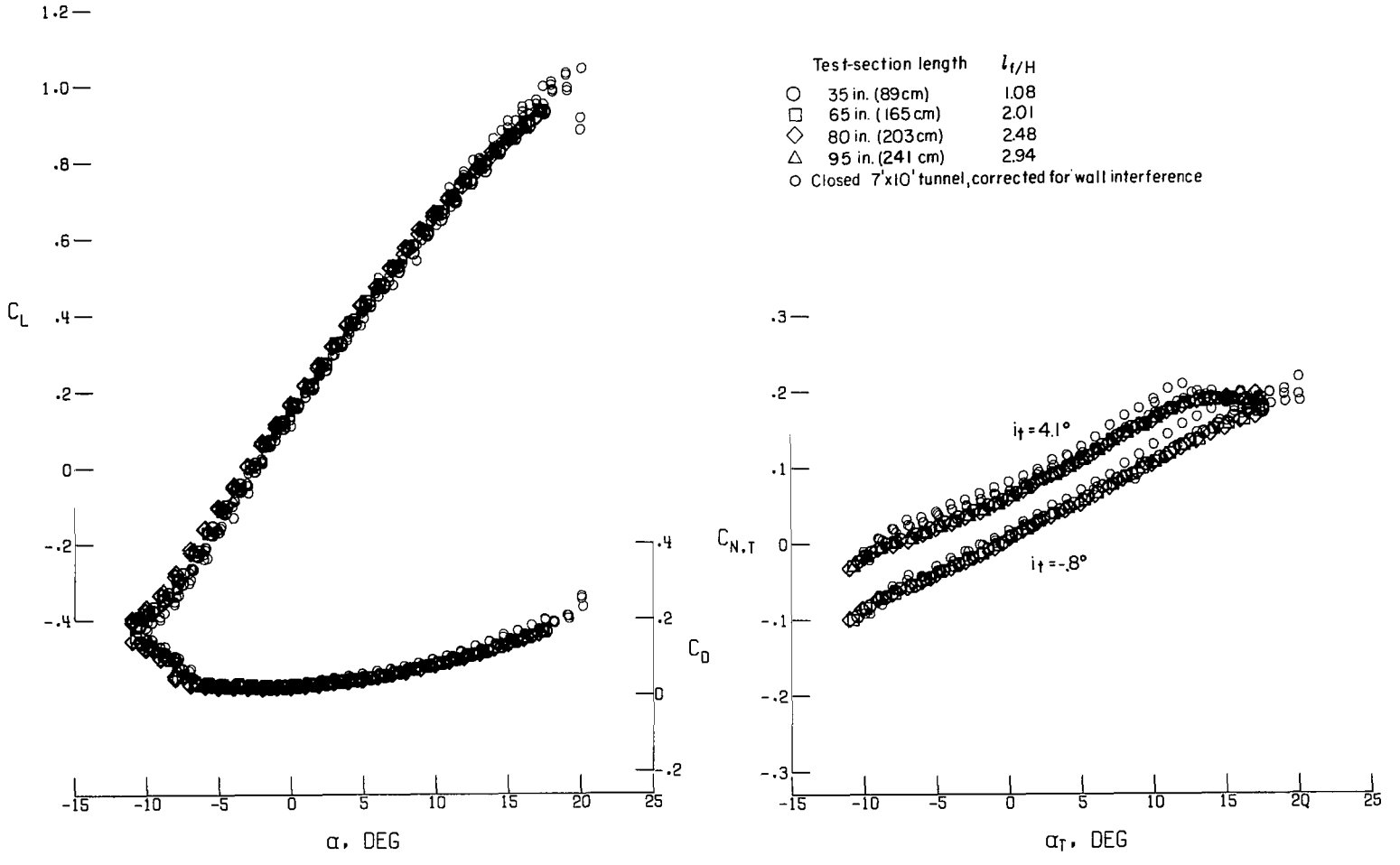

(a) $C_\mu = 0$.

Figure 13.- Effect of test-section length in model tunnel with 10-percent slotted sidewalls and screened floor on lift, drag, and tail-normal-force coefficients of jet-flap model.

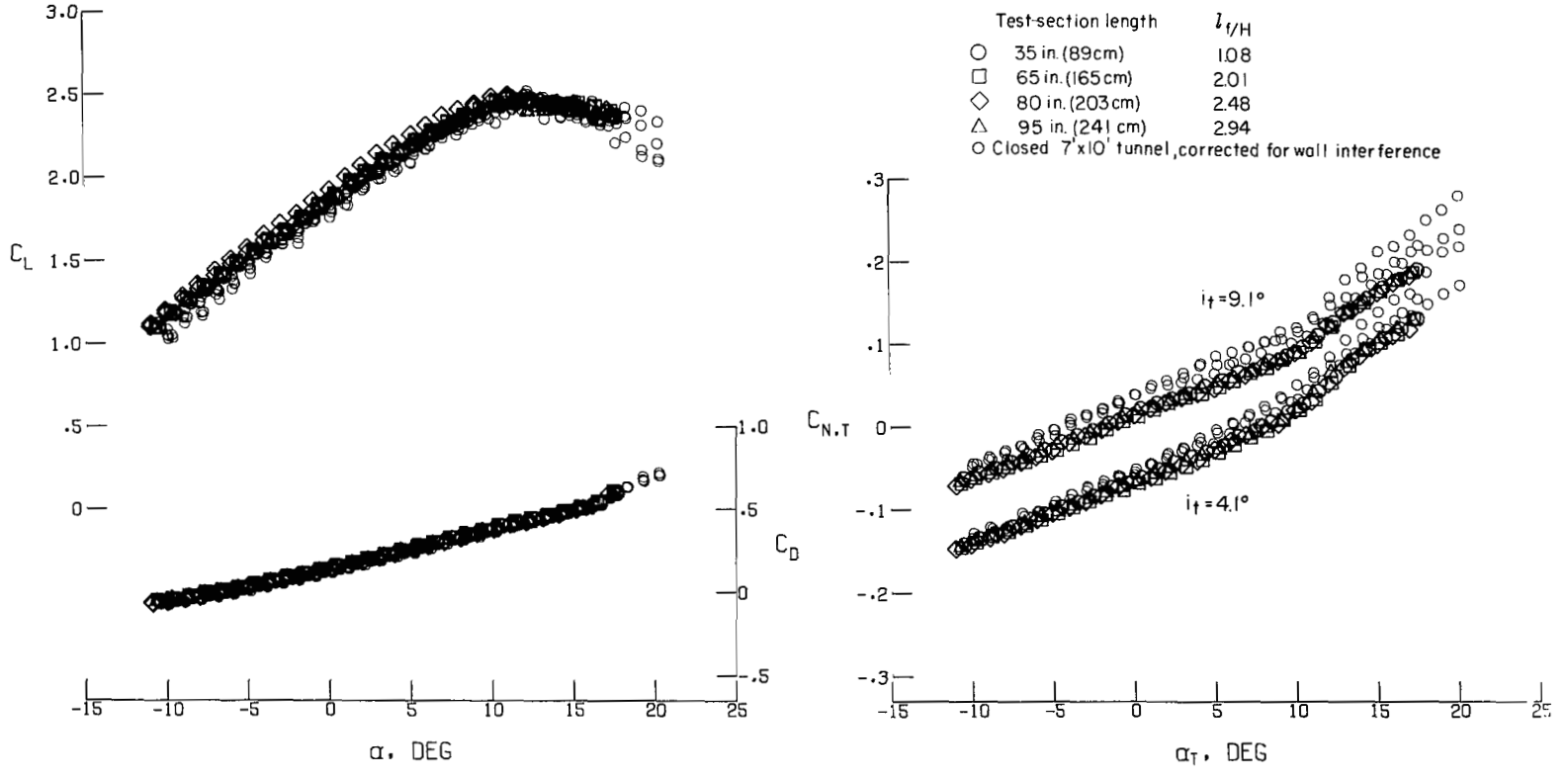

(b) $C_\mu = 0.5$.

Figure 13.- Continued.

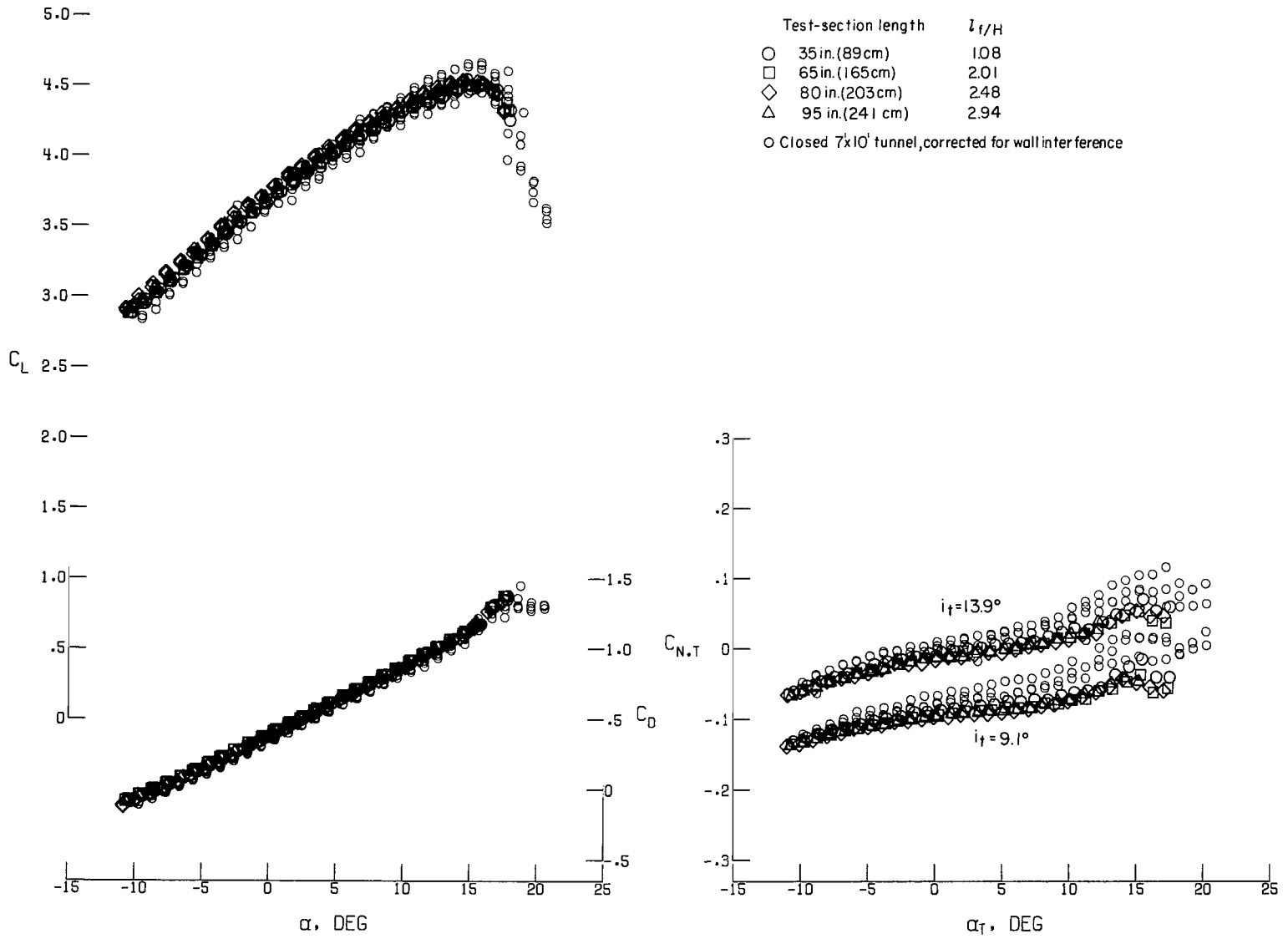

(c) $C_\mu = 1.5$.

Figure 13.- Continued.

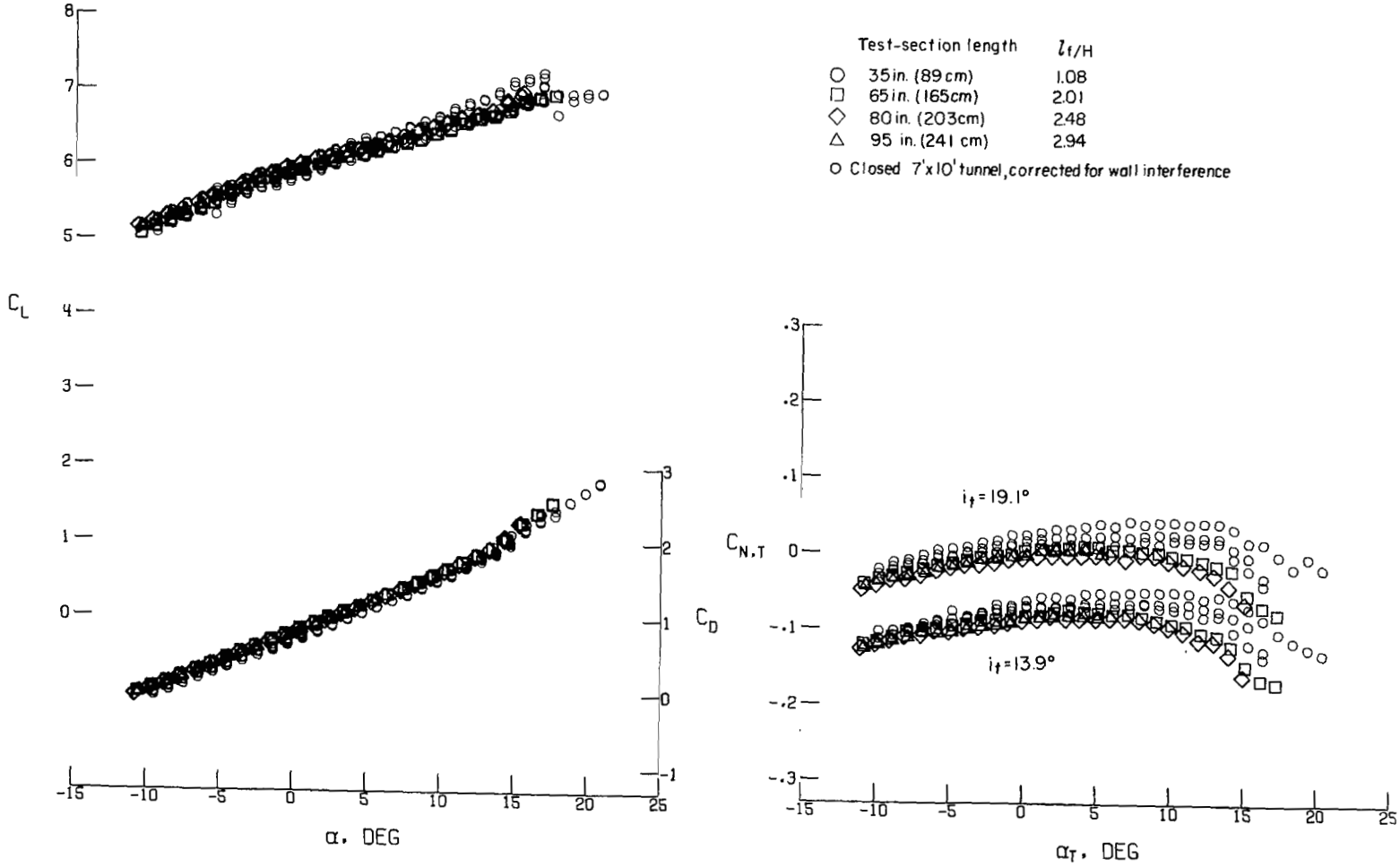

(d) $C_\mu = 3.0$.

Figure 13.- Continued.

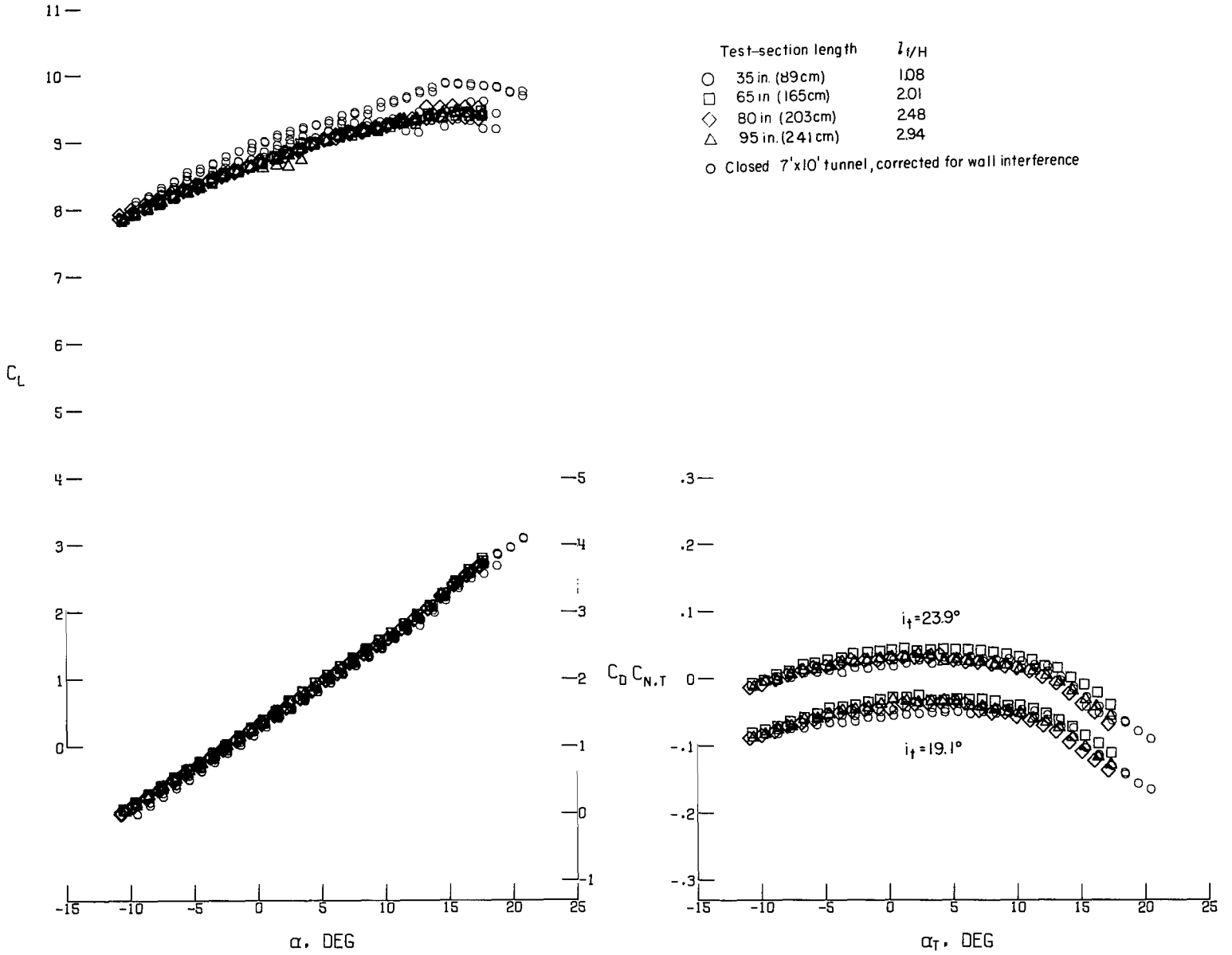

(e) C_μ = 5.0.

Figure 13.- Continued.

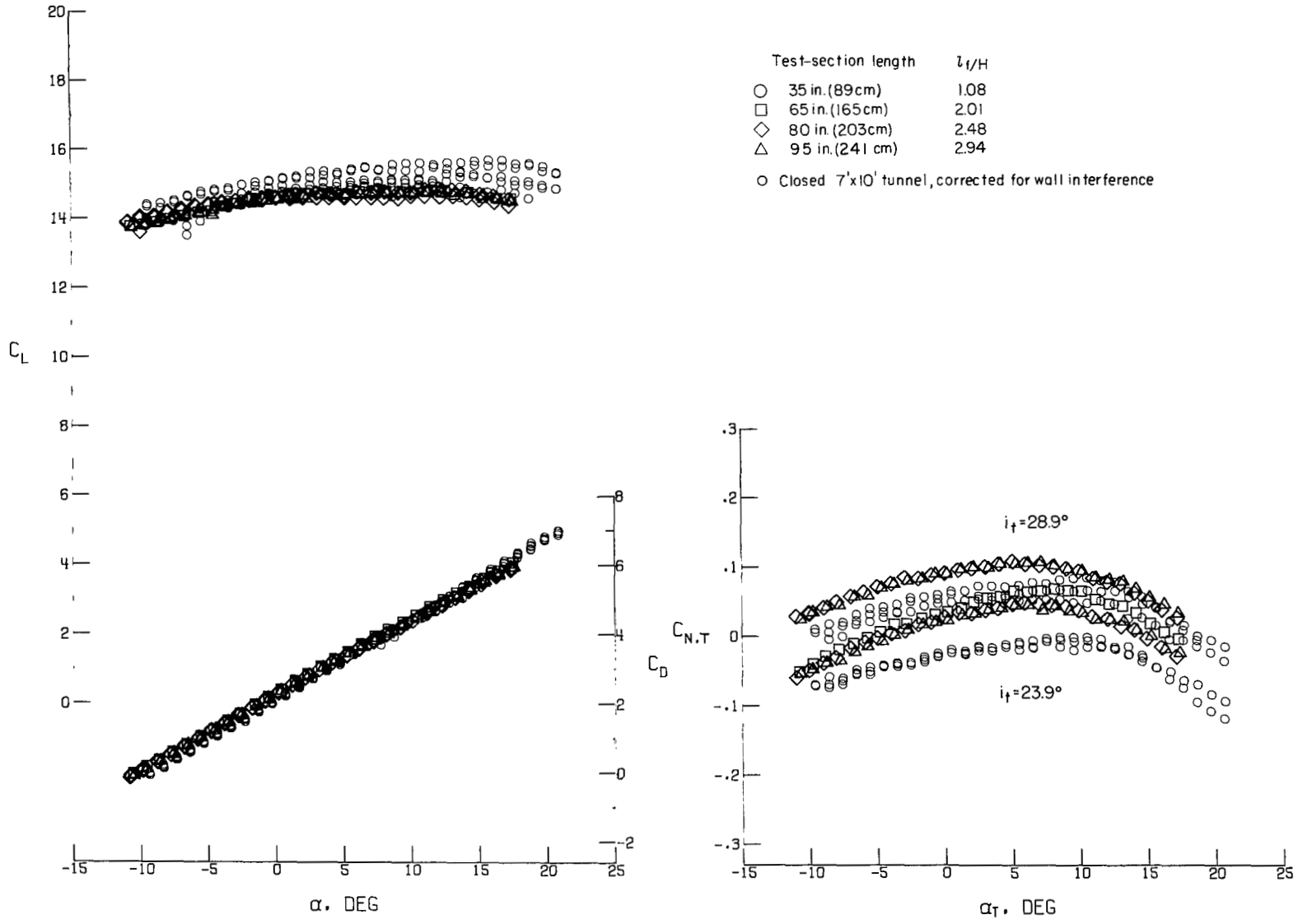

(f) C_μ = 10.0.

Figure 13.- Concluded.

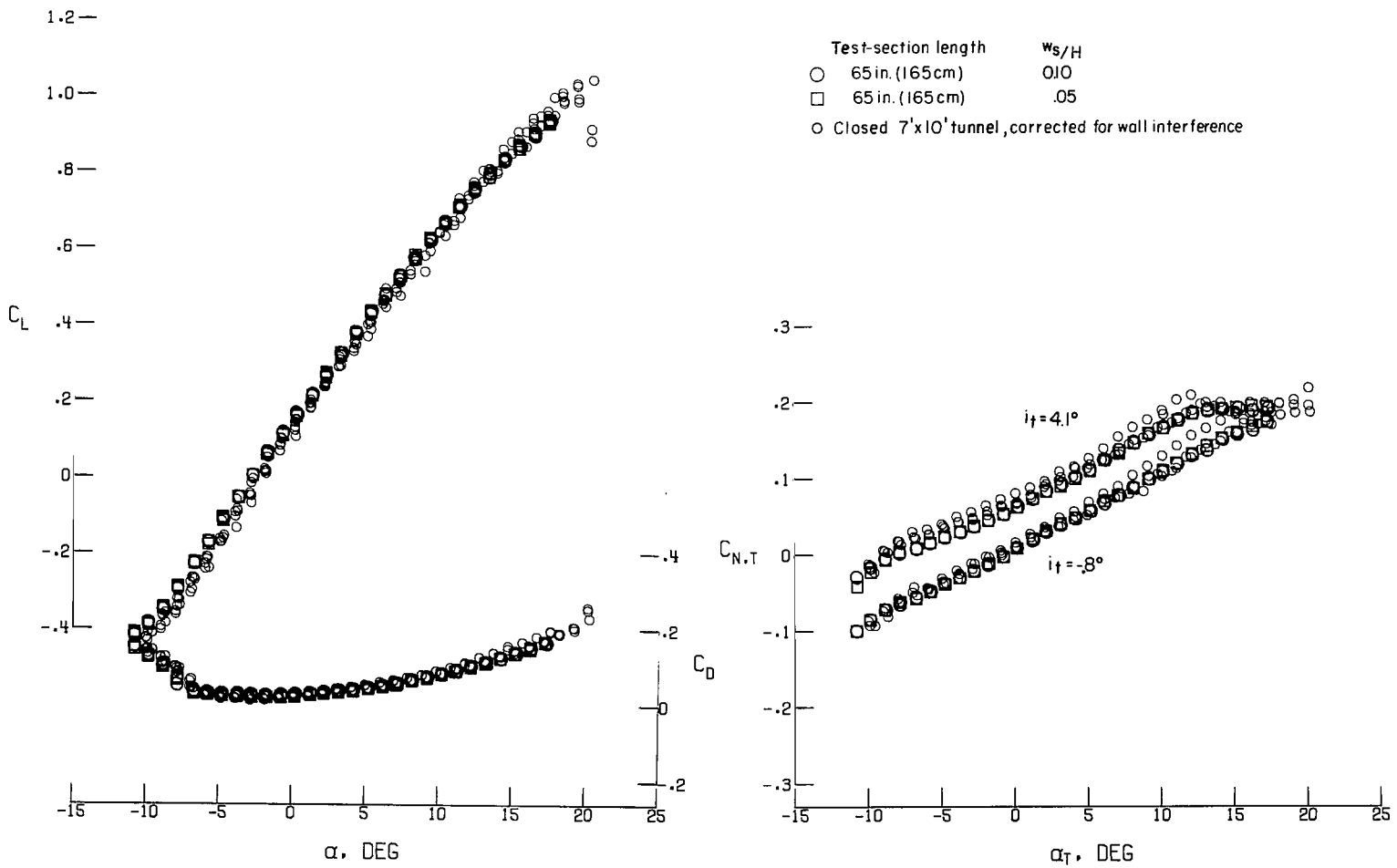

(a) $C_\mu = 0.$

Figure 14.- Effect of slot opening in model tunnel with 5- and 10-percent slotted sidewalls and screened floor on lift, drag, and tail-normal-force coefficients of jet-flap model.

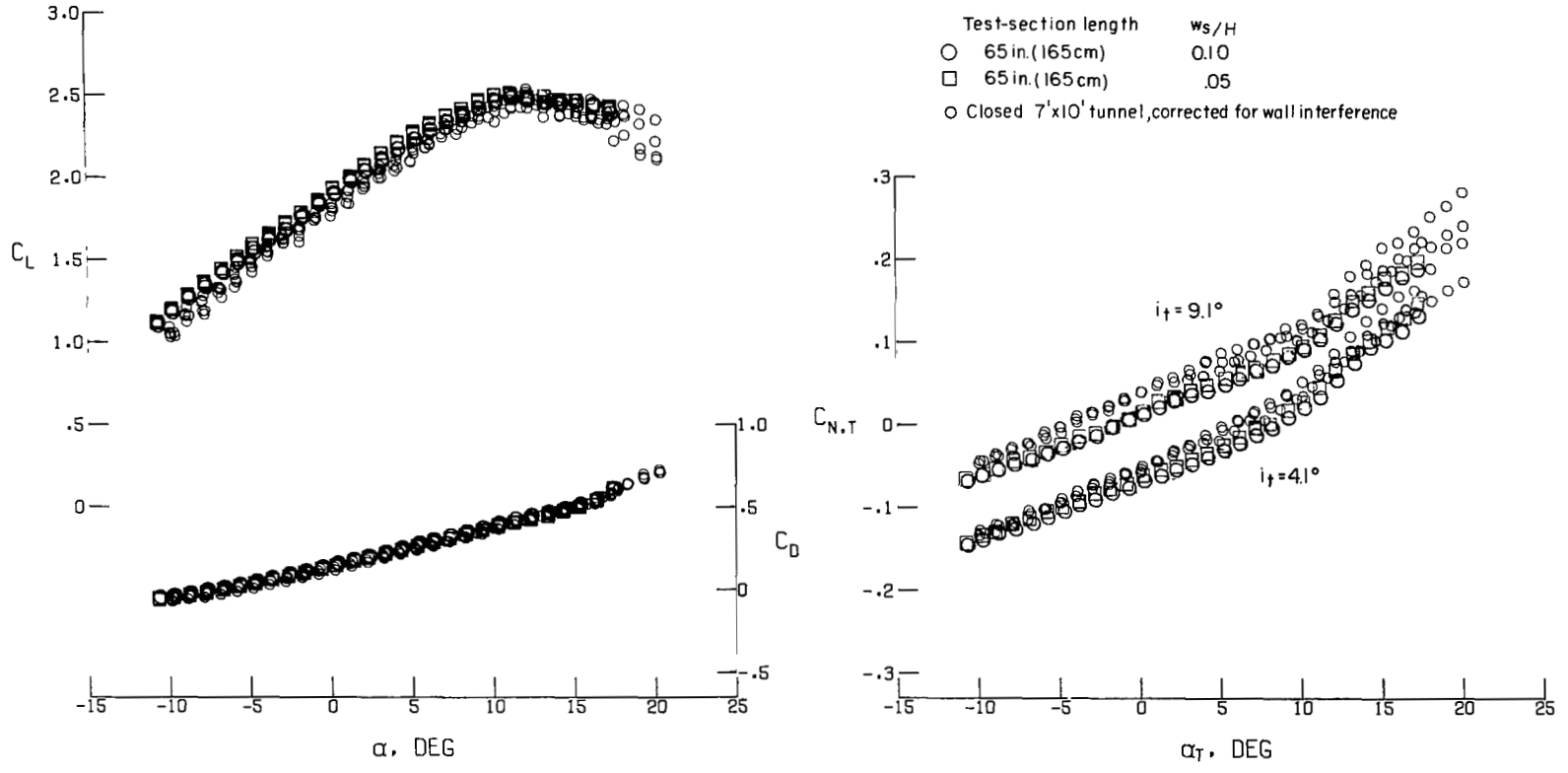

(b) $C_\mu = 0.5$.

Figure 14.- Continued.

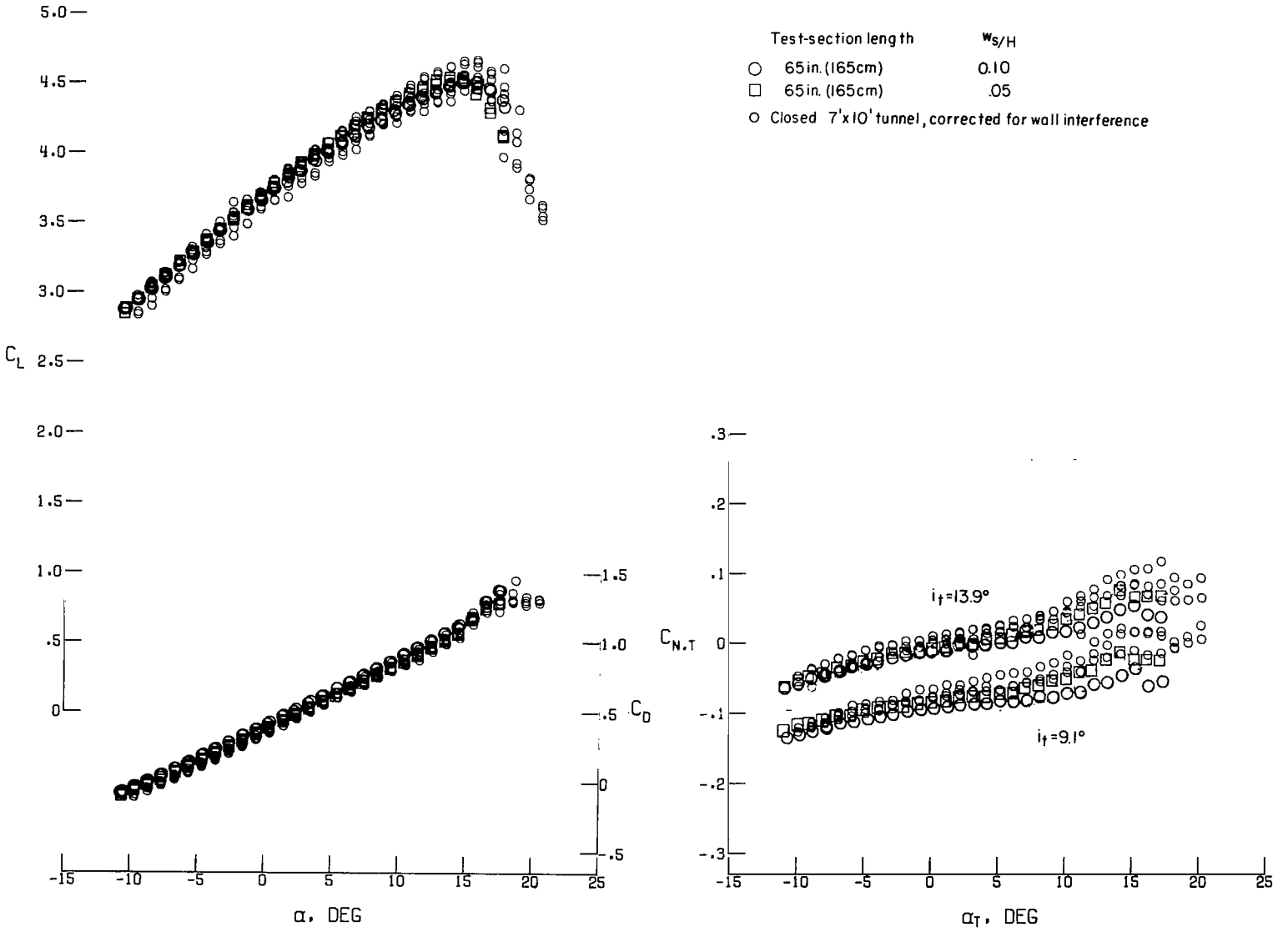

(c) $C_\mu = 1.5$.

Figure 14.- Continued.

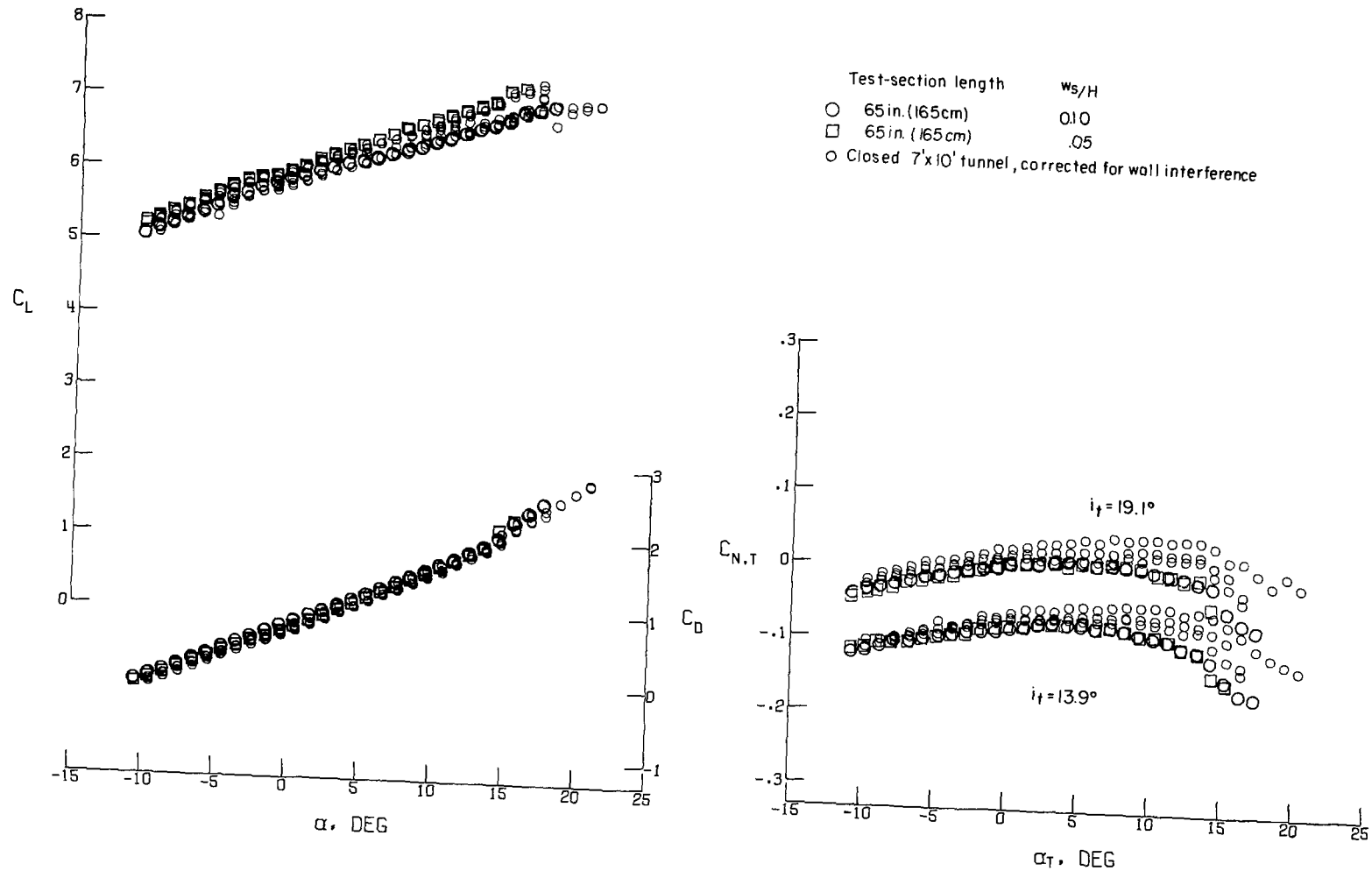

(d) $C_\mu = 3.0$.

Figure 14.- Continued.

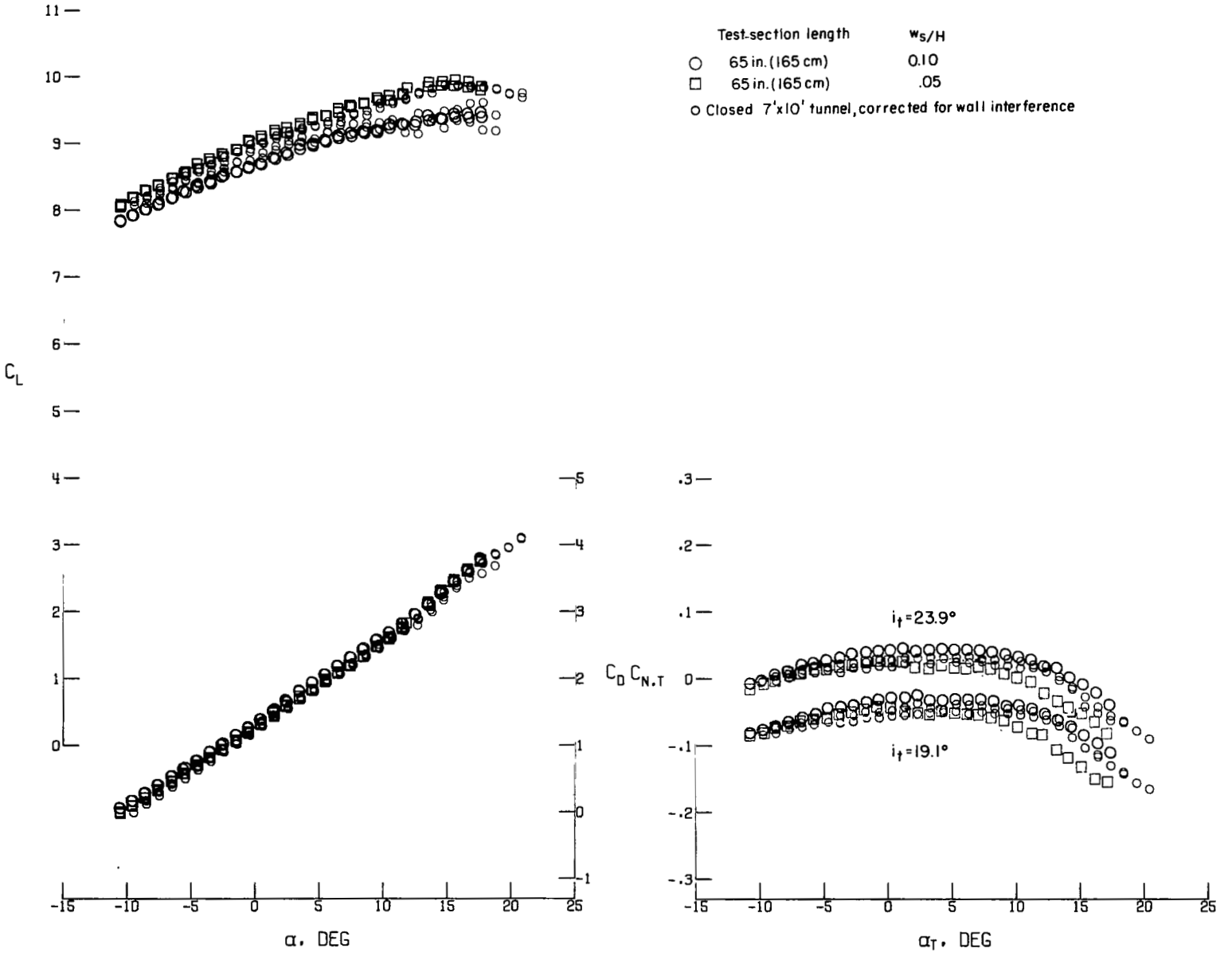

(e) C_μ = 5.0.

Figure 14.- Continued.

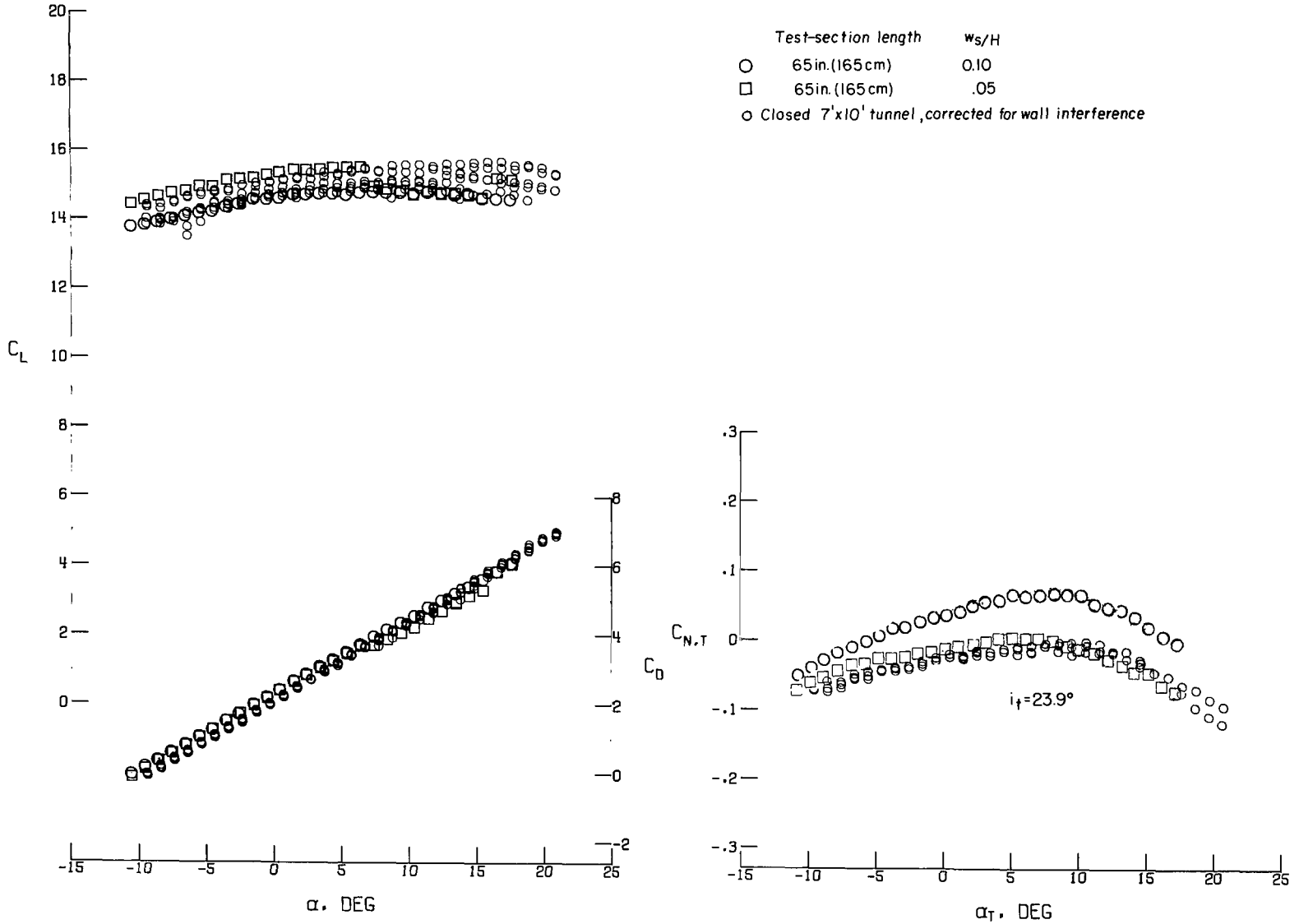

(f) C_μ = 10.0.

Figure 14.- Concluded.

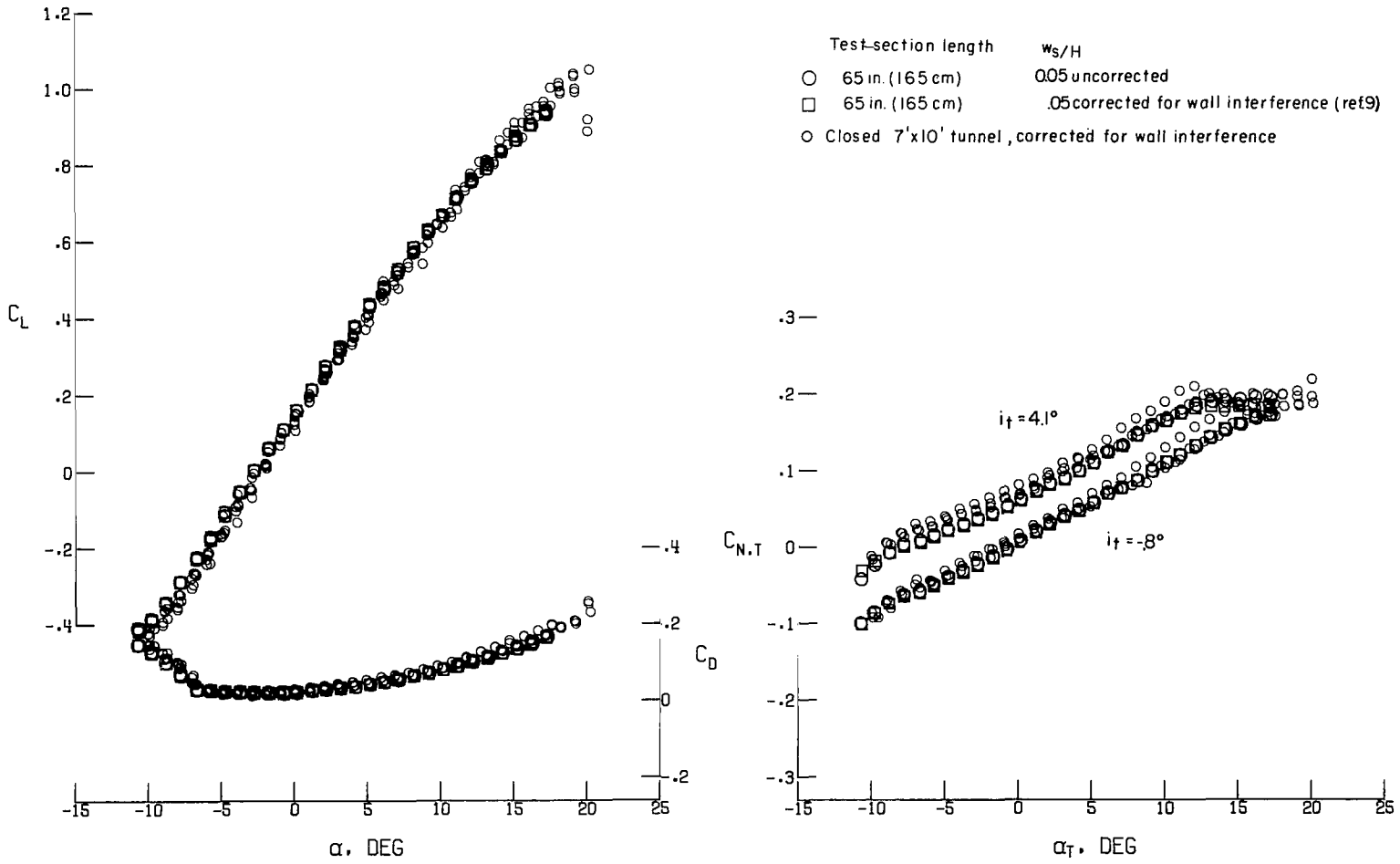

(a) $C_\mu = 0$.

Figure 15.- Effect of wall corrections applied to model tunnel with 5-percent slotted sidewalls and screened floor on lift, drag, and tail-normal-force coefficients (corrections applied from ref. 9).

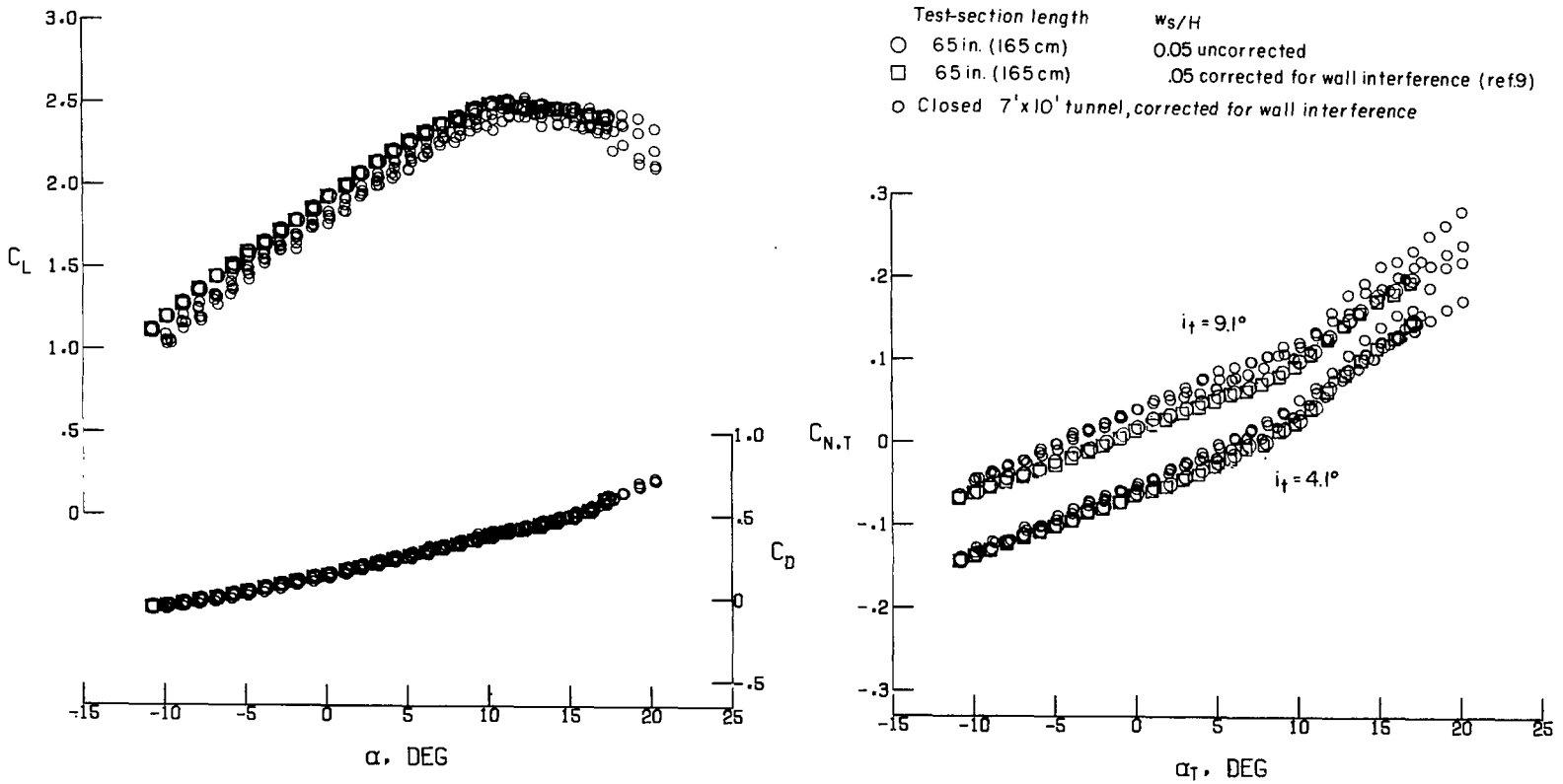

(b) $C_\mu = 0.5$.

Figure 15.- Continued.

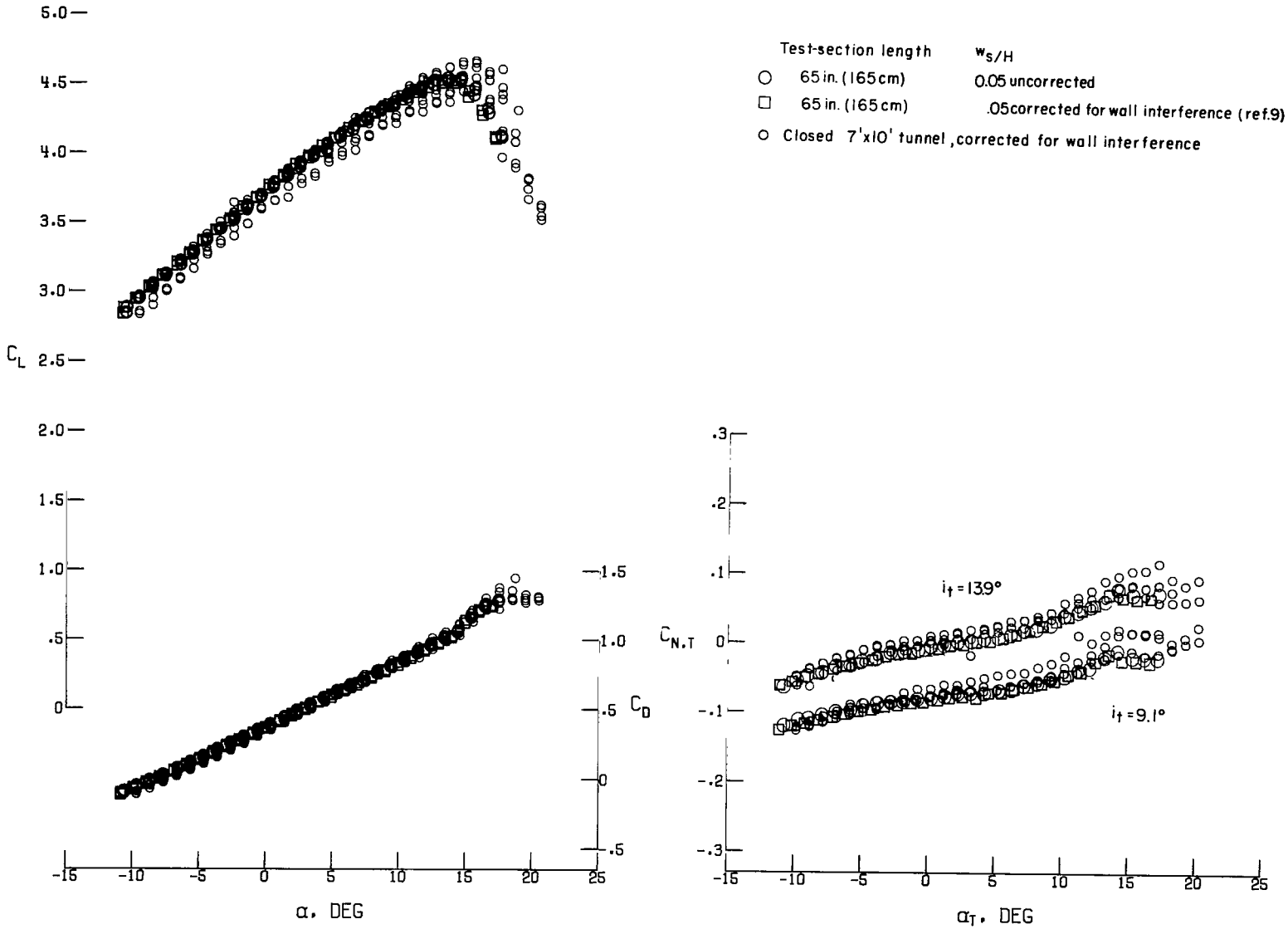

(c) $C_\mu = 1.5$.

Figure 15.- Continued.

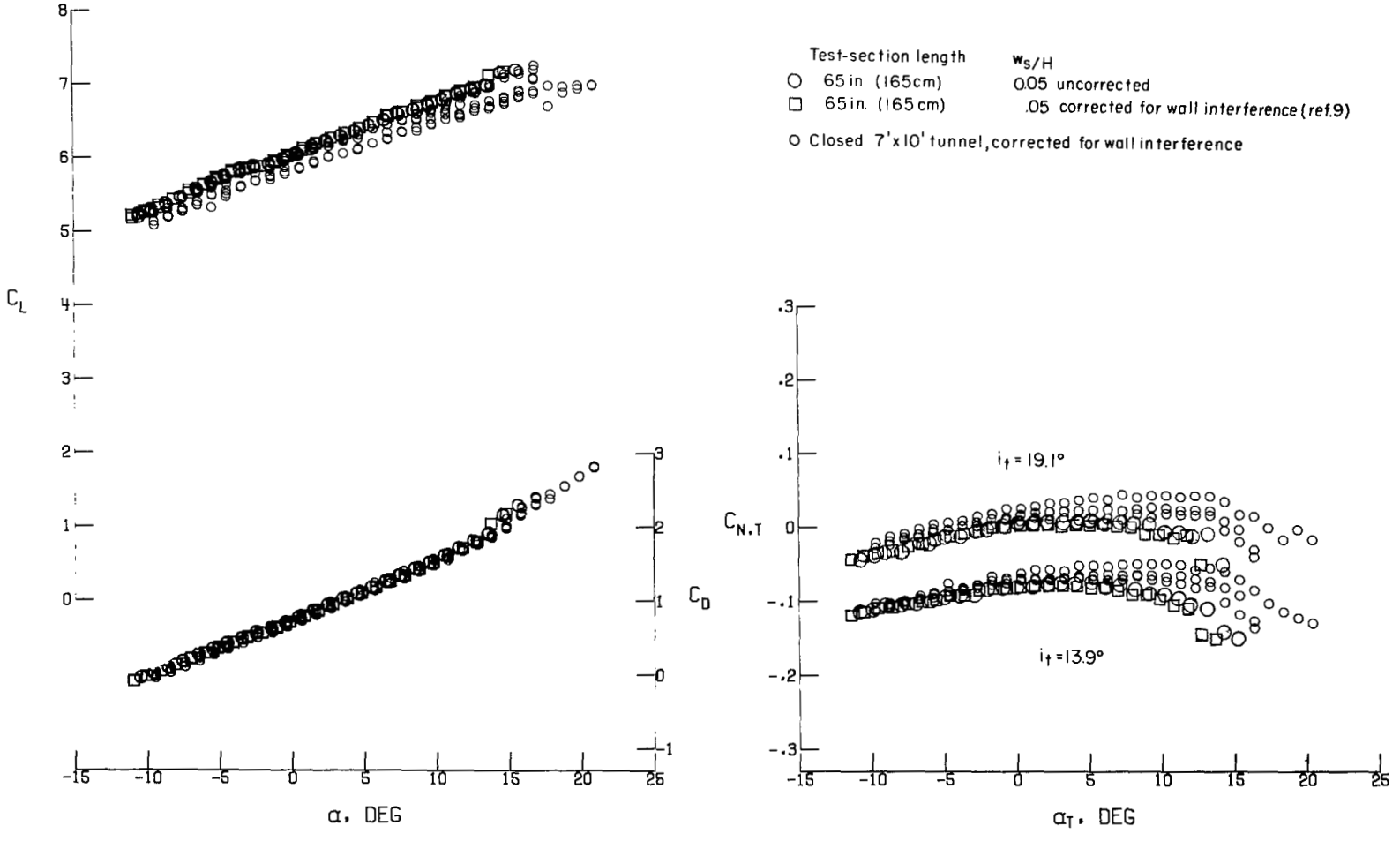

(d) $C_\mu = 3.0$.

Figure 15.- Continued.

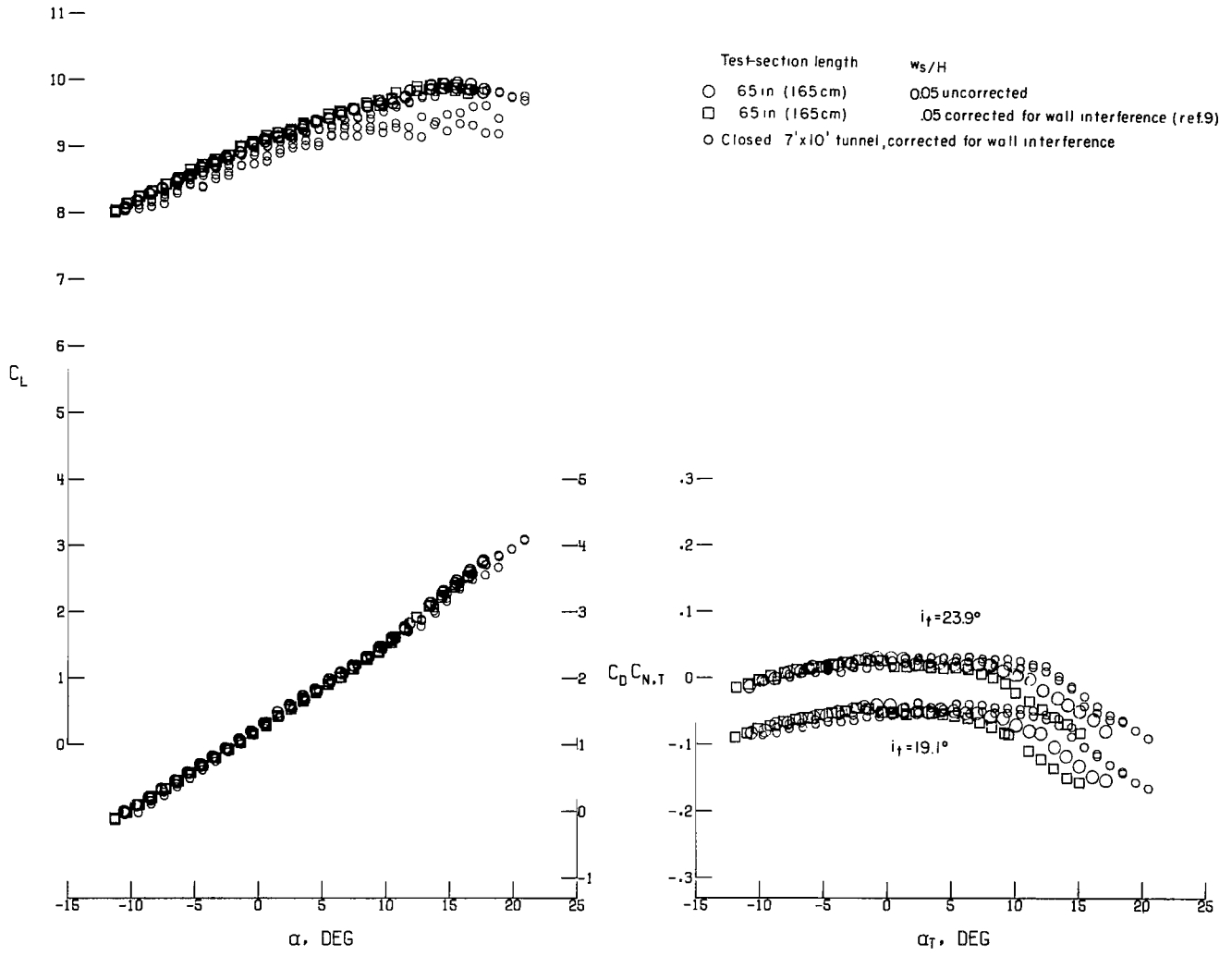

(e) C_μ = 5.0.

Figure 15.- Continued.

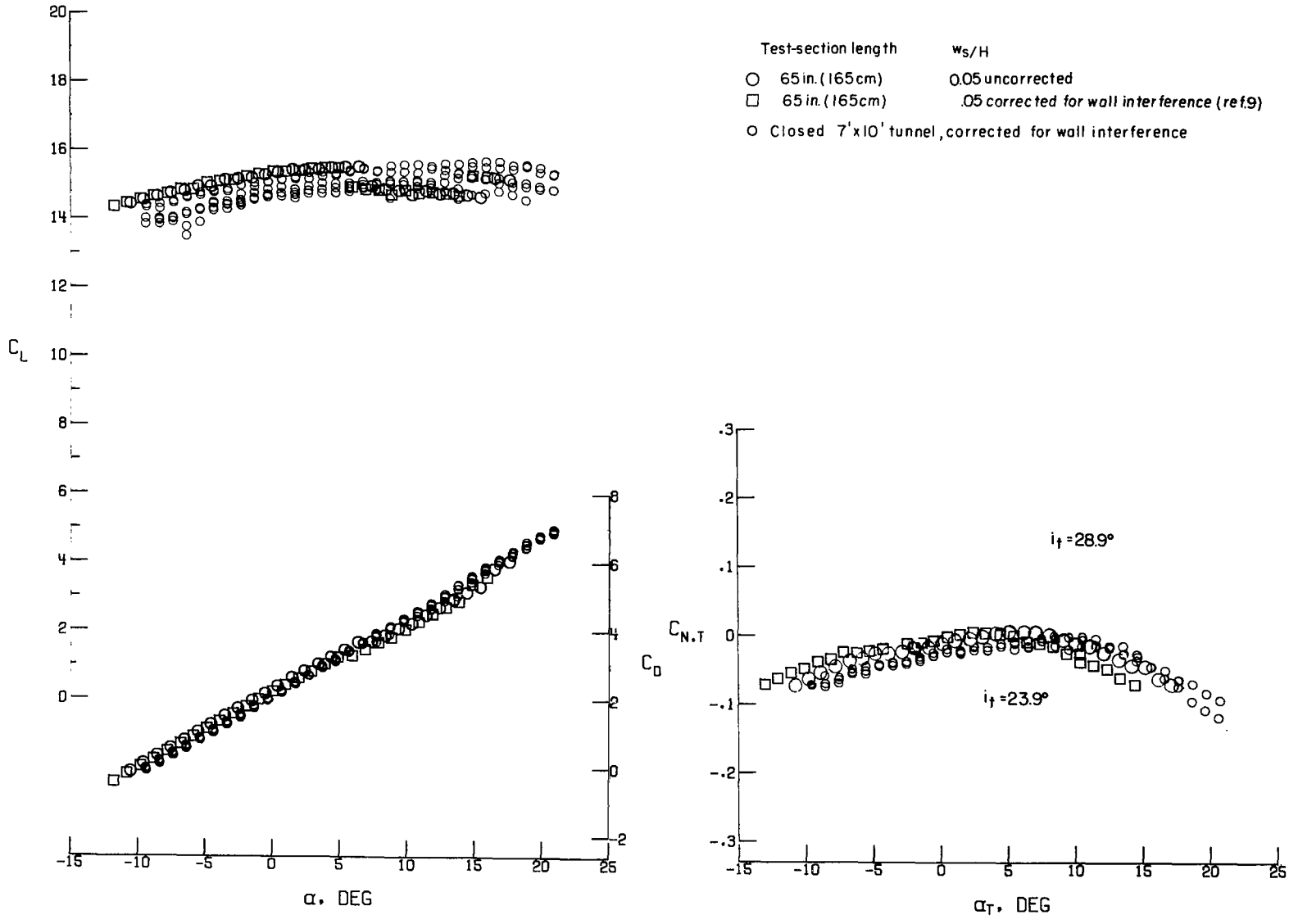

(f) C_μ = 10.0.

Figure 15.- Concluded.

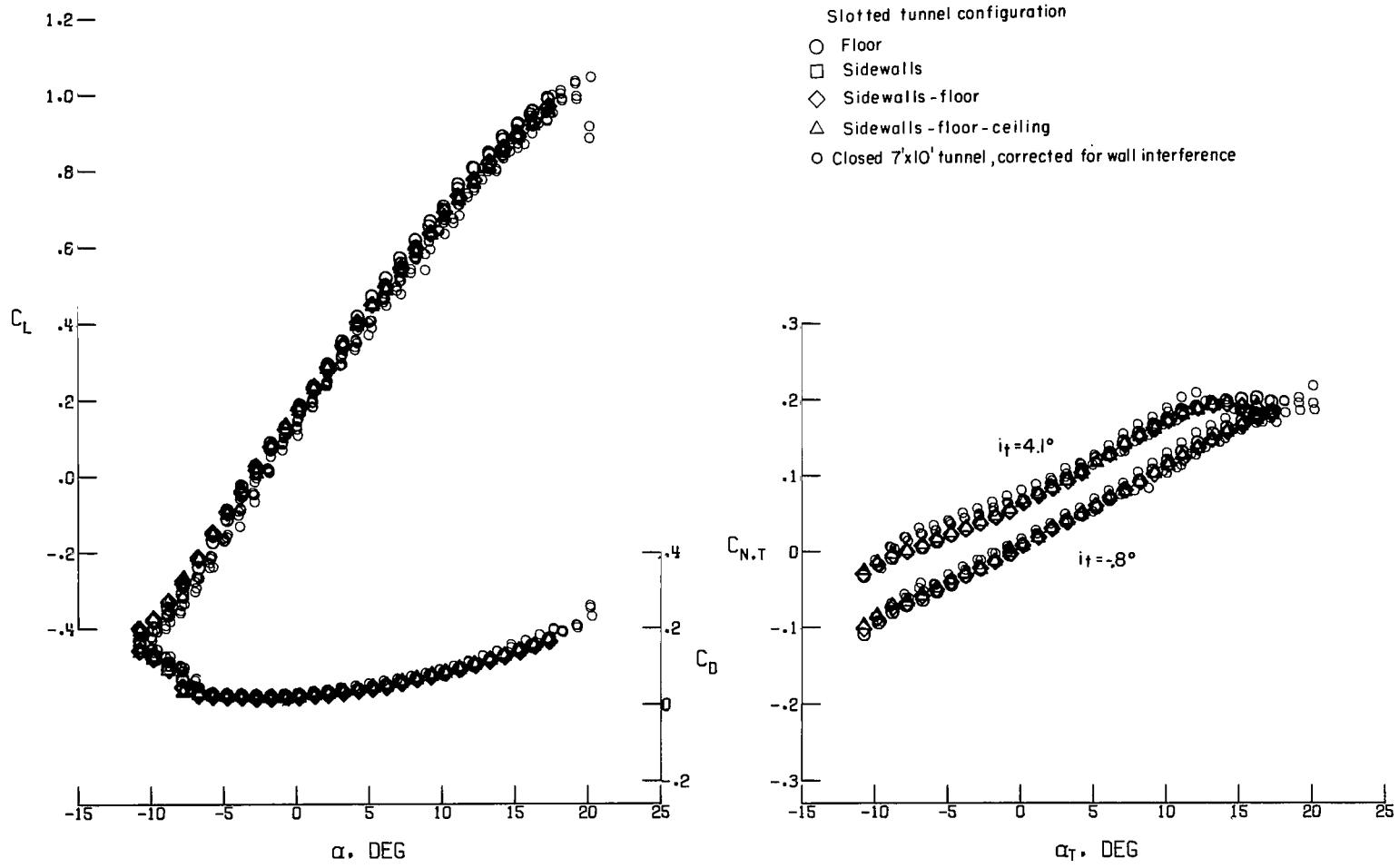

(a) $C_\mu = 0$.

Figure 16.- Effect of slotted boundaries on four different wall configurations on lift, drag, and tail-normal-force coefficients.

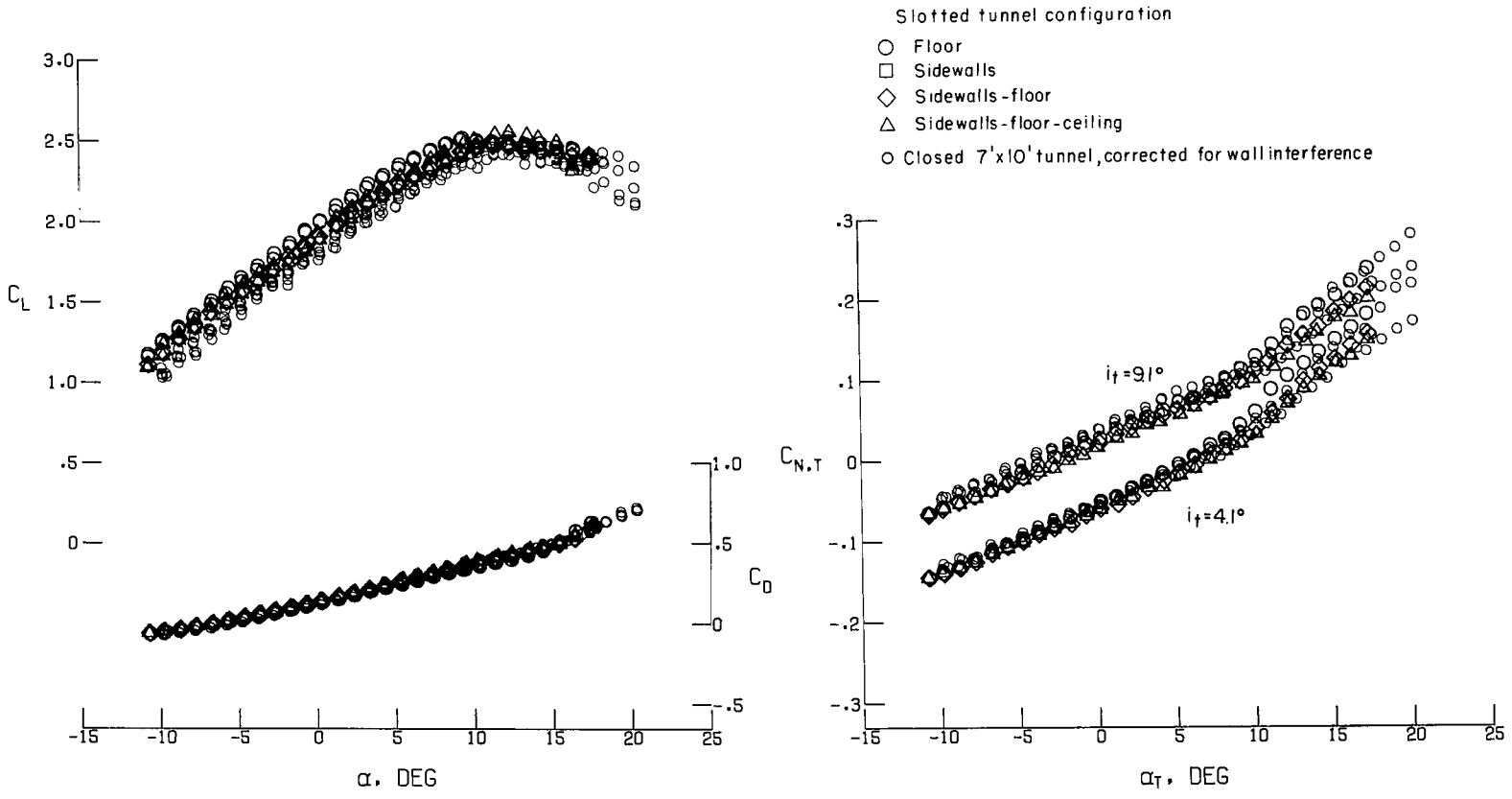

(b) $C_\mu = 0.5$.

Figure 16.- Continued.

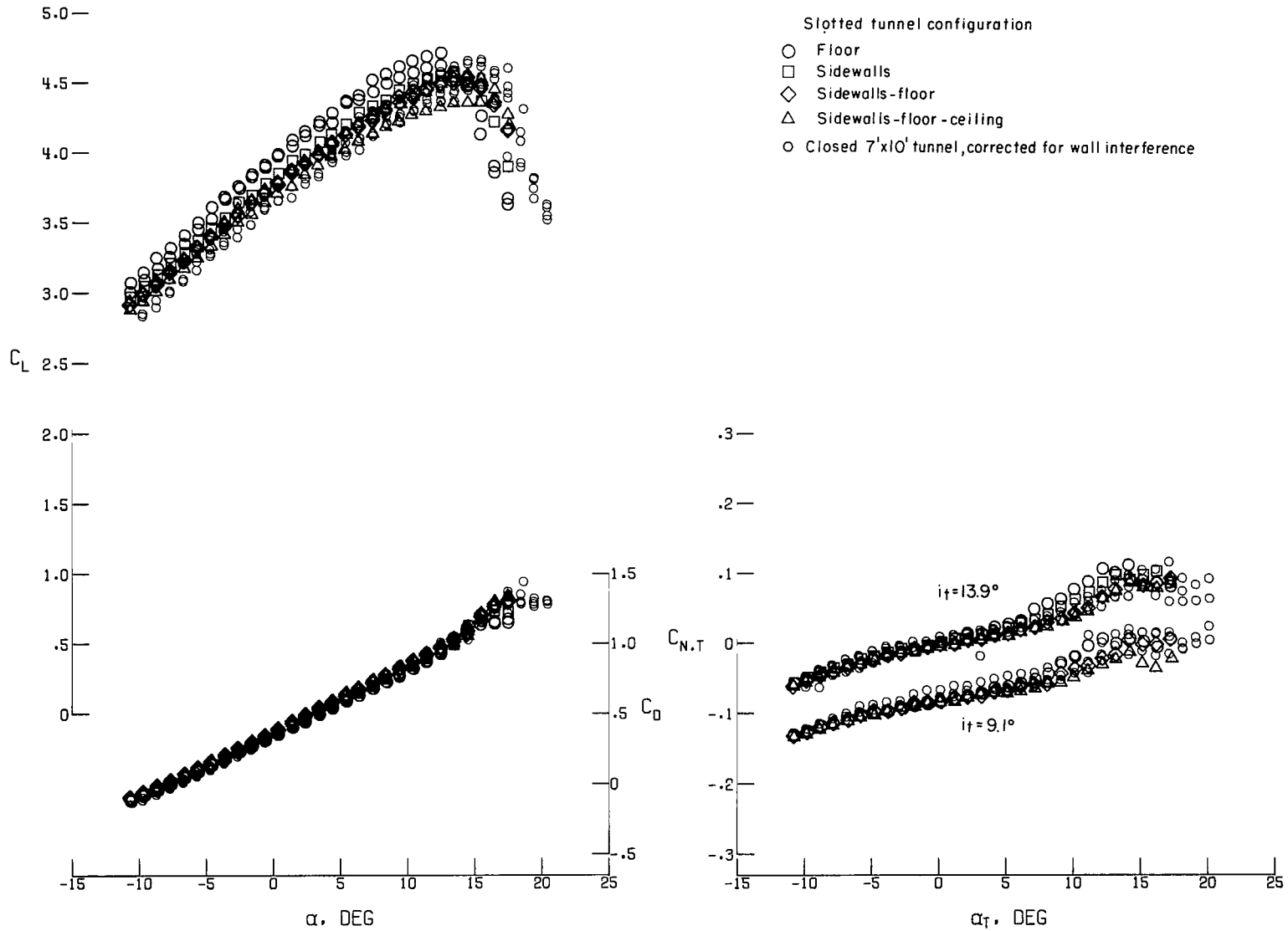

(c) $C_\mu = 1.5$.

Figure 16.- Continued.

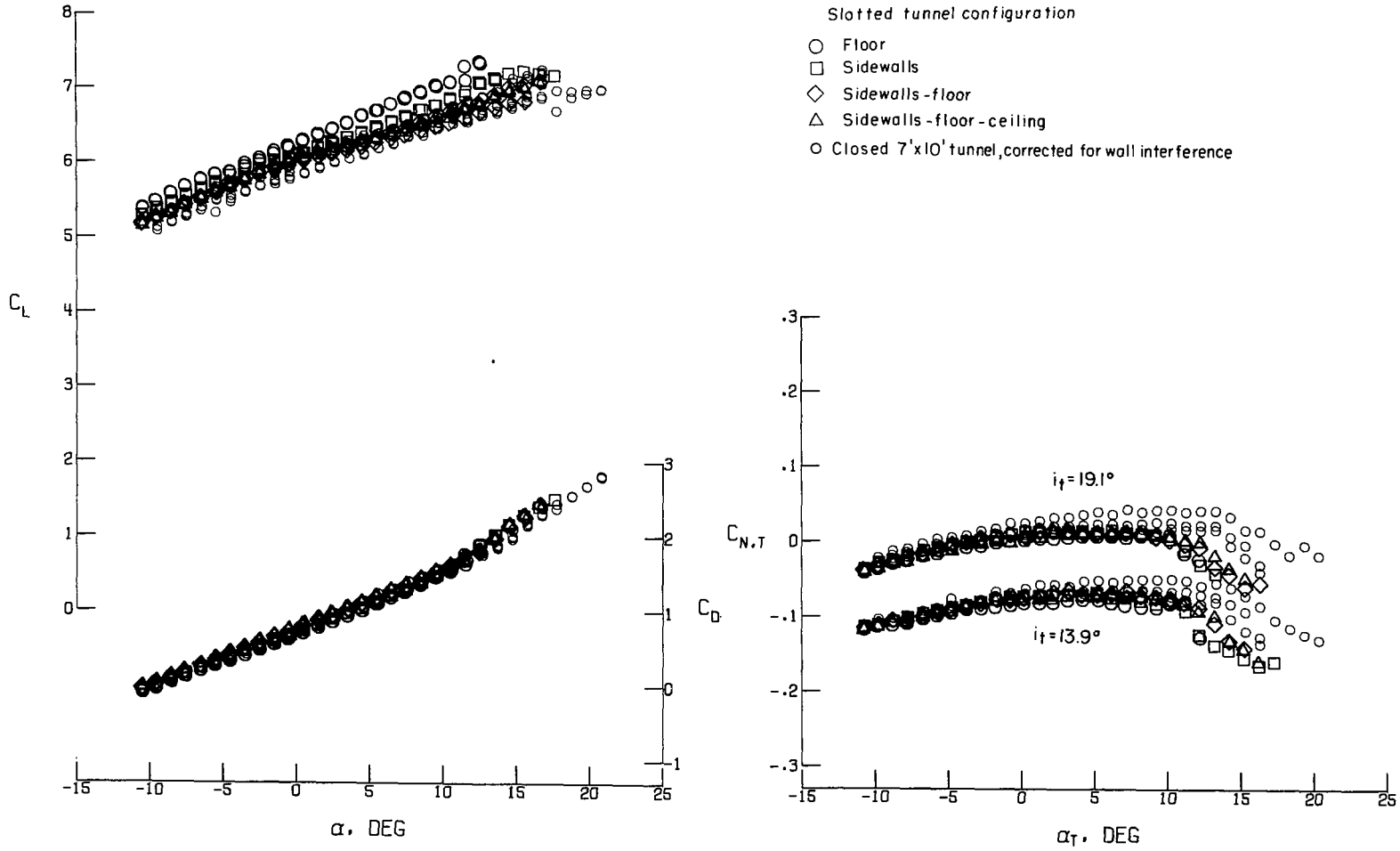

(d) $C_\mu = 3.0$.

Figure 16.- Continued.

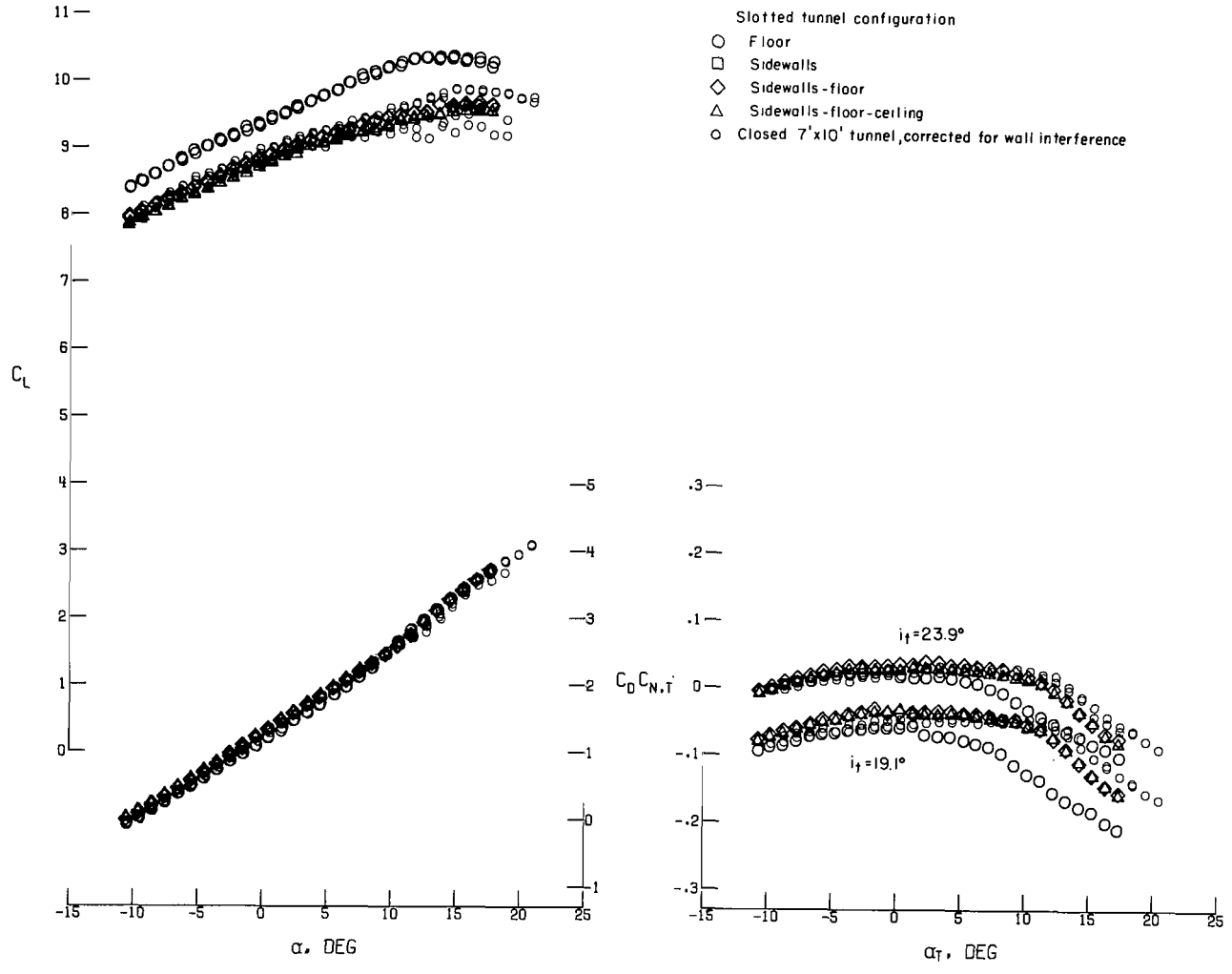

(e) C_μ = 5.0.

Figure 16.- Continued.

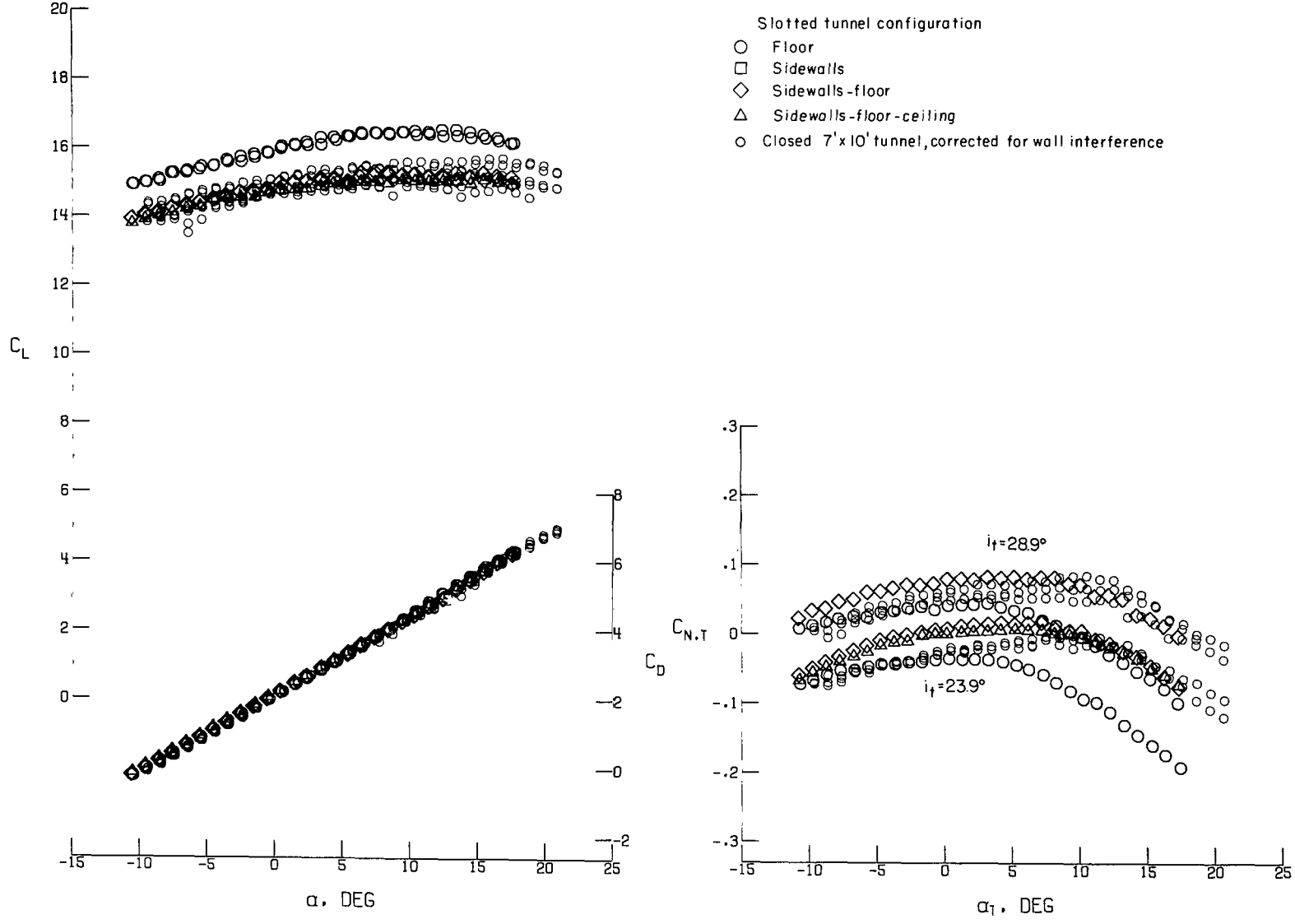

(f) C_μ = 10.0.

Figure 16.- Concluded.

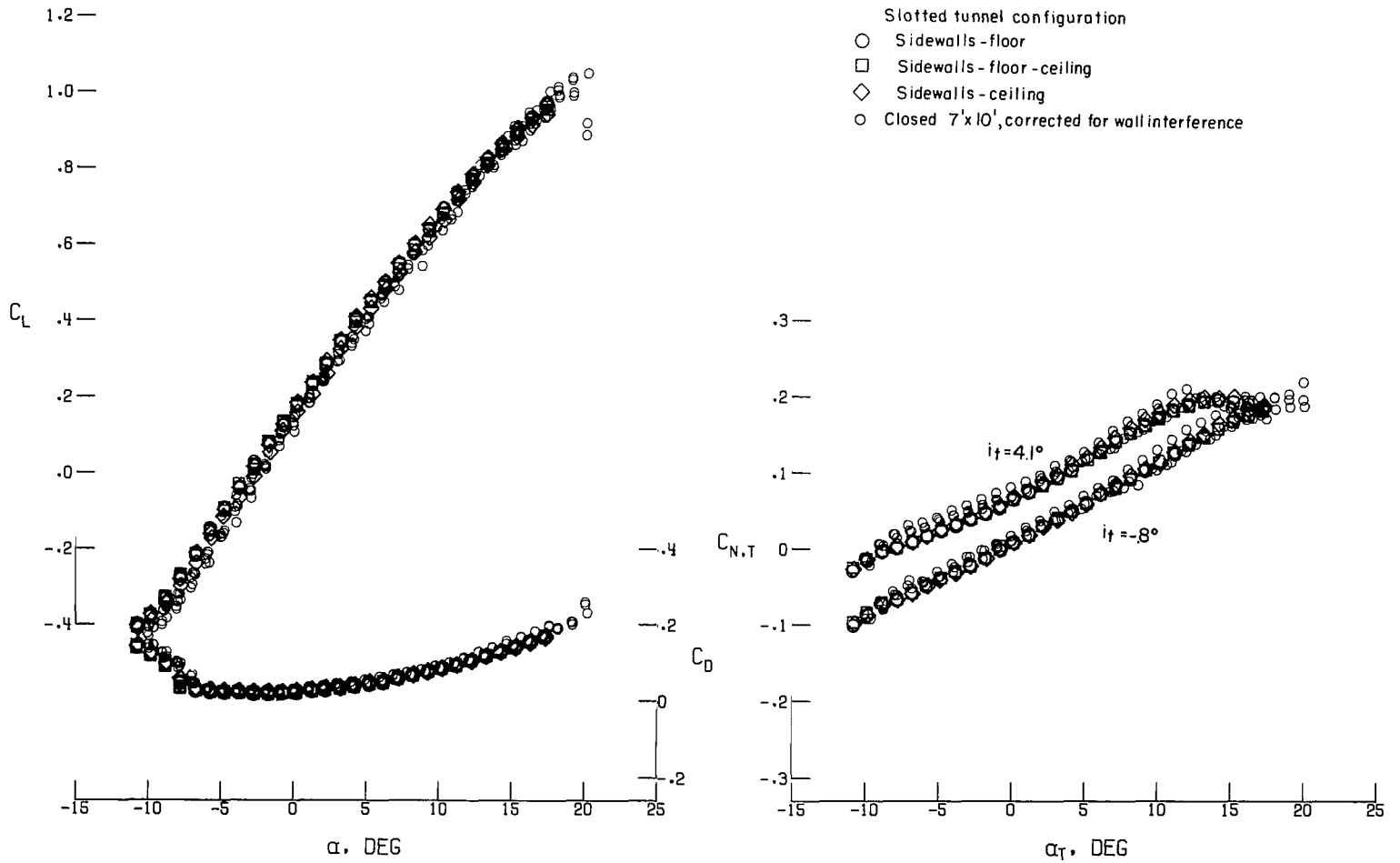

(a) $C_\mu = 0$.

Figure 17.- Effect of slotted boundaries on three different wall configurations on lift, drag, and tail-normal-force coefficients.

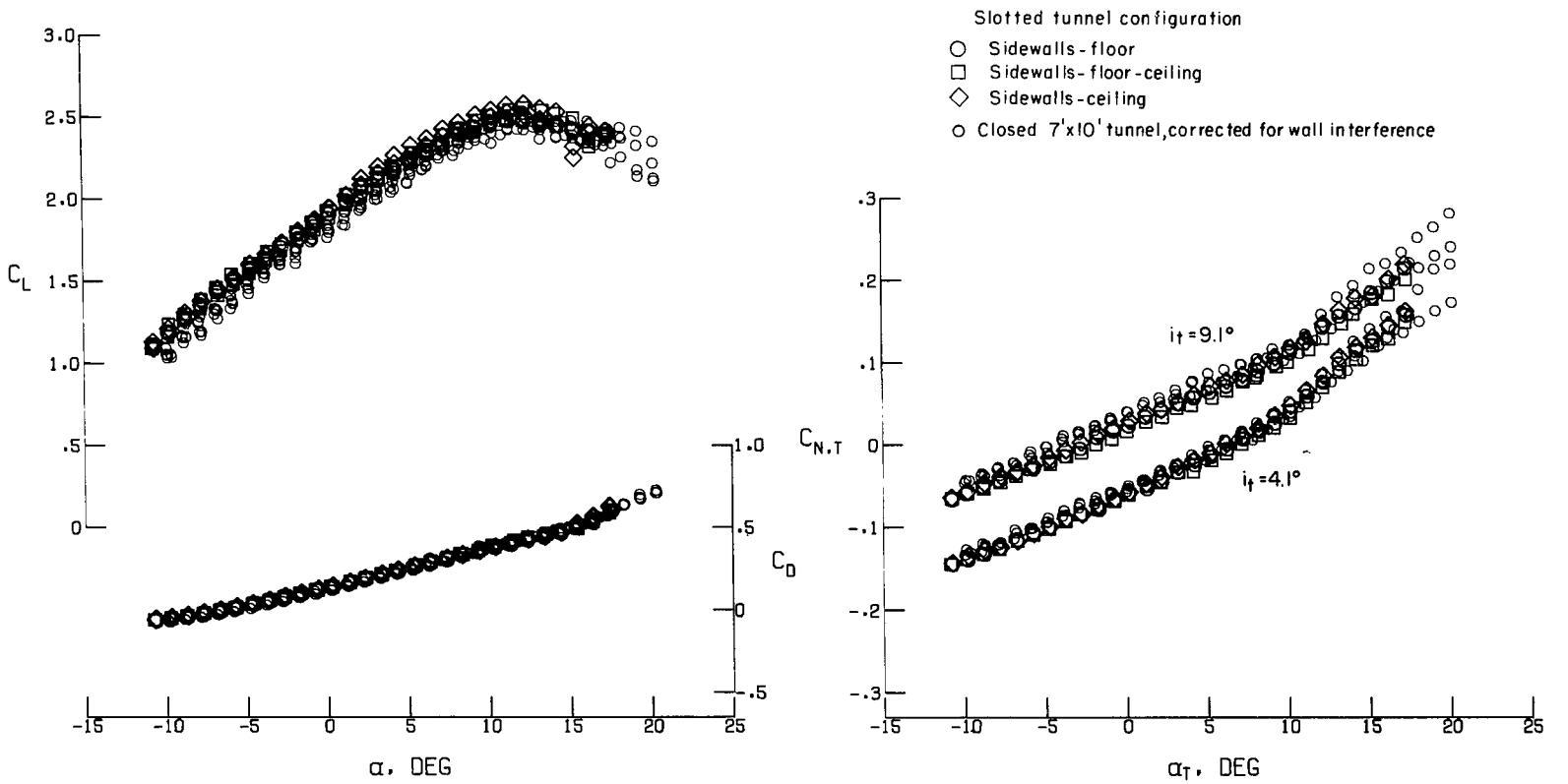

(b) $C_\mu = 0.5$.

Figure 17.- Continued.

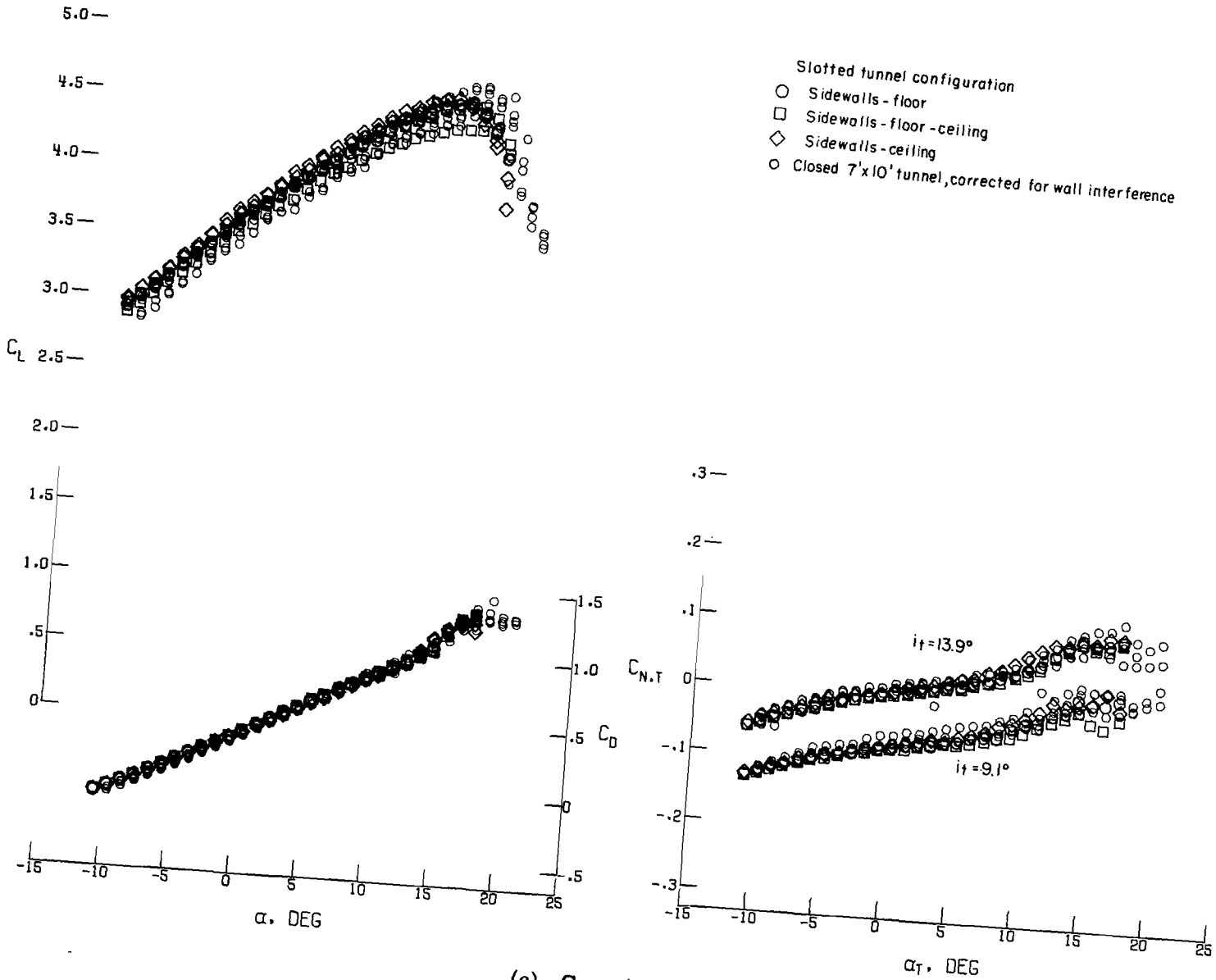

(c) C_μ = 1.5.

Figure 17.- Continued.

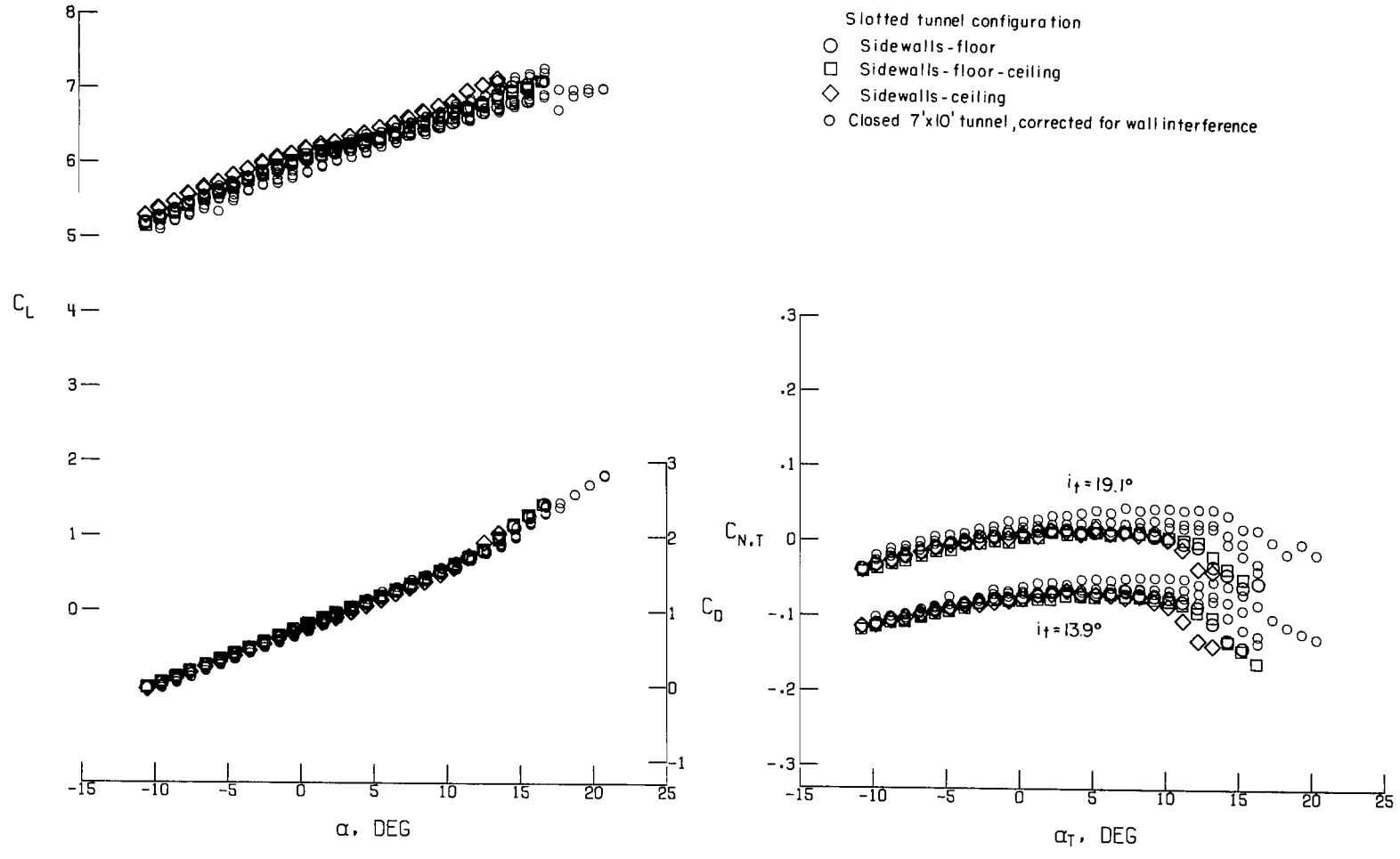

(d) C_μ = 3.0.

Figure 17.- Continued.

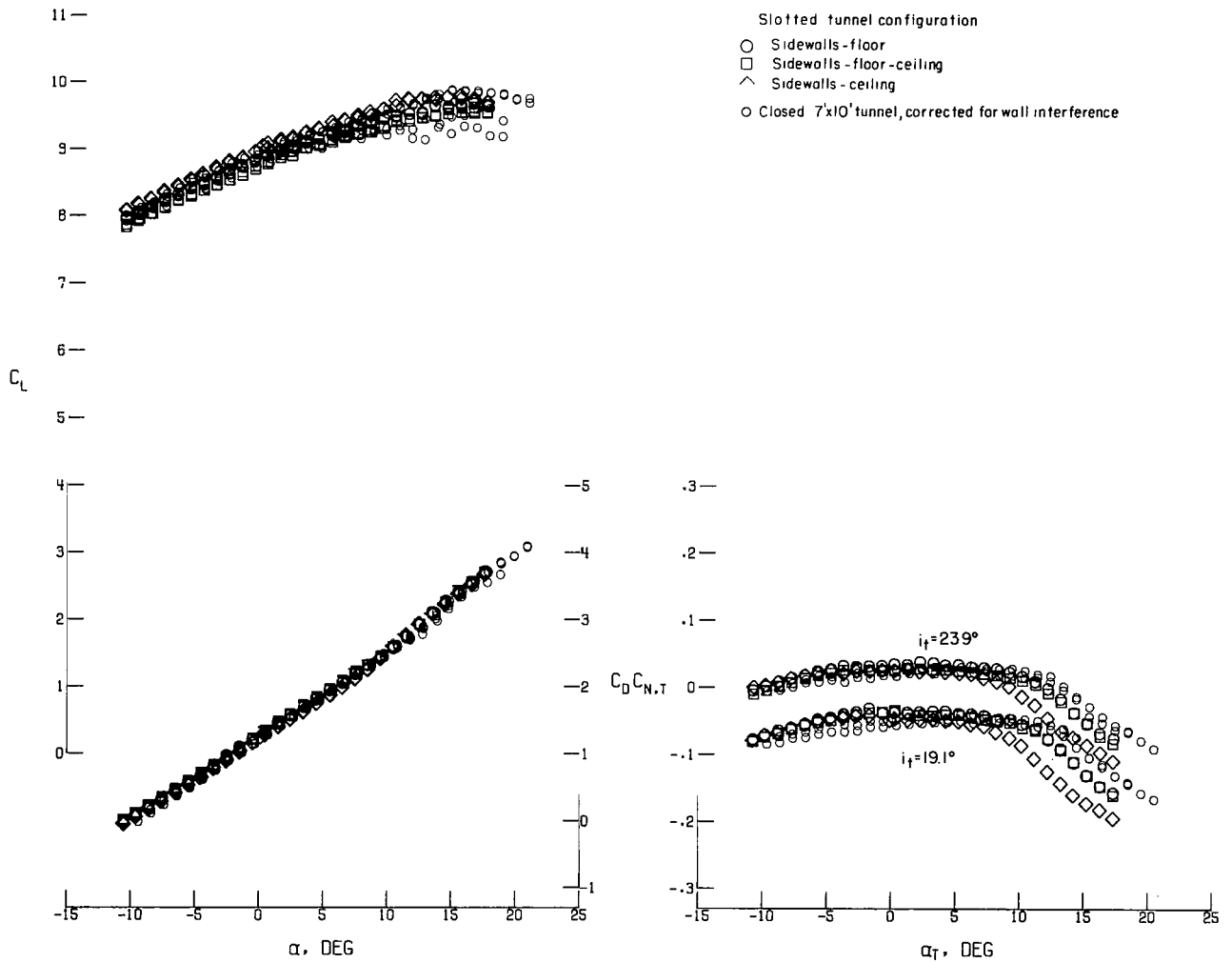

(e) C_μ = 5.0.

Figure 17.- Continued.

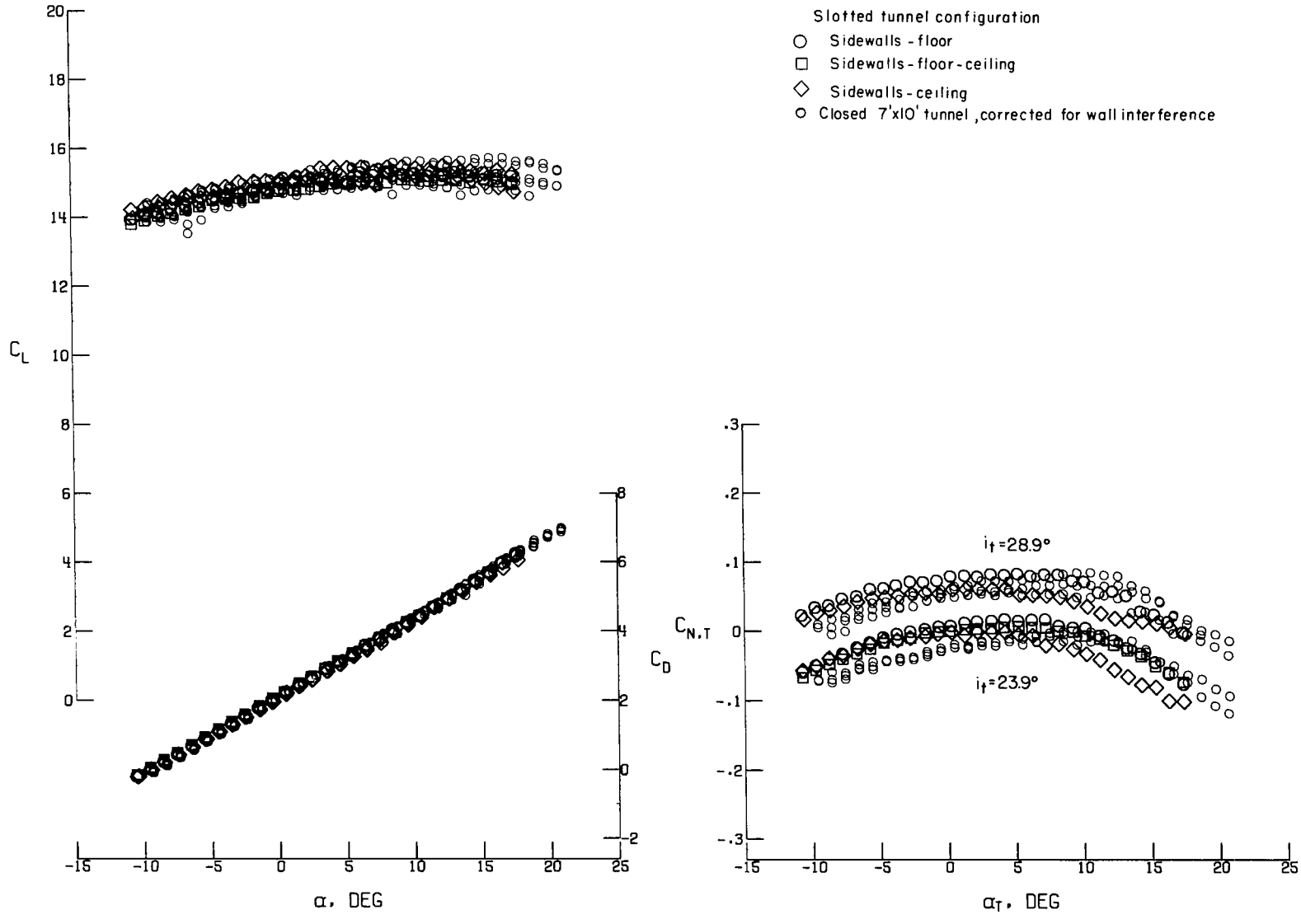

(f) C_μ = 10.0.

Figure 17.- Concluded.

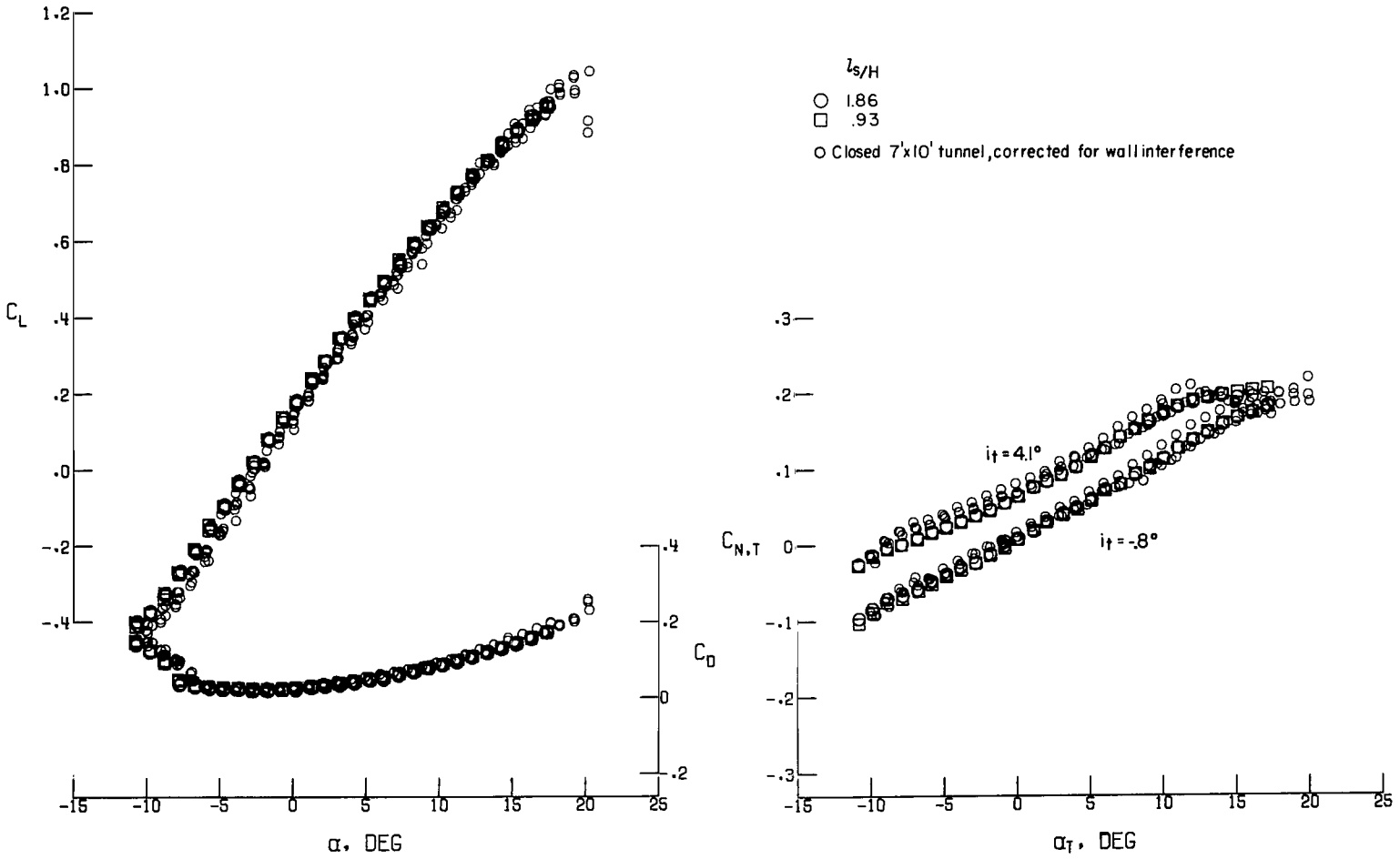

(a) $C_\mu = 0$.

Figure 18.- Effect of sidewall slot length in model tunnel with sidewalls, floor, and ceiling slotted on lift, drag, and tail-normal-force coefficients.

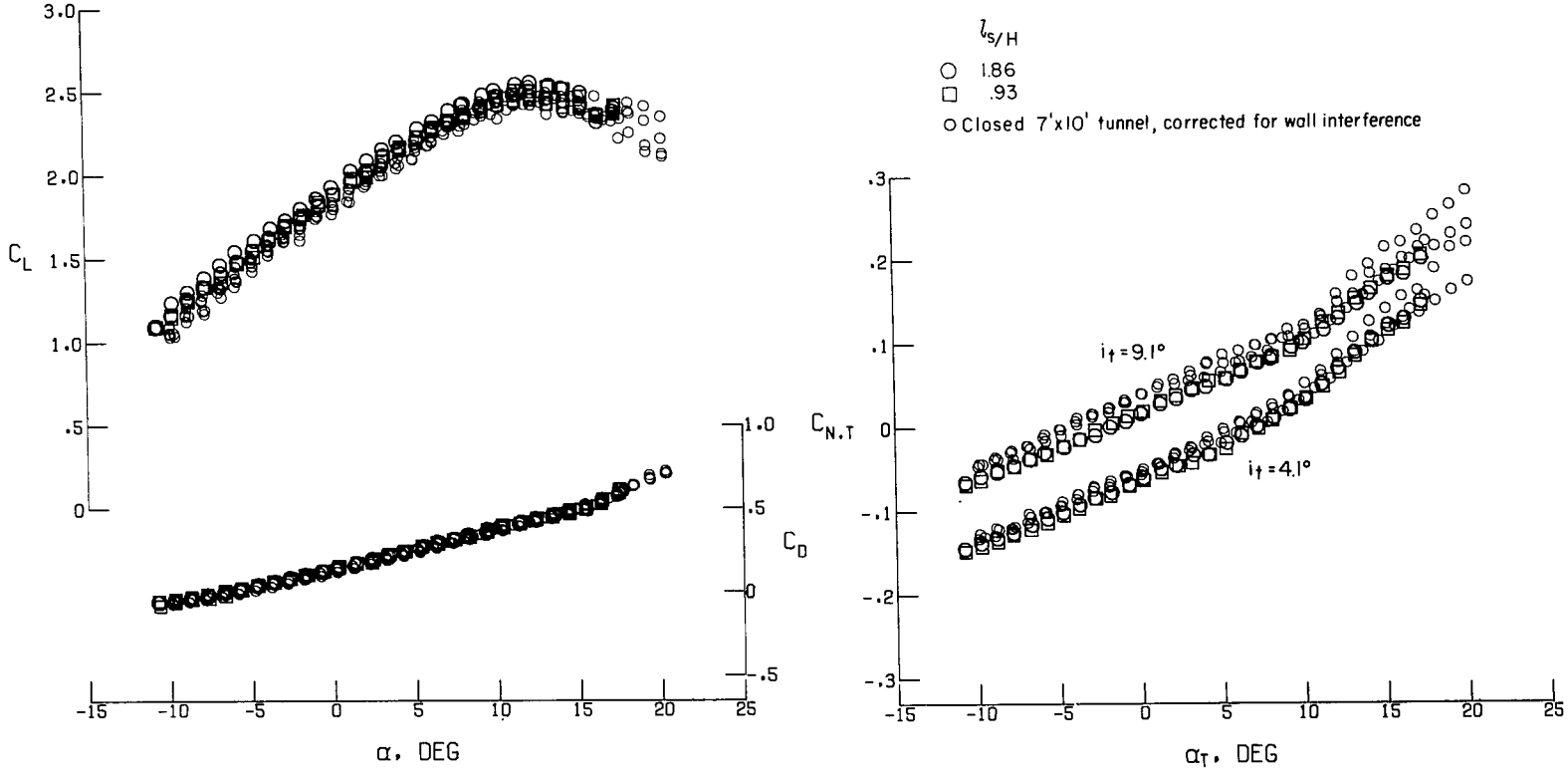

(b) $C_\mu = 0.5$.

Figure 18.- Continued.

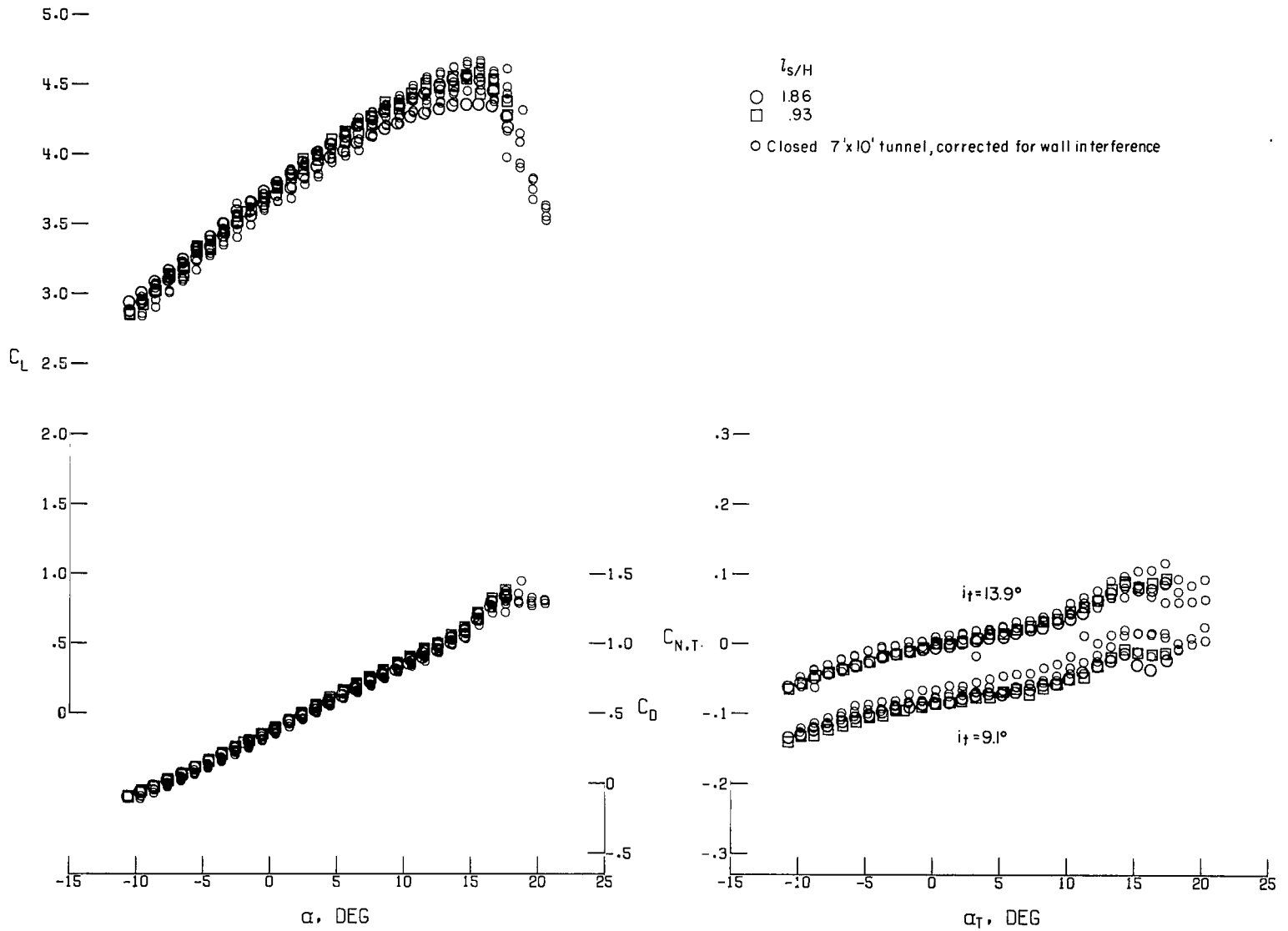

(c) $C_\mu = 1.5$.

Figure 18.- Continued.

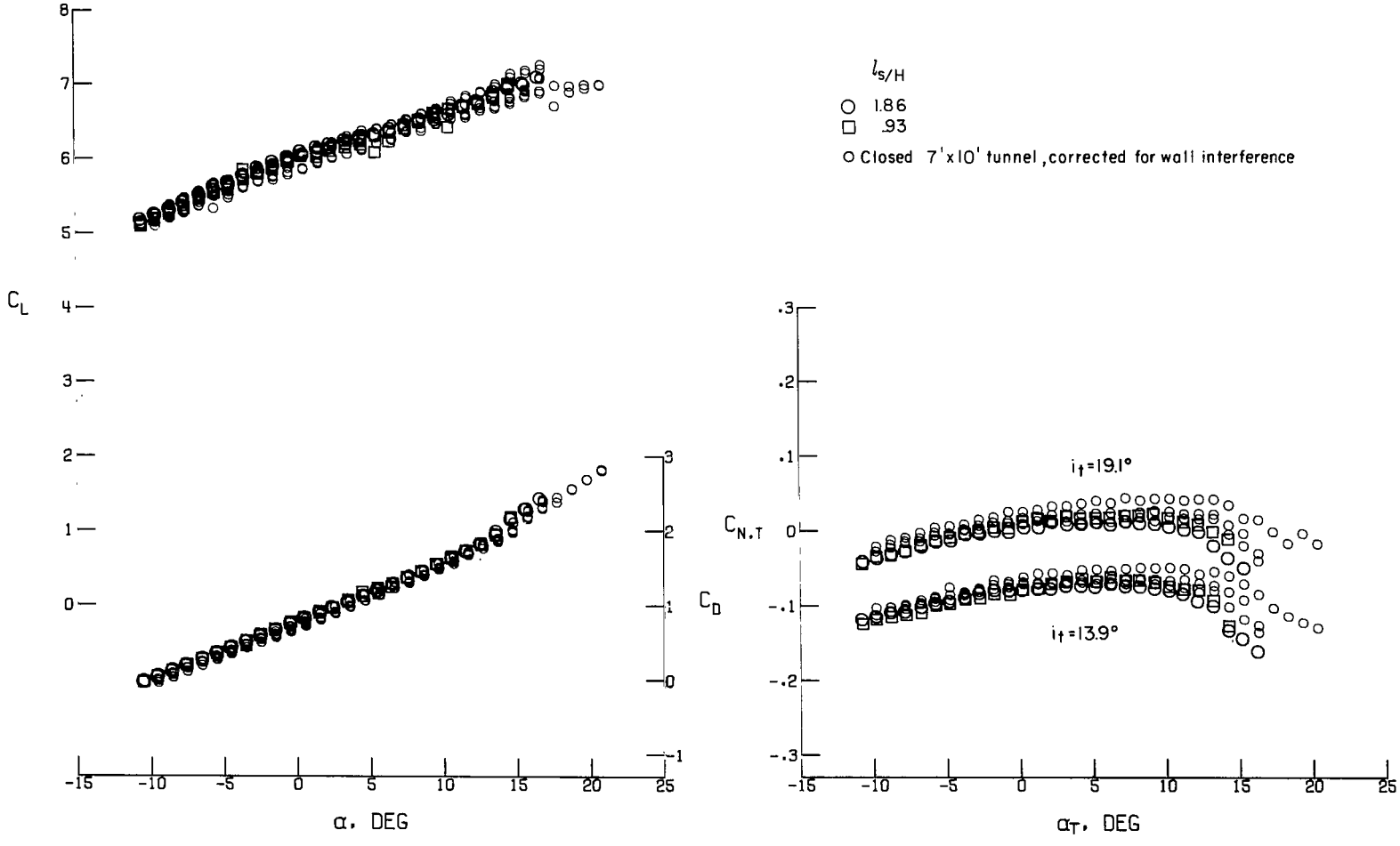

(d) C_μ = 3.0.

Figure 18.- Continued.

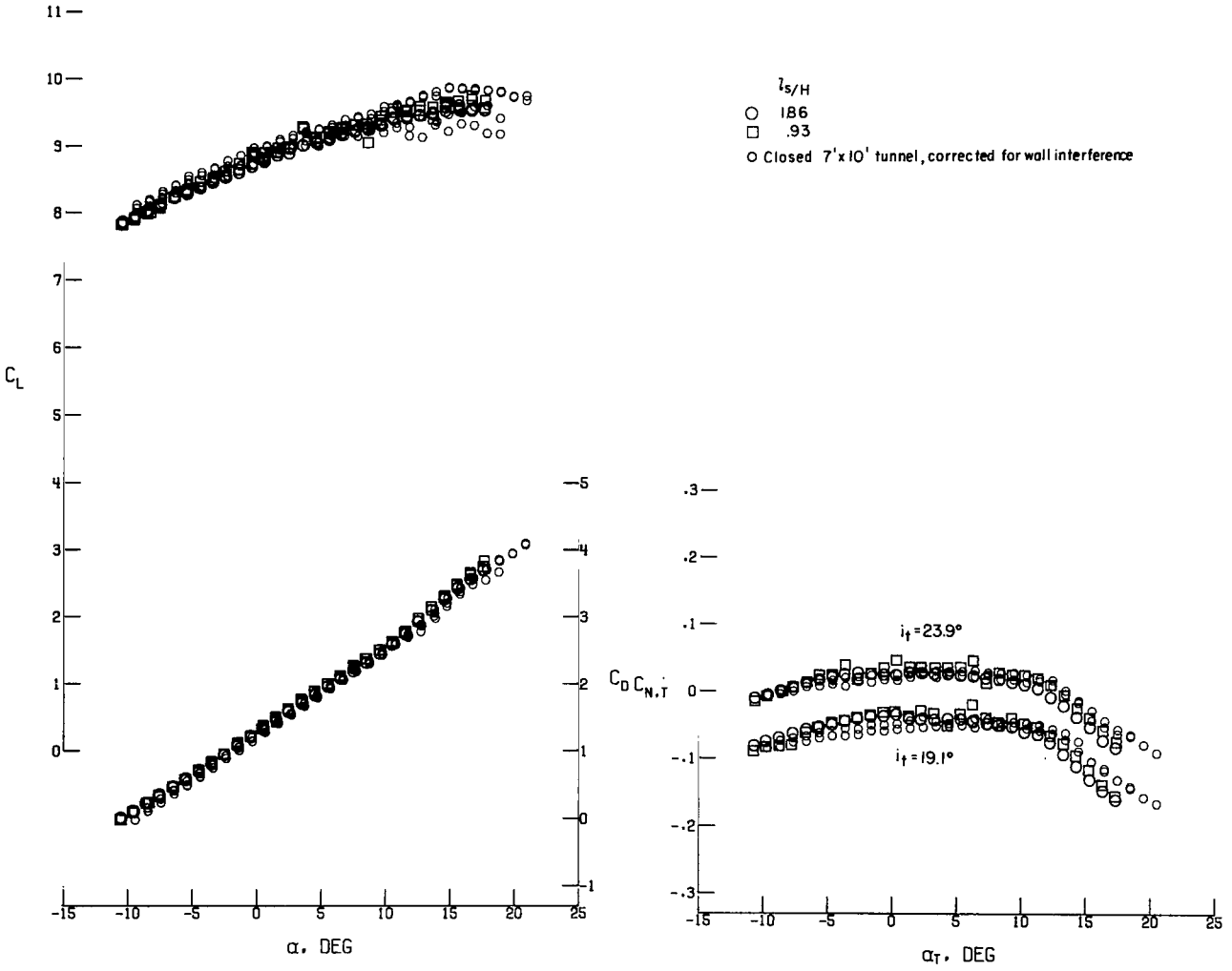

(e) C_μ = 5.0.

Figure 18.- Continued.

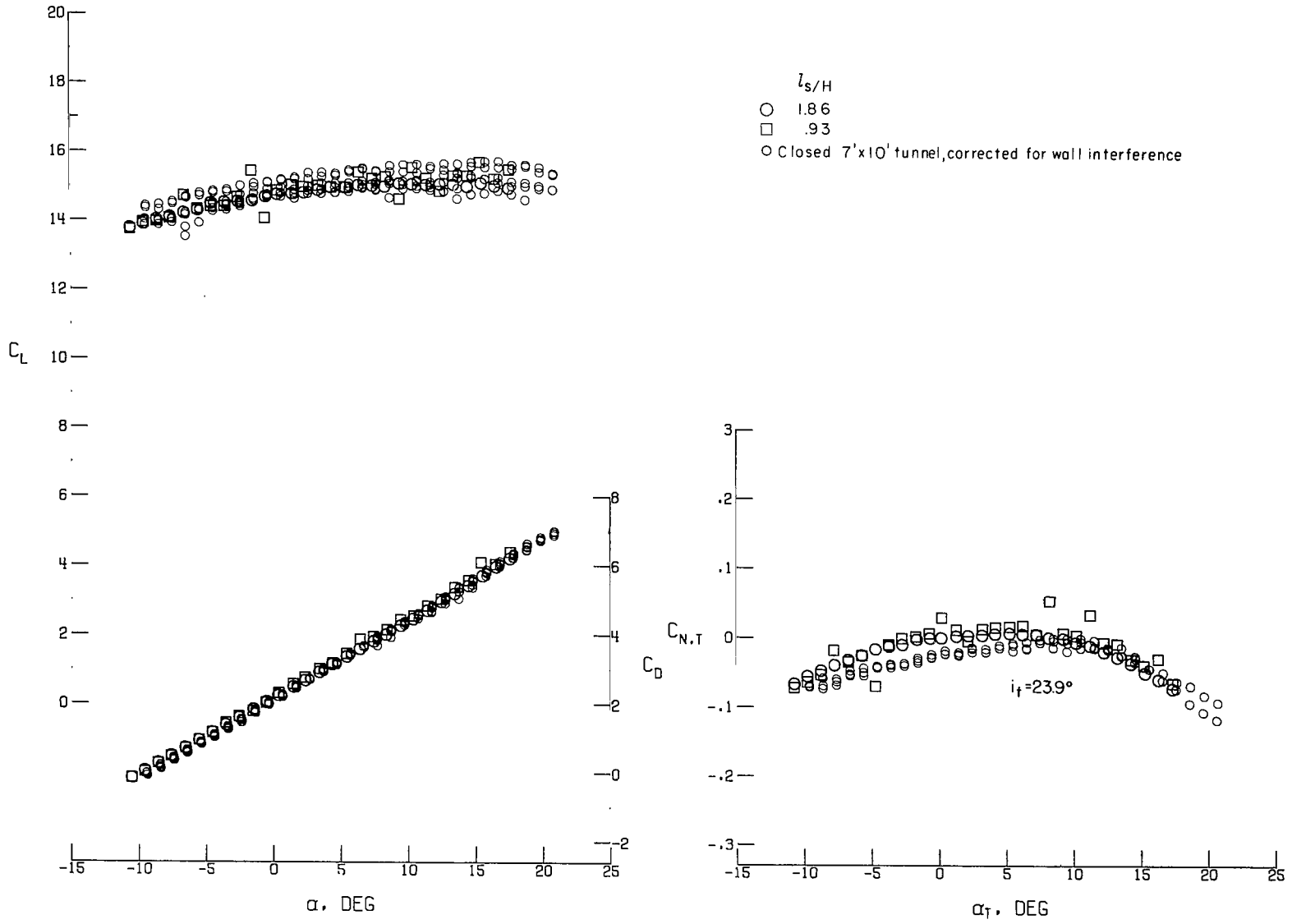

(f) C_μ = 10.0.

Figure 18.- Concluded.

"The aeronautical and space activities of the United States shall be conducted so as to contribute . . . to the expansion of human knowledge of phenomena in the atmosphere and space. The Administration shall provide for the widest practicable and appropriate dissemination of information concerning its activities and the results thereof."

— NATIONAL AERONAUTICS AND SPACE ACT OF 1958

NASA SCIENTIFIC AND TECHNICAL PUBLICATIONS

TECHNICAL REPORTS: Scientific and technical information considered important, complete, and a lasting contribution to existing knowledge.

TECHNICAL NOTES: Information less broad in scope but nevertheless of importance as a contribution to existing knowledge.

TECHNICAL MEMORANDUMS: Information receiving limited distribution because of preliminary data, security classification, or other reasons.

CONTRACTOR REPORTS: Scientific and technical information generated under a NASA contract or grant and considered an important contribution to existing knowledge.

TECHNICAL TRANSLATIONS: Information published in a foreign language considered to merit NASA distribution in English.

SPECIAL PUBLICATIONS: Information derived from or of value to NASA activities. Publications include conference proceedings, monographs, data compilations, handbooks, sourcebooks, and special bibliographies.

TECHNOLOGY UTILIZATION PUBLICATIONS: Information on technology used by NASA that may be of particular interest in commercial and other non-aerospace applications. Publications include Tech Briefs, Technology Utilization Reports and Technology Surveys.

Details on the availability of these publications may be obtained from:

SCIENTIFIC AND TECHNICAL INFORMATION OFFICE

NATIONAL AERONAUTICS AND SPACE ADMINISTRATION

Washington, D.C. 20546